SIMULATION AND DESIGN OF ION TRAPS USING THE METHOD OF FUNDAMENTAL SOLUTIONS

By

Trevor Taylor

Bachelor of Science – Physics
University of Nevada, Las Vegas
2021

A thesis submitted in partial fulfillment
of the requirements for the

Master of Science – Physics

Department of Physics and Astronomy
College of Sciences
The Graduate College

University of Nevada, Las Vegas
May 2024

UNLV | GRADUATE COLLEGE

Thesis Approval

The Graduate College
The University of Nevada, Las Vegas

April 16, 2024

This thesis prepared by

Trevor Taylor

entitled

Simulation and Design of Ion Traps using the Method of Fundamental Solutions

is approved in partial fulfillment of the requirements for the degree of

Master of Science – Physics
Department of Physics and Astronomy

Yan Zhou, Ph.D.
Examination Committee Chair

David Shelton, Ph.D.
Examination Committee Member

Zhaohuan Zhu, Ph.D.
Examination Committee Member

Balakrishnan Naduvalath, Ph.D.
Graduate College Faculty Representative

Alyssa Crittenden, Ph.D.
Vice Provost for Graduate Education & Dean of the Graduate College

Abstract

In this thesis I apply the numeric method, the Method of Fundamental Solutions (MFS), to solve for the fields create by ion traps in various configurations, such as quadrupole ion traps, linear ion traps, toroidal ion traps, and toroidal surface ion traps. The traps are then designed to maximize desired qualities such as minimization of their anharmonicity, and their ability to shuttle ions. A particular focus will be on the toroidal surface ion trap, as well as its ability to shuttle ions. This trap is planned for future experiments involving measurement of the electron Electric Dipole Moment.

Acknowledgements

I would like to acknowledge my thesis advisor committee for providing great help in preparing this thesis, and for their excellent guidance in academic class to provided me with the tools to carry out this research.

Trevor Taylor

University of Nevada, Las Vegas

May 2024

Table of Contents

List of Tables

List of Figures

Chapter 1

Introduction

1.1 Ion Traps

Ion traps are one of the most important tools for Atomic, Molecular, and Optical (AMO) physics as they allow for keeping ions in a single location for a long time. This allows for ions, which would normally fly away given any stray electric field, to be studied. Precision Spectroscopy [30], Atomic Clocks [31], and mass spectroscopy, have all relied on ion traps greatly. Recently the demands of ion traps have changed due to advancements such as quantum computing, which do not only have to keep ions in a single place, but also shuttle them around, and merge a single ion in a trap site with another ion in a different trap site [11]. In addition to quantum computing, tests of translational symmetry [27], as well as searches for the electron Electric Dipole Moment (eEDM) [42], require surface ion traps with a toroidal trapping volume. In the latter, the ions will be constrained to certain positions along the ring and shuttled along it. This thesis will focus on simulating such a trap and also demonstrating which design parameters of the trap are vital.

1.2 Method of Fundamental Solutions

In order to simulate the electric potential caused by ion traps, the Method of Fundamental Solutions (MFS) will be used. The MFS aims to represent the potential on the boundary of some object by a summation of charges outside the domain. This has much in common with the well known method of images, with the only difference being that the MFS is an approximation method and does not require one to know the exact position in which to place charges. In addition, the error on such an approximation method can be found by the uniqueness principle. In this way the MFS presents itself as an intuitive, easy to program, and easy to analyze numeric method. I believe that these

qualities make it worth investigation, and while it might not be able to handle all of the geometries a method such as the Boundary Element Method (BEM) or Finite Element Method (FEM) can, its short learning curve can allow for many to begin their own numerical investigations in a short time.

Chapter 2

Ion Traps

2.1 Theory

In order for an ion to be trapped in a local minimum it must be trapped in all three spatial dimensions, we can also note that the potential trapping the ion must follow Laplace's equation.

$$\nabla^2 V = \frac{\partial^2 V}{\partial x^2} + \frac{\partial^2 V}{\partial y^2} + \frac{\partial^2 V}{\partial z^2} = 0 \tag{2.1}$$

A simple potential to try is then a quadratic potential in each of the three directions

$$V(x, y, z) = \alpha x^2 + \beta y^2 + \gamma z^2 \tag{2.2}$$

which will trap provided that $\alpha, \beta, \gamma > 0$. However if we plug this into Laplace's equation we see

$$\nabla^2 V = \alpha + \beta + \gamma \neq 0 \tag{2.3}$$

Since we are only trapping in each direction if each of these coefficients is positive. This leads to the conclusion that an ion cannot be trapped in one spot by a purely electrostatic field. Since we cannot apply a static potential then there might be a chance to trap an ion if we apply an RF potential. Let us first consider the case of being in the xy plane only, meaning $\gamma = 0$, and note a solution to Laplace's equation occurs if $\alpha = -\beta$.

Our potential at one moment of time is then

$$V(x, y) = \alpha(x^2 - y^2) \tag{2.4}$$

This potential is a quadrupole potential if we let $\alpha = 1/r_0^2$, and now if we modulate it by $U+V\cos\Omega t$ we get the equation,

$$V(x,y,t) = (U - V\cos\Omega t)\frac{(x^2-y^2)}{r_0^2} \tag{2.5}$$

with U being a DC voltage and V being an RF voltage. Intuitively this corresponds to a potential in which the potential "flaps". Often this potential is compared to a rotating saddle, however, the rotating saddle does not have this form [17]. Now by noting that $-\nabla V = E$ and $m\ddot{x}/e = E$ we get, the set of equations,

$$\ddot{x} = -\frac{e}{mr_0^2}(U - V\cos\Omega t)x \tag{2.6}$$

$$\ddot{y} = \frac{e}{mr_0^2}(U - V\cos\Omega t)y \tag{2.7}$$

$$\ddot{z} = 0 \tag{2.8}$$

with e being the ion's charge and m being the ion's mass. If we then make the substitutions

$$\frac{4eU}{mr_0^2\Omega} = a \tag{2.9}$$

$$\frac{2eV}{mr_0^2\Omega} = q \tag{2.10}$$

$$\Omega t = 2\zeta \tag{2.11}$$

Then our equations become

$$\frac{d^2x}{d\zeta^2} + (a - 2q\cos 2\zeta)x = 0 \tag{2.12}$$

$$\frac{d^2y}{d\zeta^2} - (a - 2q\cos 2\zeta)y = 0 \tag{2.13}$$

which can be recognized as the Mathieu's differential equation [16]. Now intuitively these equations should be unstable for some values of a, q and stable for others, for example, in the very low limit of rotation $\Omega = 0$ this is just a static potential which we know cannot trap an ion. To look for the regions of stability we can solve the eigenvalue problem associated with this equation.

$$\frac{d^2x}{d\zeta^2} + (a - 2q\cos 2\zeta)x = \lambda x \tag{2.14}$$

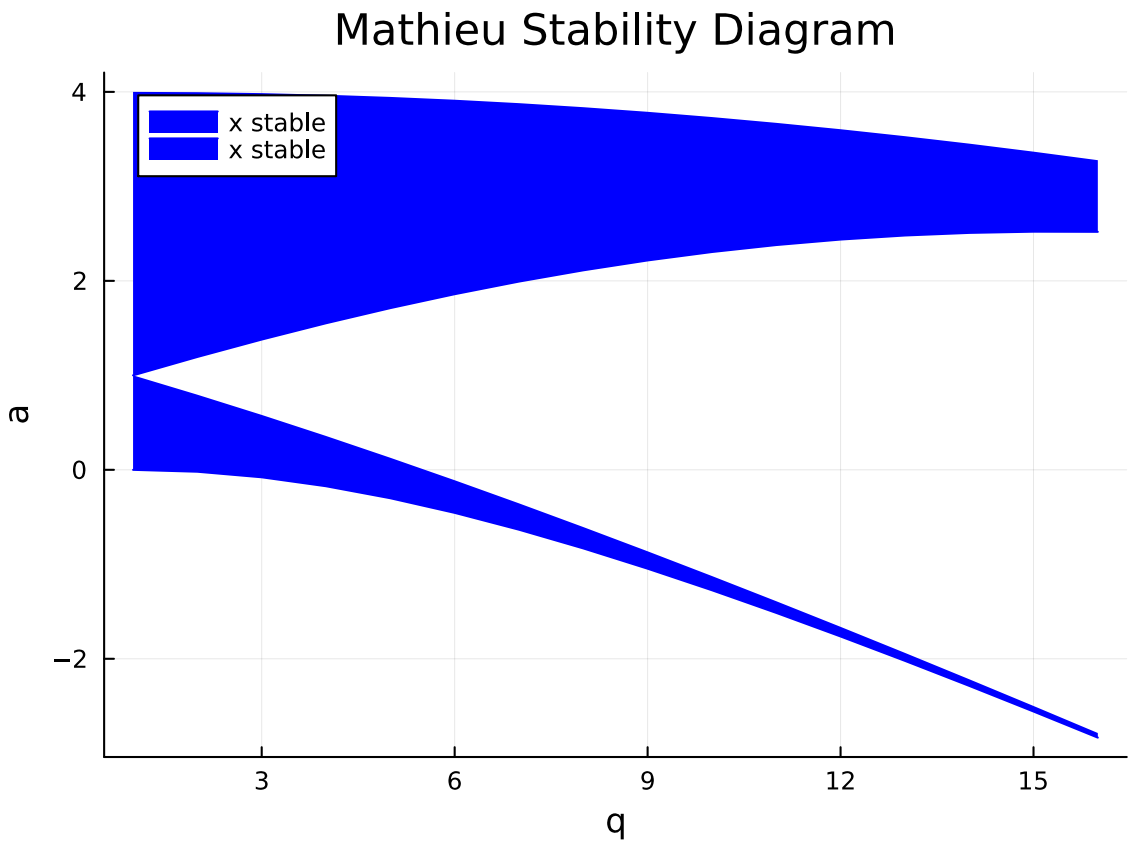

Figure 2.1: Stability diagram for the Mathieu equation

We can solve this using many techniques, but using a spectral method as in [38], we can obtain the stability diagram shown in Figure 2.1.

With the shaded areas being regions of stability and non-shaded being unstable. We can also note that our ion must obey both Eq 2.12 and Eq 2.13 and thus it must obey two stability diagrams, which are mirrored over the q axis because of the minus sign difference between the two equations. The stability diagrams for both are shown in Figure 2.2.

The equations do not trap in the z direction and thus do not form traps, but mass filters. If we want to form an ion trap then we need to have an equation which includes the z direction. One solution is $\alpha = 1$, $\beta = 1$ $\gamma = -2$, which would correspond to the equation

$$\phi = \phi_0(\frac{x^2 + y^2 - 2z^2}{4r_0^2}) \tag{2.15}$$

with ϕ_0 being a scalar. If we make a transformation to cylindrical coordinates by letting $r^2 = x^2+y^2$, we then get the equation

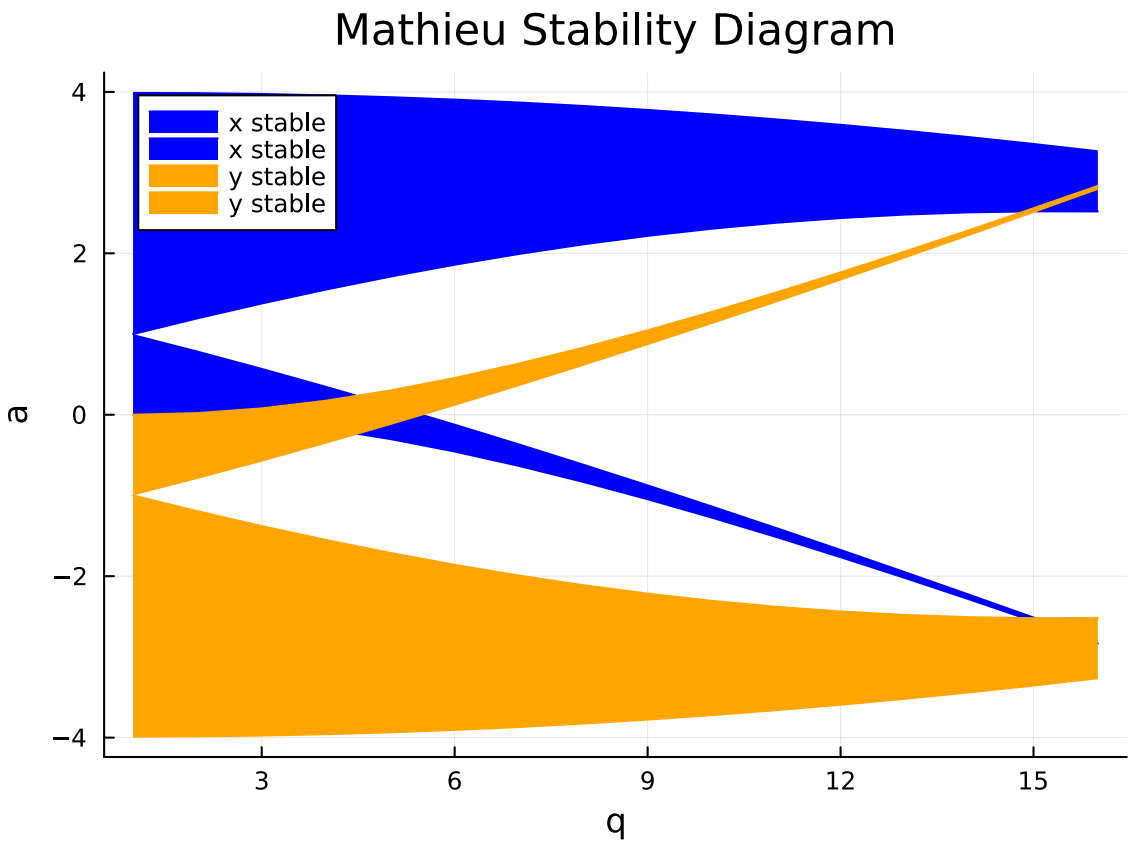

Figure 2.2: Stability diagram for the Mathieu equations in both the x and y directions

$$\phi = \phi_0(\frac{r^2 - 2z^2}{4r_0^2}) \tag{2.16}$$

which has the same form as the two dimensional trap, just with the exception that the z axis is scaled by a factor of 2. The Mathieu equations and stability diagrams end up looking nearly the same except for this factor of 2.

2.2 Ion Motion in an Ion Trap

With the Mathieu equations we can simulate the motion of an ion in an ion trap. The results of a simulation of a two dimensional ion trap, with the initial parameters of $a = 0.01$, $q = 0.2$, starting at the center of the trap with a value of $x = 1$, $v_x = 2$, $y = 1$, and $v_y = 1$, give the plot shown in Figure 2.3. We can also see the dynamics for a longer time period to confirm it is trapped in Figure 2.4.

We can see two types of motion in this simulation. There appears to be a slower oscillations,

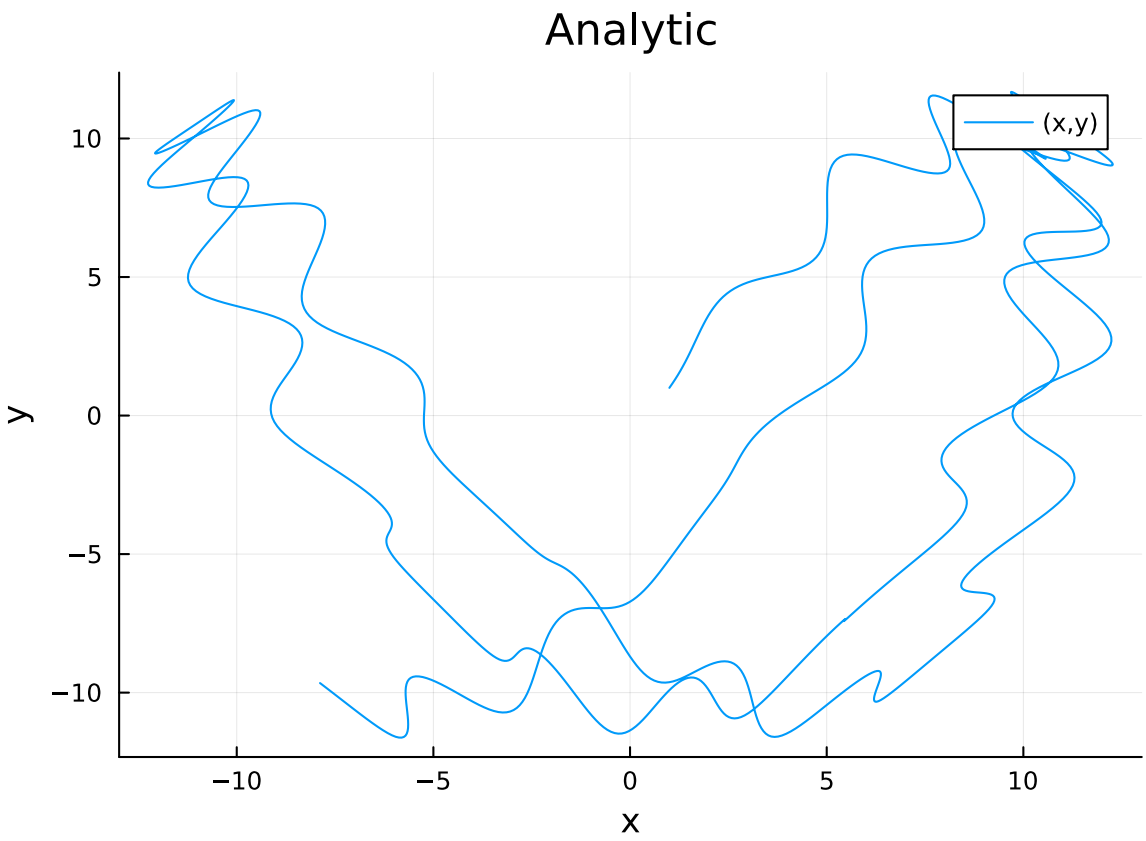

Figure 2.3: Solution to Mathieu equation with $a = 0.01, q = .2, x = 1, y = 1, v_x = 1.1e-6, v_y = 1e-6$

referred to as secular motion, and a much faster oscillation called micromotion. The micromotion is a consequence of the $cos(wt)$ variation in the applied voltage, and the frequency of the micromotion will correspond to that frequency. The secular motion's frequency can be found by utilizing a "pseudopotential" approximation. This approximation replaces the unstable saddle like potential of the trap with its time averaged electric field potential given by Eq 2.17.

$$\Phi = \frac{e^2}{4m\Omega}|\phi|^2 \tag{2.17}$$

Using this we see that if we were to plug in our quadrupole potential of $x^2 - y^2$ we would get something proportional to $x^2 + y^2$ which will obviously trap an ion in one spot. One last thing to note is the interaction between micromotion and the pseudopotential. As seen in Figure 2.3 the squiggles that represent the micromotion are much greater the farther away from the center the ion is. In this way if there was a force which pushed the ion away from the center of the ion trap, the micromotion would be greater, and this increase in micromotion from the normal amount is

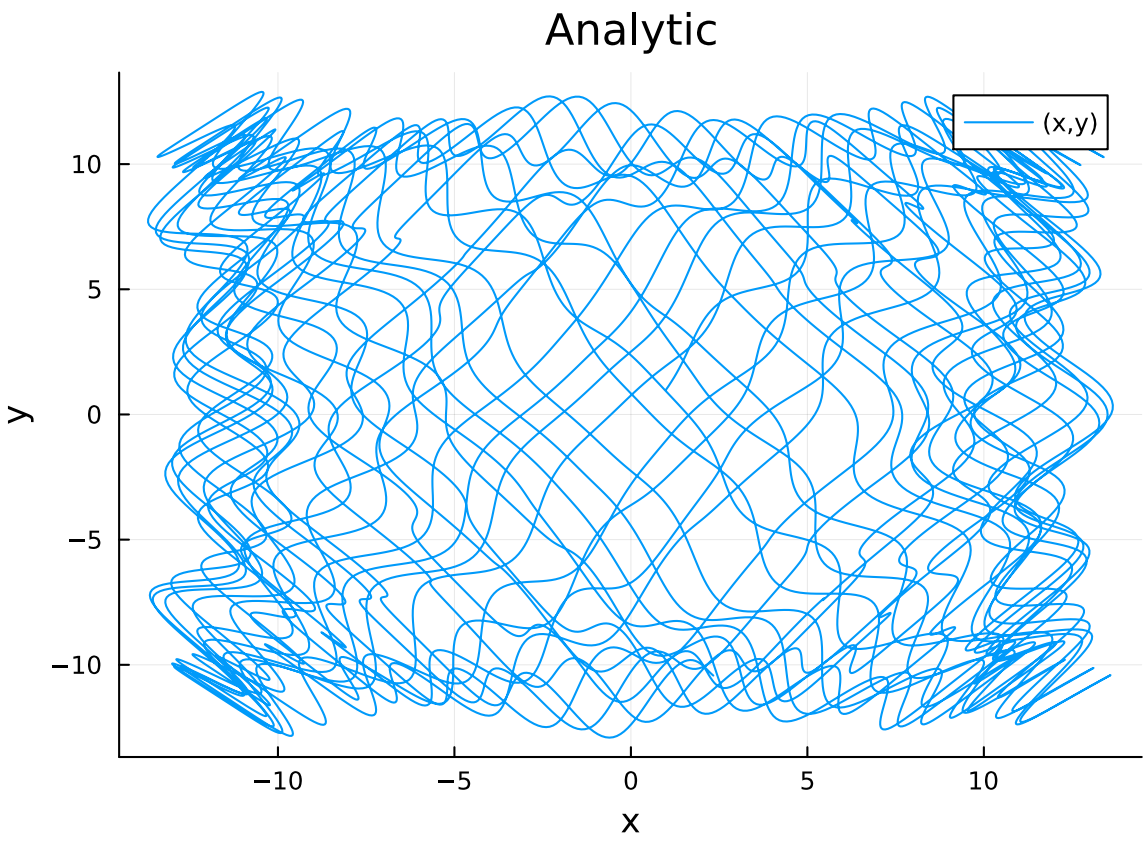

Figure 2.4: Solution to Mathieu equation with $a = 0.01, q = .2, x = 1, y = 1, v_x = 1.1e-6, v_y = 1e-6$

called excessive micromotion [5]. This type of effect is mainly caused by misalignment of the ion trap, and for many of the traps presented in this thesis, this effect will be present unless explicitly compensated for.

2.3 Trap Geometry

While we have seen the ideal potentials for these traps we have not considered the way in which to create these potentials. The easiest way to construct the potentials is to place electrodes shaped to follow the equipotential contours of the potential. In this way the shape of the electrodes will satisfy the boundary conditions of the potential and thus must be the solution through the uniqueness principle. We can first look at the potential for a 2d hyperbolic trap. The potential is given by

$$V(x, y) = \frac{(x^2 - y^2)}{r_0^2} \tag{2.18}$$

and let us pick the equipotential lines for $V = \pm 1$. We then get the implicit equations

$$\pm r_0^2 = x^2 - y^2 \tag{2.19}$$

which will form four different hyperbolas, and then extruding these out will give us an electrode structure that will create a quadrupole potential with a minimum that lies on a line. A CAD rendering of the trap can be shown in Figure 2.5

Another ideal geometry is that for a 3d ion trap. It will be given by the implicit equation below.

$$\pm r_0^2 = r^2 - 2z^2 \tag{2.20}$$

Since this trap has a radial geometry, we can note that it will trap in 3d, and a rendering is shown in Figure 2.6. Note that the rendering has a cutout, purely to show the structure of the trap since the internal structure is not easily viewable without it.

One thing to note is that hyperbolic electrodes are not easily machinable, and as a results many ion traps feature simpler designs, such as replacing hyperbolic electrodes with cylinders. This forms an ion trap with a trapping region along a line. One modification can then be done which is to add endcaps which will provide trapping in the z direction. This is commonly referred to as a linear ion trap, and this thesis will call it a four rod trap, due to it being made of four rods. It is shown in Figure 2.7.

Another class of ion traps are those which only have electrodes which lie on a surface. These traps are easy to manufacture using photolithography. The most common design is the five wire ion trap, which has five rectangular electrode strips. The ion will be trapped above the surface of the trap by an RF voltage applied to the second and fourth electrodes. The other most electrodes are often broken up into many control electrodes to provide trapping in along the axis of translational symmetry.

2.4 Anharmonic Terms

While the previous section mentioned ion traps which featured a perfect quadrupole potential, it is not often the case that our potential is a perfect quadrupole, as any deviation from this model, such as truncating the electrodes, will distort the electric field. To explain this distortion we can describe our field in terms of some expansion. For a 2d quadrupole potential one possible choice is the Harmonic Polynomials as shown below.

$$\phi_n = \frac{Re((x+iy)^n)}{r_0^n} \tag{2.21}$$

We can note that for $n = 2$ we get a quadrupole potential. For $n = 0$ we get a constant potential, for $n = 1$ we get a dipole potential. For $n = 3, 4, 5, \ldots$ we get the 2d version of the hexapole, octupole, decapole, dodecapole. These terms are also referred to as 6-pole, 8-pole, 10-pole, based on how many times their potential changes from positive to negative when traversing a circle around the potential's center. In this way a quadrupole can also be referred to as a 4-pole potential. Using these terms we can then say that the potential of an ion trap is given by a series expansion.

$$V = \sum_{0}^{\infty} A_i \phi_i \tag{2.22}$$

In this way any deviations from the ideal quadrupole geometry, will change the values of A_i such that A_2 is no longer the only solution. One example of this is the "stretched" ion trap geometry, which has the vertical electrodes separated more than the horizontal electrodes. This ends up contributing an addition octupole component to the field [14].

The effects of these terms which deviate from a perfect quadrupole can be considered negligible if the ions do not deviate much from the center of the trap. This is the case often assumed for ion traps, which want to keep ions stored for a long time, and which only have a few ions. In the case of a mass spectrometer, which wants ions to fly away if they have a certain ratio of their mass to their charge, these effects have a greater impact.

These terms can cause certain parts of the stability region to have "black canyons" where they would normally be stable but are unstable due to nonlinear resonances [12]. They will also couple orthogonal motional modes together and cause additional heating [36].

2.5 Toroidal Ion Traps

A major focus of this thesis will be on ion traps which feature a toroidal trapping volume. While these designs have existed in the form of ion storage rings [9] since the 1970s, and in terms of mass spectrometers [26] since the early 2000s, only recently has there been extensive studying on these traps.

D.E. Austin et all [18] have studied the motion in terms of toroidal harmonics, which serve as a multipole expansion which is valid in the toroidal geometry. However, when analyzing the

stability of the ion in a pure toroidal quadrupole, they saw many nonlinear effects, and chaos in their stability diagram. They have recently proposed to include certain ratios of the toroidal hexapole as well to improve their stability diagram [19]. However, from their analysis it appears that using the toroidal harmonics to design an ion trap does not provide obvious intuition as to what the addition of certain harmonics will do, as compared to the standard multipole analysis where there is more of an intuition as to what the higher order terms do.

If the toroidal harmonics are not the best expansion to use to gain an intuitive understanding of the trap then a perturbative analysis might be better. Zhou et al, [41] discusses the case of a curved ion guide and find a perturbative expansion in terms of harmonic polynomials. Concluding that as the curvature of the trap becomes greater, more harmonic terms such as the hexapole and octupole increase in strength.

The specific trap that there will be a focus on in this thesis, is the trap proposed by Zhou et al, [42], which is a surface ion trap with a toroidal trapping volume, shown in Figure 2.9, similar to the NIST Ring Ion Trap [37], with a major change being that the outer electrodes are to transport the ions in a circular fashion, instead of purely to shim unwanted Electric Fields. A similar trap [39] rotates the ions in a similar circular fashion, but not so each ion forms its own trap site along the ring. Overall, this trap design has not had the shuttling feature of it or any analysis of its higher order harmonics performed. The aim of this thesis will then be to simulate and analyze the toroidal surface trap using the Method of Fundamental Solutions, and to investigate its feasibility.

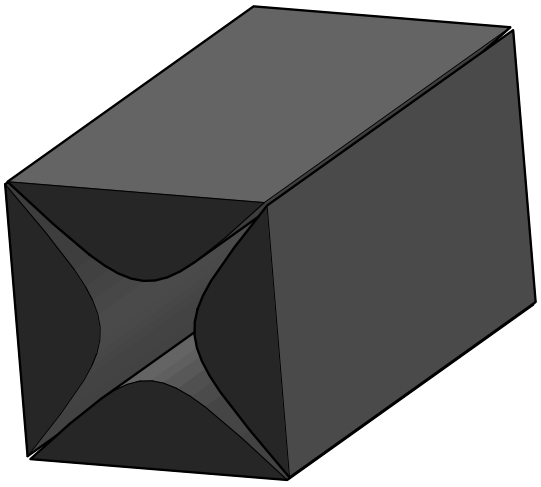

Figure 2.5: CAD rendering of a hyperbolic linear ion trap which produces the ideal quadrupole potential. The top and bottom electrodes are set to a voltage V, and the left and right electrodes will be set to a voltage -V

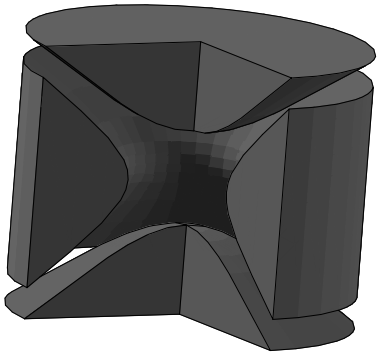

Figure 2.6: CAD rendering of a 3d hyperbolic ion trap, with a cutout, which produces the ideal quadrupole potential in 3d.

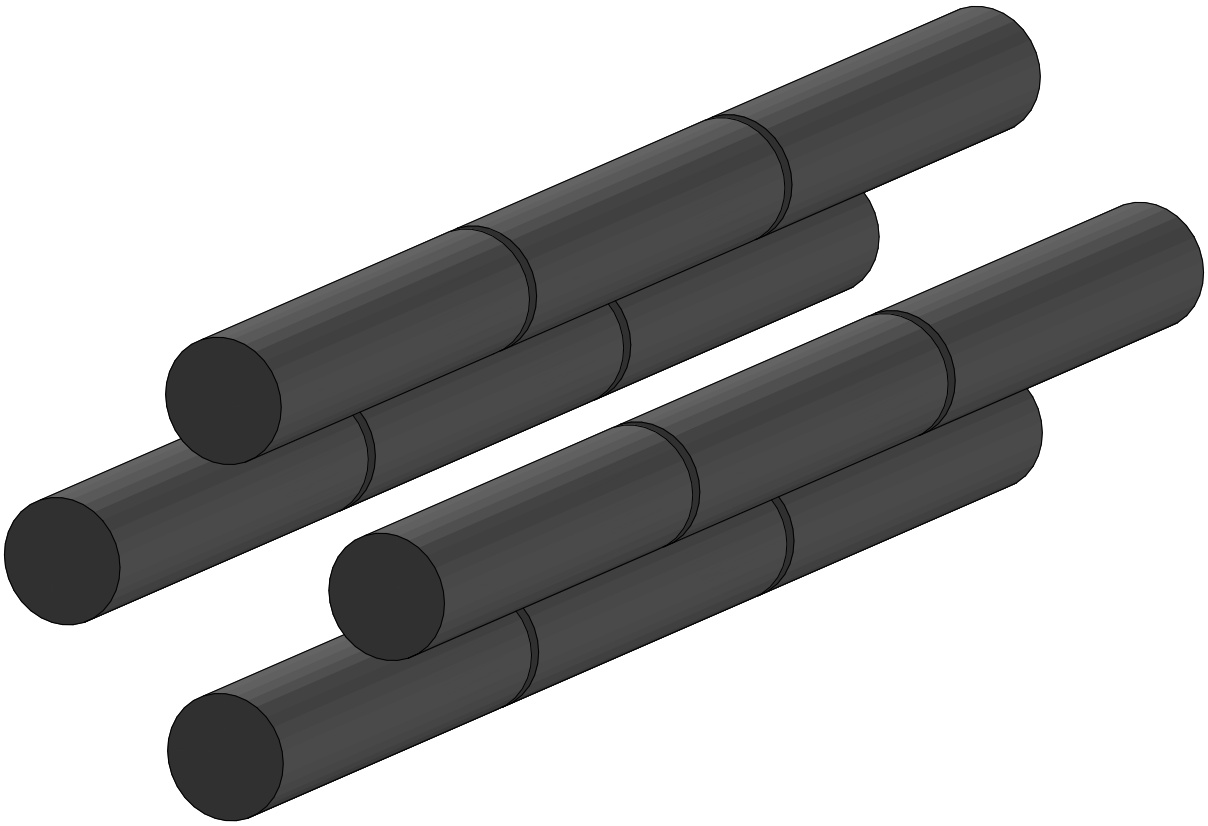

Figure 2.7: A Four Rod Linear ion trap geometry. The voltages are the same as in the 2d hyperbolic trap, but an additional DC voltage is applied on the two outer sets of four electrodes to trap ions in the center

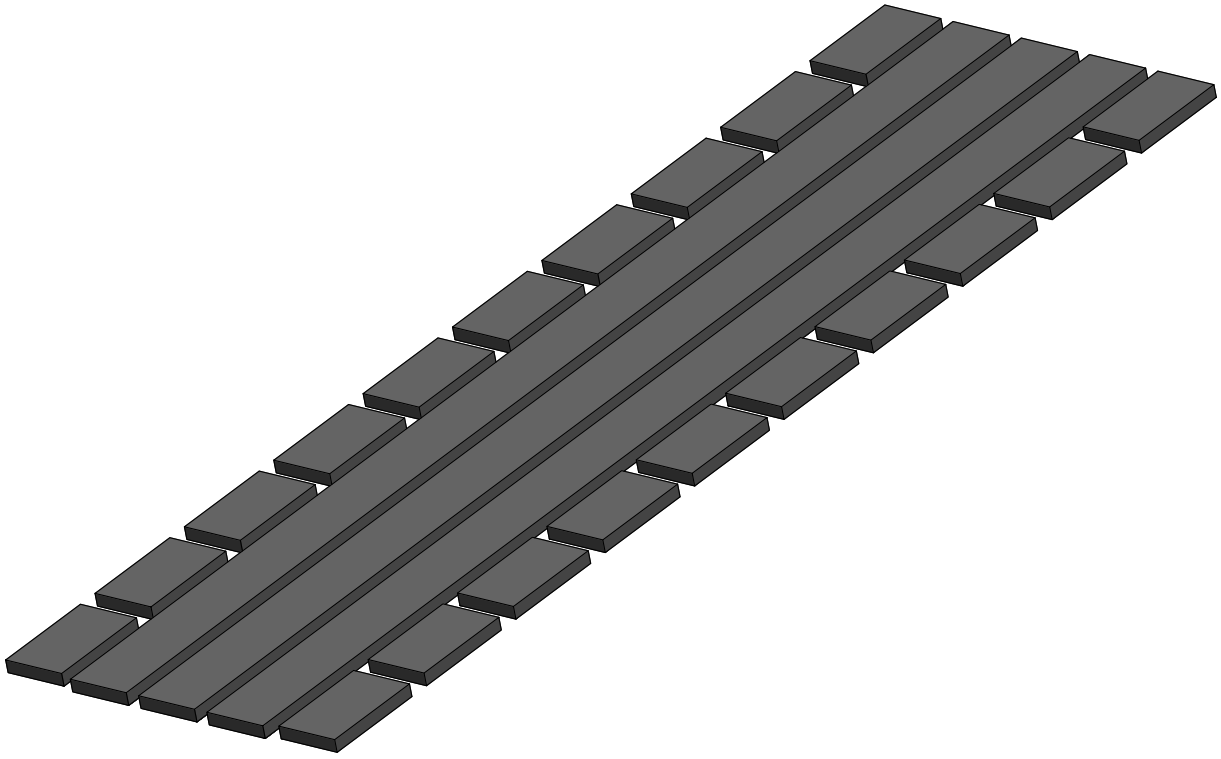

Figure 2.8: A five wire ion trap geometry. The three innermost wires provide a RF trapping potential above the trap. The outer electrodes provide trapping along the axis of the trap

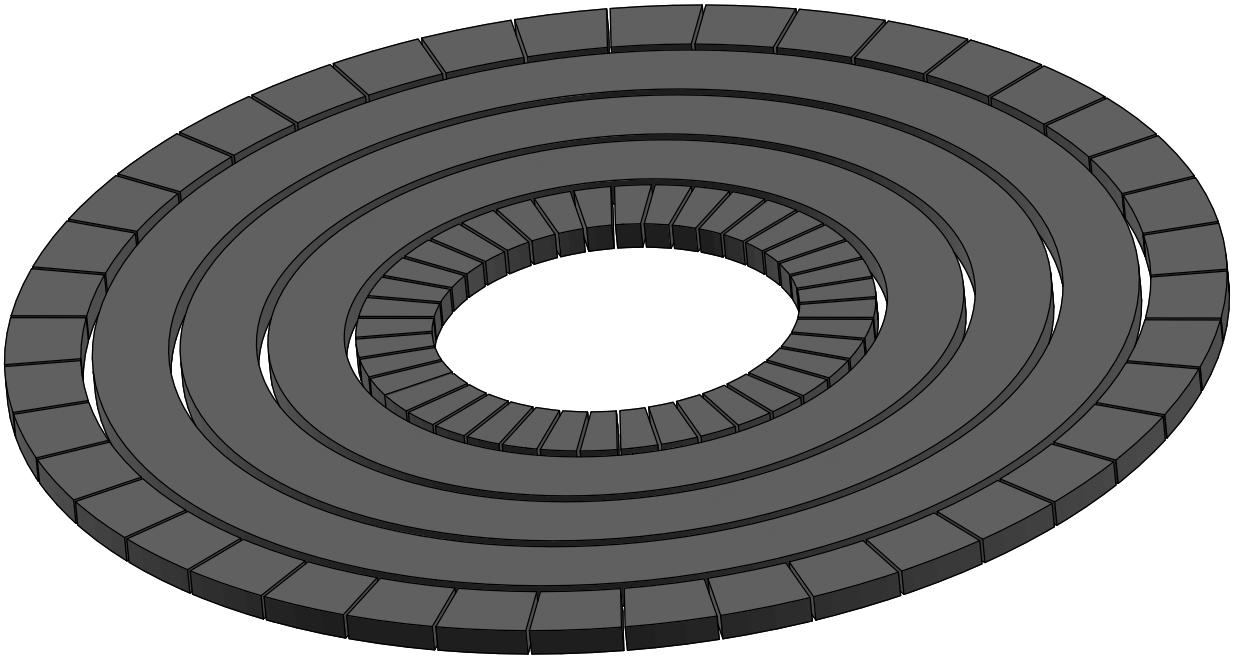

Figure 2.9: CAD rendering of a toroidal surface trap. The three rings will have RF voltages of V,0,V applied to them, and will form a trapping reigon above the surface. On the outside and inside of the three rings are 96 control electrodes which can be used to create a confining potential tangential to the ring

Chapter 3

Method of Fundamental Solutions

This chapter will focus on the main numeric tool used in this thesis to calculate the electric potential of ion traps, the Method of Fundamental Solutions (MFS). While there are many techniques to calculate electric potentials such as the Finite Difference Method (FDM), the Finite Element Method (FEM), and the Boundary Element Method (BEM), in my opinion, the MFS aligns with physical intuition the best out of these methods. In one way, the MFS is nothing but a generalized Method of Images, without the need of knowing the exact locations of where to place charges. Using this intuition we will describe the MFS and demonstrate many of its nice advantages.

3.1 Method of Images

A well known technique in Electrostatics is the Method of Images. It is a technique for satisfying the boundary conditions, by placing charges outside of the domain, and tuning their amplitudes such that they correctly reproduce the boundary conditions. The most basic example of this technique is a positive charge (+q) located a distance z above an infinite grounded electrical plane with a normal to the z direction. We now wish to find a set of charges such that this set together with our original positive charge satisfies the boundary conditions, of which a negative charge (-q) placed at (-z) will satisfy these requirements.

While this method works for this case, and a few others (such as a sphere or a 90 degree corner) it unfortunately does not work for much else. This is due to a high requirement of symmetry in the problem for this to work, and for most problems, they do not have the symmetry necessary. However, if we loosen our requirements of exactly solving the system, to just finding an approximation to the system, then the method of images once again becomes useful.

Let us consider the same problem but we only roughly know where the image charge should go. If we misplace the image charge this would surely go terribly but let us instead distribute N charges, z_i in a circle of radius d, around the proper place for the image charge (0,-z). Now we wish to find the magnitude of each of the charges such that they solve the boundary conditions. We can take N_b points, labeled by x_i, on the boundary where we know the potential we want is negative of the potential due to the positive charge, and set up a linear least squares system to find the appropriate magnitudes, c_i of the charges to satisfy these boundary conditions.

The linear least squares system is shown in Eq 3.1, with the notation $||x_i - z_i||)_2$ being the Euclidean distance between a the points x_i and z_i. For the image charge problem, we let $\psi = 1/r$ and the function f being the potential due to the charge above the grounded plane.

$$\begin{bmatrix} \psi(||x_1 - z_1||_2) & \psi(||x_2 - z_1||_2) & \dots & \psi(||x_n - z_2||_2) \\ \psi(||x_1 - z_1||_2) & \psi(||x_2 - z_2||_2) & \dots & \psi(||x_n - z_2||_2) \\ \vdots & \vdots & \ddots & \vdots \\ \psi(||x_1 - z_n||_2) & \psi(||x_2 - z_n||_2) & \dots & \psi(||x_n - z_n||_2) \end{bmatrix} \begin{bmatrix} c_1 \\ c_2 \\ \vdots \\ c_n \end{bmatrix} = \begin{bmatrix} f(x_1) \\ f(x_2) \\ \vdots \\ f(x_n) \end{bmatrix} \tag{3.1}$$

We can then take the standard image charge problem and discretize it. Let us have 50 boundary points, distributed from -50 to 50 on the x axis and 10 image charge points. The image charge points will be distributed on a circle of radius $d = 0.1$. This configuration is shown in Figure 3.1. Now if we set the values at each of the boundary points to be the value of the charge located above the plane, we have everything to determine the values of our charges. In addition, since we know what the true solution to the problem is, we can test our solution on a 10x finer boundary, to see how well this method worked. Doing so we get an error of 5.7e-11, which is very good. We can also investigate how this method performs as we vary the number of charges. The results are shown in Figure 3.2. We see that nearly for every additional image charge we add, the error decreases by an order of magnitude until about 10. This kind of convergence is exponentially convergent.

We can also perform another test by moving the center of the circle which houses our image charges to $y = -0.95$, which is off of the true location of the image charge by 0.05. The error is shown in Figure 3.3 and we see that the results are not as good, but still reach an error of $1e-8$. This highlights an interesting difference to many methods, in that we can choose where to distribute our image charge points, and this affects our solution. A final test we can do to see this, is distribute our image charges on a circle which does not enclose the true solution, say at (0,-0.7). We can see the results in Figure 3.4, and we see that the results get to $1e-2$ which is much worse

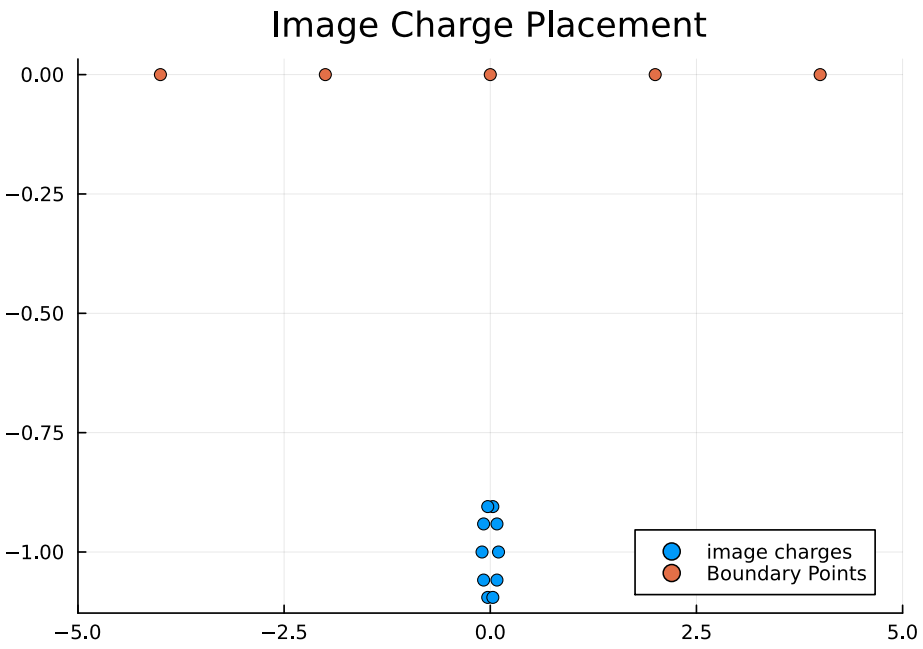

Figure 3.1: Configuration of charges for the standard image charge problem. Note that the image has been cropped and the boundary points go from -50 to 50.

than the previous results. This is to be expected since we have chosen quite a bad choice of image charge locations.

One advantage not yet mentioned is that while we only used the boundary to determine the values of charges, the field everywhere is given by the summation of each charge individually. This is different to the Finite Difference Method or the Finite Element Method, which require an explicit mesh, and only solves for values on that mesh. They typically require a mesh of the domain of space, and for this problem the domain is infinite. In addition, ion traps usually trap ions in a very small volume far away from the electrodes, which presents a difficult in creating the mesh because the region where the ion is trapped will have to have a finer mesh. Since the image charge method only requires a boundary it is referred to as a boundary method. This feature is quite useful for many ion trap designs as they are exterior Laplace problems, and the domain is usually infinite. This eliminates the need to truncate our domain, and eliminates truncation errors.

Overall we can see that through discretizing the method of image charges, and adding more image charges than necessary we could obtain a numeric method that only involves the boundary of our domain, is exponentially convergent, and is simple to program solver for Laplace's equation. These additions to the method of images turn it into the Method of Fundamental Solutions (MFS).

Figure 3.2: The error as we add more image charges, with the image charges being distributed on a circle of radius .1 around (0,-1)

3.2 Method of Fundamental Solutions

Let us consider a Dirichlet Boundary Value Problem for Laplace's equation

$$\nabla^2\phi(x) = 0, x\epsilon\Omega \tag{3.2}$$

$$\phi(x) = g(x), x\epsilon\Gamma \tag{3.3}$$

With a domain, Ω, and the boundary of the domain is, Γ. If we want to solve this problem then we must solve both equations, eq 3.2 and eq 3.3. If we want to solve eq 3.2, then a simple approach would be to just use functions that already solve the equation. The simplest thing would be to use the Fundamental Solutions of Laplace's Equation

$$G(r, r') = ln(||r - r'||_2) \tag{3.4}$$

in 2D, and

$$G(r, r') = 1/(||r - r'||_2) \tag{3.5}$$

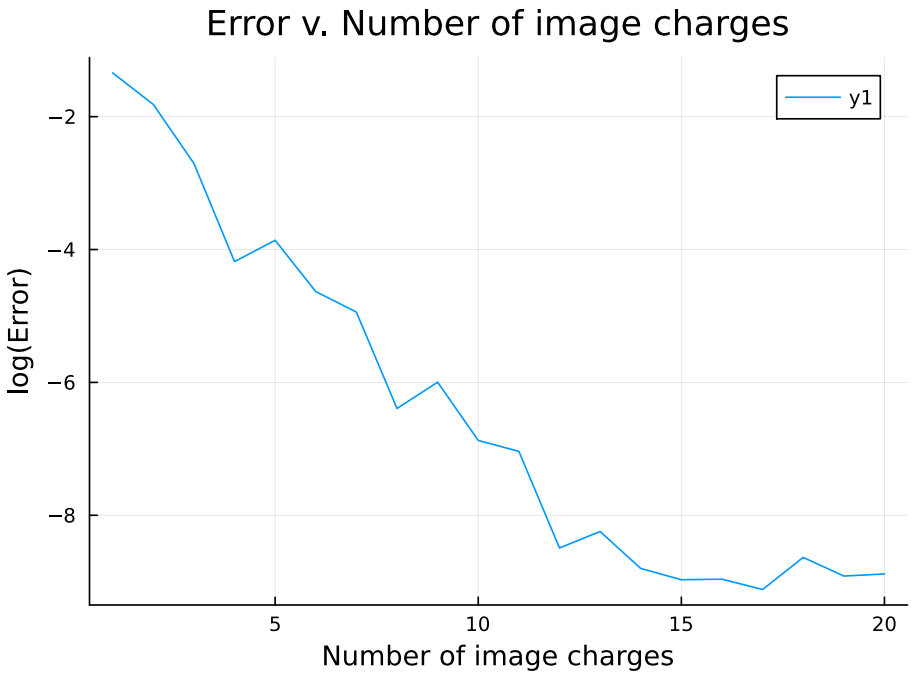

Figure 3.3: The error as we add more image charges, with the image charges being distributed on a circle of radius .1 around (0,-0.95)

in 3D, where $||\cdot||_2$ indicates the L^2 norm or Euclidean Distance. Since all of these functions satisfy Laplace's equations, then a linear combination of them can be used to satisfy boundary conditions. Thus we can write an approximate solution $\hat{\phi}$ as

$$\hat{\phi}(x) = \sum_{i=1}^{N} c_i G(x, x_i) \tag{3.6}$$

where y_i are the locations of each Fundamental solutions and

One of the best things about the Method of Fundamental Solutions is that there are many fundamental solutions to choose from. This allows the user to custom tailor their fundamental solutions to the problem at hand, and include symmetries in the fundamental solutions. Likewise, by changing the fundamental solution from one of Laplace's equation to one of the Helmholtz equation, the PDE being solved can easily be changed. For example, if one is dealing with a domain that has axial symmetry then a Fundamental solution that has that symmetry can be used to reduce the dimension of the problem by 1. An example of a Fundamental solution with this symmetry is the potential, due to a ring of charge of radius, R, lying on the xy plane, at a distance r from the symmetric axis and a height of z,

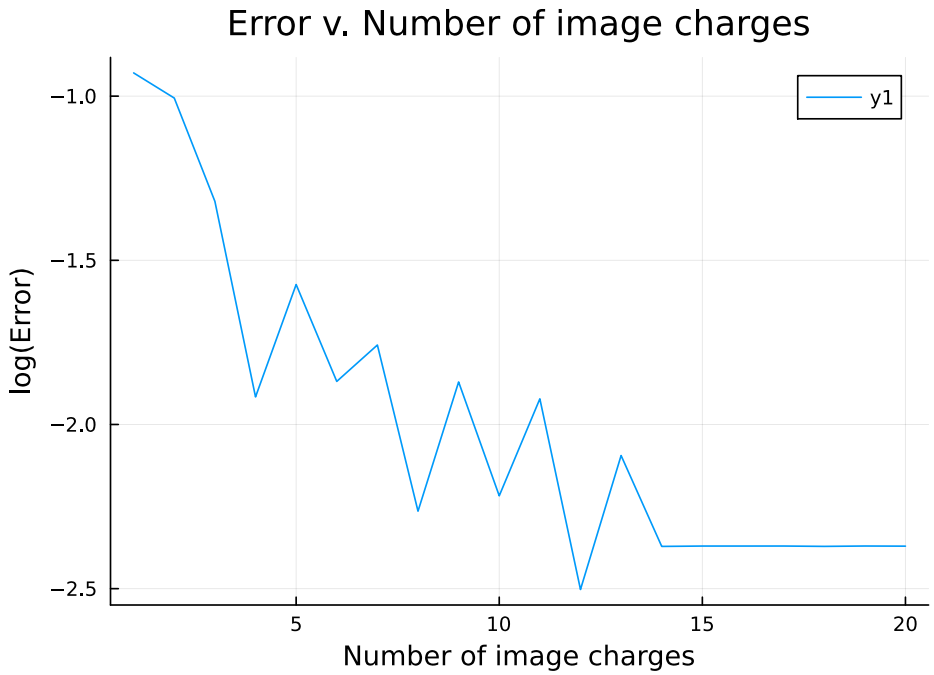

Figure 3.4: The error as we add more image charges, with the image charges being distributed on a circle of radius .1 around (0,-0.7)

$$V_{ring} = \frac{Q}{4\pi\epsilon}\frac{1}{2\pi}\frac{K(k)}{\sqrt{q}} \tag{3.8}$$

with K being a complete Elliptic integral of the 1st Kind, and

$$q = r^2 + R^2 + a^2 + 2rR$$

$$k = \sqrt{\frac{4rR}{q}}$$

A plot of the potential for a ring of radius 1 is shown in Figure 3.5. One can see that such a potential is not symmetric inside and outside of the ring, which is to be expected, and we can note that the potential is higher inside of the ring than outside of the ring. While this asymmetry is not a fundamental problem, we will see later on that this asymmetry causes many difficulties in our intuitive understanding of ion traps which have this kind of symmetry.

Another possibility is given by the fact that a summation of fundamental solutions is itself a fundamental solution. So if the domain repeats itself linearly 5 times then we can mimic this behavior by summing up fundamental solutions that have the same behavior, for example in 2d

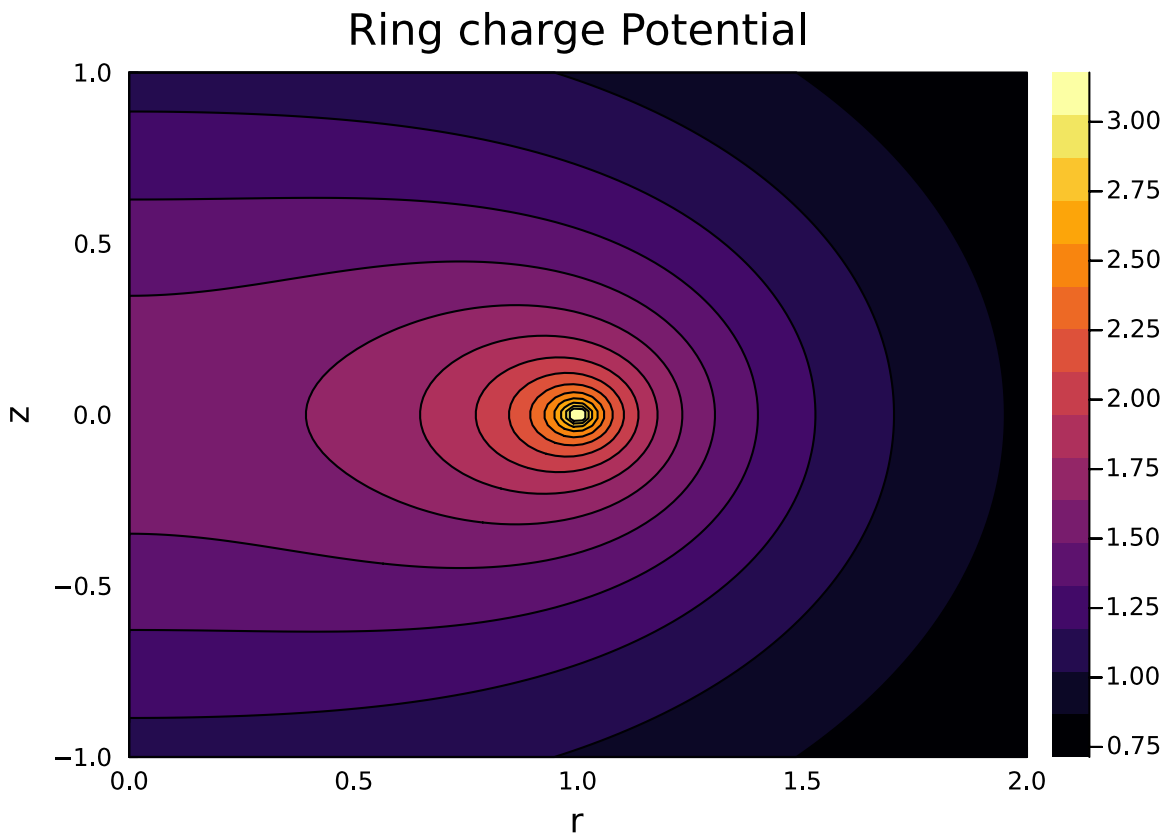

Figure 3.5: Potential due to a ring of charge with radius 1

$$\phi(x) = \sum_{i=0}^{5} log(||r - (r - i * d_i)||_2)$$

where d would be like a lattice spacing constant form solid state physics. This fundamental solution can capture the a domain repetition type effect rather simply. In addition, this can deal with unequal domain repetitions or even radial domain repetitions in a very similar manner. Doing so reduces the size of the linear system we solve, by replacing many charges with a more complicated fundamental solution. Since inverting a matrix has a time complexity of $\mathcal{O}(n^3)$, reducing the number of image charges by a factor of five would reduce the computation time by 125 times.

Lastly we can talk about some of the finer details of the Fundamental solution in 2d, $ln(r)$, which would represent a line of charge. Such a solution appears simple at first but there are many subtle difficulties. To start, we can note that $ln(1) = 0$ which can cause a problem if we were to distribute our fundamental solutions on a circle of radius 1. In this case, the point at the center of the circle will always be 0 since it is always a distance of 1 away from every point, thus if the

potential we want to find is not 0 at the origin, then this choice of fundamental solutions cannot get the correct answer. Another thing to note is that $ln(\infty) \neq 0$, which is a problem if we are solving an exterior Laplace equation which requires that the field goes to 0 at infinity. In this case we can truncate the domain by a circle and force that the potential on that circle to go to 0. Note that this is not the case when using the 3d Fundamental Solution or when using a ring charge as the solution, as those automatically satisfy the boundary condition at infinity.

3.2.2 Ill Conditioning

The MFS produces dense matrices due to the global support of the fundamental solution (it does not go to 0 after a certain point). In addition, since the charge points must lie on a fictitious boundary far away from the real boundary, the matrices produced are not diagonally dominant. These facts lead to the condition number of the MFS being around 1e17 or higher. Despite this condition number, when the matricies are solved using standard gaussian elimination, and the error is checked on the boundary, good results are obtained. This has led to Drombosky et al [10] proposing an alternate definition of the condition number called, the effective condition number, which for the equation

$$Ax = b \tag{3.9}$$

takes the form of

$$\kappa_{eff} = \frac{||b||}{\sigma_m ||x||} \tag{3.10}$$

with σ_m being the smallest singular value of the matrix A. The standard condition number is given by the ratio of the largest to smallest singular value of the matrix A.

$$\kappa = \frac{\sigma_1}{\sigma_m} \tag{3.11}$$

From this we can see that the difference between the effective condition number and normal condition number is

$$\eta = \sigma_1 \frac{||x||}{||b||} \tag{3.12}$$

Essentially, while the matrix is ill-conditioned the values of the rhs matter. If the norm of the boundary conditions is small then the system behaves much better than the original condition

number would predict. So while the condition number appears very large, if solved using standard gaussian elimination then the answers obtained can be very good. However, this does present a problem, in that iterative solvers do not work well with the MFS, since they require that the matrix is not ill-conditioned. So there is some care necessary when solving a MFS problem.

3.2.3 Harmonic Boundary Conditions

One special case to note for MFS is that when our boundary conditions are harmonic, i.e. the boundary conditions also satisfy Laplace's equation. This is often used because the error within the domain can then be evaluated. However, this has historically lead to some confusion about placement of source points. When working with a harmonic function often one sees that the error becomes better as the points are placed further away from the boundary. However, this is due to the fact that when the sources are placed far away they approximate the harmonic polynomials, as shown by Schaback [33]. In this way there is no surprise that the solution becomes better, because the harmonic polynomials are able to represent any harmonic function. However, in the case of non-harmonic boundary conditions, the advise of placing charge points far away from the boundary breaks down. In these cases the best place to put charge points is unknown, which is one of the most criticized parts of the MFS.

Many papers have tried ways to solve this issue and some methods are

1. To place the fictitious boundary based on the normals of the real boundary and then to adjust how far away it is using a method such a cross validation [7].

2. Greedy methods, where you place each charge one by one, and place them such that the new charges expand the approximation space [33].

3. Perform a conformal transformation mapping the exterior of the desired shape onto the exterior of the unit circle [24].

In general, finding the optimal fictitious boundary is a main challenge in the MFS. While there are methods that do not need this fictitious boundary such as the Singular Boundary Method [15], and the Boundary Knot Method [8], in my own experience I have found the standard MFS to be more accurate once a good fictitious boundary is located. Luckily in the case of ion traps, there are only a few simple objects, such as sphere, rings, and rectangles which build up most of the trap. Once a suitable fictitious boundary is found for each of these, then any trap made of these is easy to simulate.

3.2.4 Singularities

Another issue is that of geometric singularities, when the boundary data is not continuous. This happens mainly at something like a corner, where the first derivative is not continuous. We also know from Classical Electricity and Magnetism [23] that around the corner we have a solution of the form

$$V(\rho, \phi) = \rho^{\frac{\pi}{\beta}} sin(\pi\phi/\beta) \tag{3.13}$$

where β is the the angle of the corner. This equation only represents the first term in an infinite series. In the case that there is only one corner, then we can note that this is a solution to Laplace's equation and we can simply add this basis function to the MFS. This has shown good results with the Motz problem [28].

This idea of adding solutions to deal with singularities has also been explored in [3], where they aimed to solve problems that feature a jump discontinuity. They added basis functions which capture this feature and were able to obtain good results as well.

In both of the previous cases, they knew what the form of solution would be and thus could easily add it to the basis set. However, the situation is much harder in three dimensions, for example the electostatic capacitance of a cube has no analytic solution [22]. This means that finding a suitable fictitious boundary in three dimensions is difficult, and this thesis will make heavy use of ring charges to reduce axially symmetric three dimensional boundaries into two dimensional boundaries. For problems without axial symmetry, many shapes such as cubical electrodes will be approximated by spheres.

Chapter 4

Simulating Ion Trap Potentials

Despite the challenges of the MFS with ill-conditioning, the fictitious boundary, and difficulty in domains with sharp geometric features, it is still able to simulated the potential of many common ion trap configurations quite well. This chapter will focus on simulating ion traps that are two dimensional as well as three dimensional, in a variety of configurations, such as hyperbolic ion traps, four rod ion traps, surface traps, as well as the toroidal versions of all of these.

4.1 2D Traps / Mass Spectrometers

To start we can focus on traps that live in two dimensions, or likewise mass spectrometers which only trap in two of the three dimensions of space. The fundamental solution to Laplace's equation in 2d is $\ln(r)$ which represents an infinite line of charge in 3d.

4.1.1 Hyperbolic Linear Mass Spectrometer

As discussed in Chapter 2, the ideal ion trap potential is a quadrupole potential. If we want to create a perfect quadrupole potential then we can do so easily by the uniqueness principle. If we have four hyperbolic curves arranged in a "+" pattern as shown in Figure 4.1, and if the top and bottom follow the +V isocontour line of the quadrupole potential, and the left and right ones follow a -V isocontour line, then the overall potential must be a quadrupole potential, since a quadrupole potential satisfies the boundary conditions.

If we use the fundamental solution of an infinite line of charge $G(r, r') = ln(||r - r'||_2)$ then this 2d potential is infinite along the z axis. We can the place our source points along the same hyperbola as the boundary points but shifted away by .4. The configuration of points is shown

in Figure 4.1. We can note that this configuration of charge points does not extend to infinity as required by hyperbolas, however, it extends far enough that it is reasonable to assume that this truncation of the domain does not effect our answer to much.

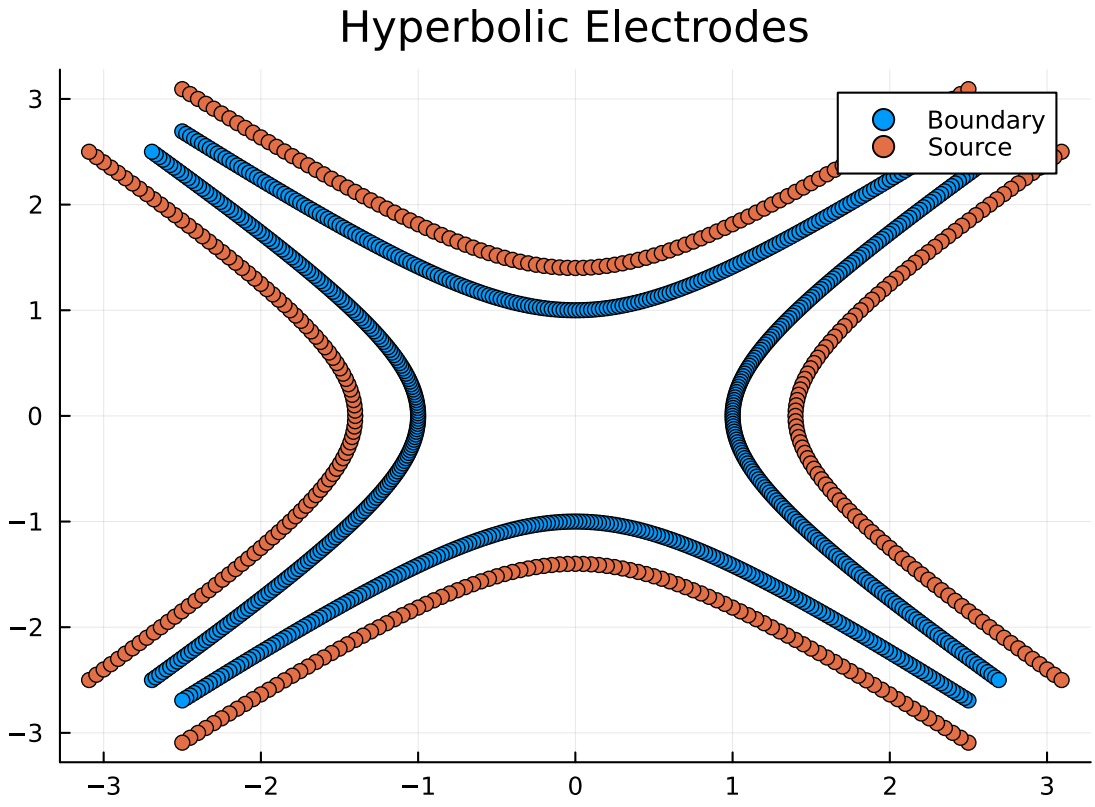

Figure 4.1: Configuration for a Hyperbolic mass spectrometer

If we distribute 804 points on the boundary and 404 source points on a fictitious boundary which is higher than the real boundary by .4, then we obtain an absolute error of 8.57e-14 as measured on a 10x finer grid of the boundary. In this case we can compare our answer to the analytic answer of

$$V(x, y) = x^2 - y^2$$

We can check this on a grid from -1 to 1 with a spacing of .01 in both the x and y directions. From this analysis we get an error of 2.20e-14. This gives us more confidence in the fact that the MFS has its maximum error on the boundary as we see that the error in the domain is less than

the error on the boundary. We can also confirm that truncating our electrodes as we did had little physical effect on the potential. We match the potential nearly to machine precision so the effect of truncation is minimal.

4.1.2 Four Rod Mass Spectrometer

Another common configuration for an ion trap is a four rod linear ion trap. This consists of approximating the hard to machine hyperbolic electrodes by cylinders. For the hyperbolic case, the hyperbola created a closed domain asymptotically. Because of this, infinity was not a part of the domain and the fundamental solution $log(r)$ was fine to use, despite it going to infinity at infinity, as confirmed by comparing our answer to an analytic answer. However, for this trap it is clear that this is a multiply connected exterior domain problem and thus infinity is included in our domain. So the fundamental solution $log(r)$ does not capture the boundary condition at infinity. While we can modify our fundamental solution to one that does have this behavior [34]

$$ln(z - \xi) - ln(z) \tag{4.1}$$

where z is the field point, and ξ is the location our source point, in my testing I found that this fundamental solution does not work with some of the methods presented later, such as clustering points near a corner. Another approach we can take is to truncate our domain by making an outer casing at a fixed radius, R, which is set to 0 Volts. Since ion traps are usually mounted in a vacuum chamber, this approximation is realistic to the experiment.

We can now set up a simulation of 4 rods uniformly placed on a circle of radius R=2 and with each of the rods having a radius r=1. The top and bottom electrodes are set to be +1V and the left and right are set to be -1V, with each being represented by 50 points. In addition we have a circle of radius 10 which we set to be 0V, represented by 100 points. Now we must place our charges and their magnitude until the boundary conditions are met. 30 sources will be place in each electrode with a radius of .4, and 80 sources will be placed on a circle of radius 12. The configuration of source points is shown in Figure 4.2 and potential create by this configuration are shown in Figure 4.3. The time of this simulation is 2.579 ms and the error, is 1e-7, determined by sampling on a boundary which had twice as many points as the original boundary.

From a quick view it appears that this potential does quite well to approximate a quadrupole potential. Later on in this thesis a harmonic analyses will be performed to fully quantify how close this trap is to the hyperbolic trap. However, one thing we can do is compare this result with

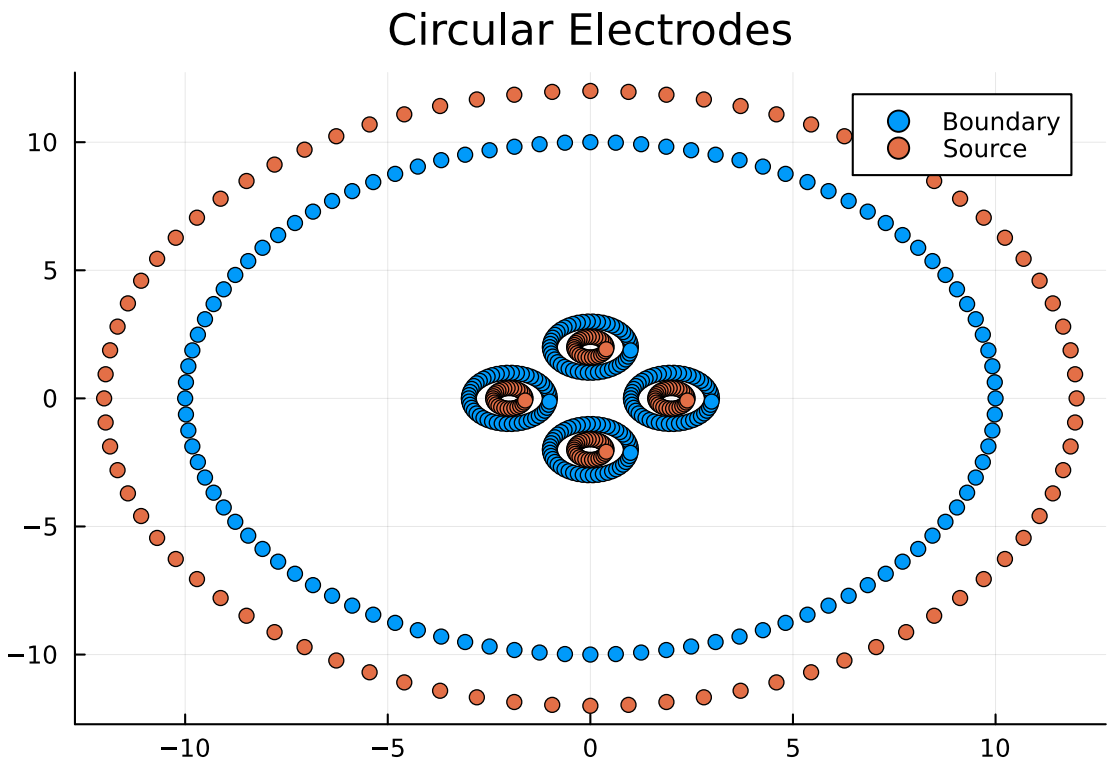

Figure 4.2: Configuration of points for a 4 rod mass spectrometer

another set of voltages. A common case of this is applying RF to only two of the electrodes, say the top and bottom, and keeping the other electrodes at ground or at a DC voltage. This is an easier experimental set up as the RF and DC voltages do not need to be mixed. We can simulate this trap, with the only change being that the top and bottom electrodes are at +2V and the left and right are held at 0V, the difference between this field and the symmetric case is shown in Figure 4.4

While one might expect these two potentials to be identical because the voltage difference in each case is the same, we must take into consideration our boundary condition at infinity. Since the boundary condition at infinity is that the field goes to 0, this fact introduces the difference between the two fields. While this effect is small in this case, only being a difference of .005 or only .5 % of the total field's amplitude, we will that later on a similar case with toroidal traps in which a far off boundary condition has a noticeable effect. Another thing to point out is that this error is much bigger than our error bars, and while it might be dismissed in a method that only asks for a few percent error, it must be considered here. However, since the MFS converges exponentially for many simple shapes, this precision is not at any significant cost.

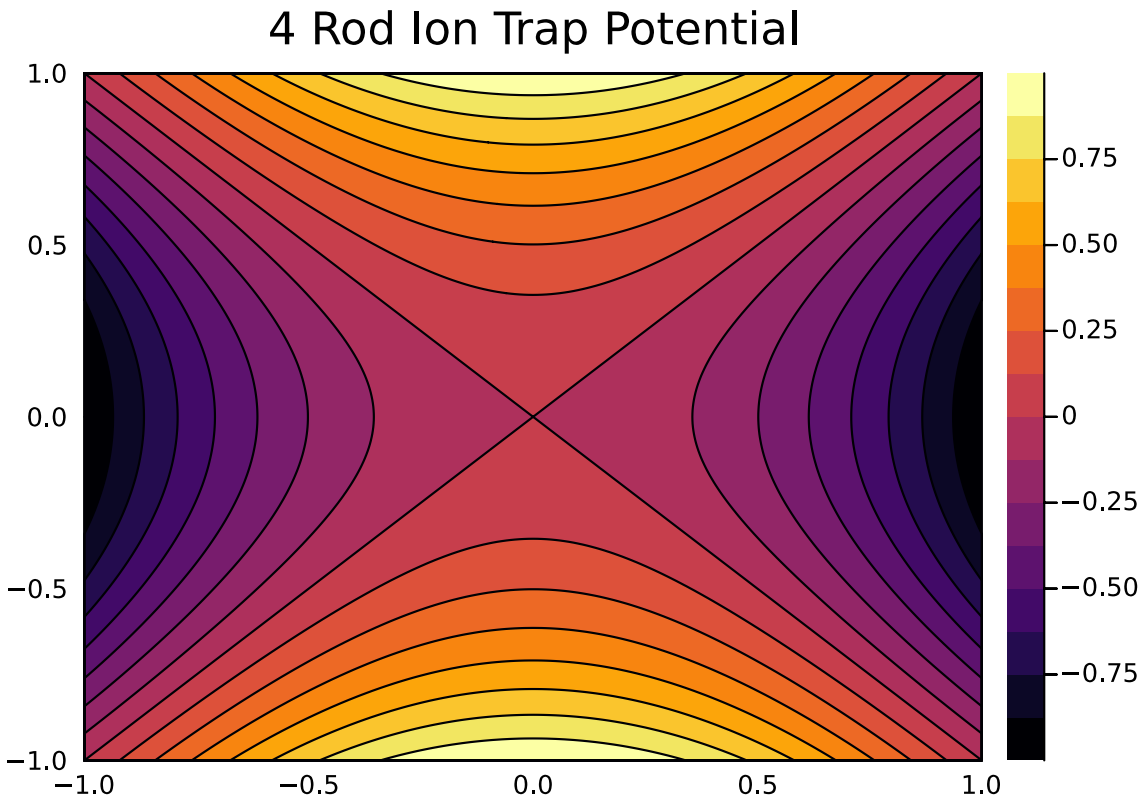

Figure 4.3: Simulated Potential of a 4 rod mass spectrometer

5 wire surface ion trap

Another trap which we can simulate is a surface ion trap. However, such a trap has a few potential problems. One being that surface traps have sharp corners which require us to place our source points carefully. In addition, the method does not do well with thin structures. We can solve the first problem by clustering points around the corners in the way as [29]. For the second problem we can see if making the electrodes full sized, having a square dimension, has a considerable effect by comparing our solution to the analytically solved field of a gapless surface ion trap.

Liu et al [29] shows a method to solve for the field when near a corner using the MFS. They first take their boundary and split it up into Ns equal segments. Then the two segements closest to the corners are split into thirds, this is then repeated recursively NSplitTimes. Then on each segment, Nb, points are placed in a Chebyskev manner. These points are the boundary points. To place the source points, we go back a step and place Nz, points on each segment in a Chebyskev manner, and then every segment is moved along the normal based on the size of the segment. This means that

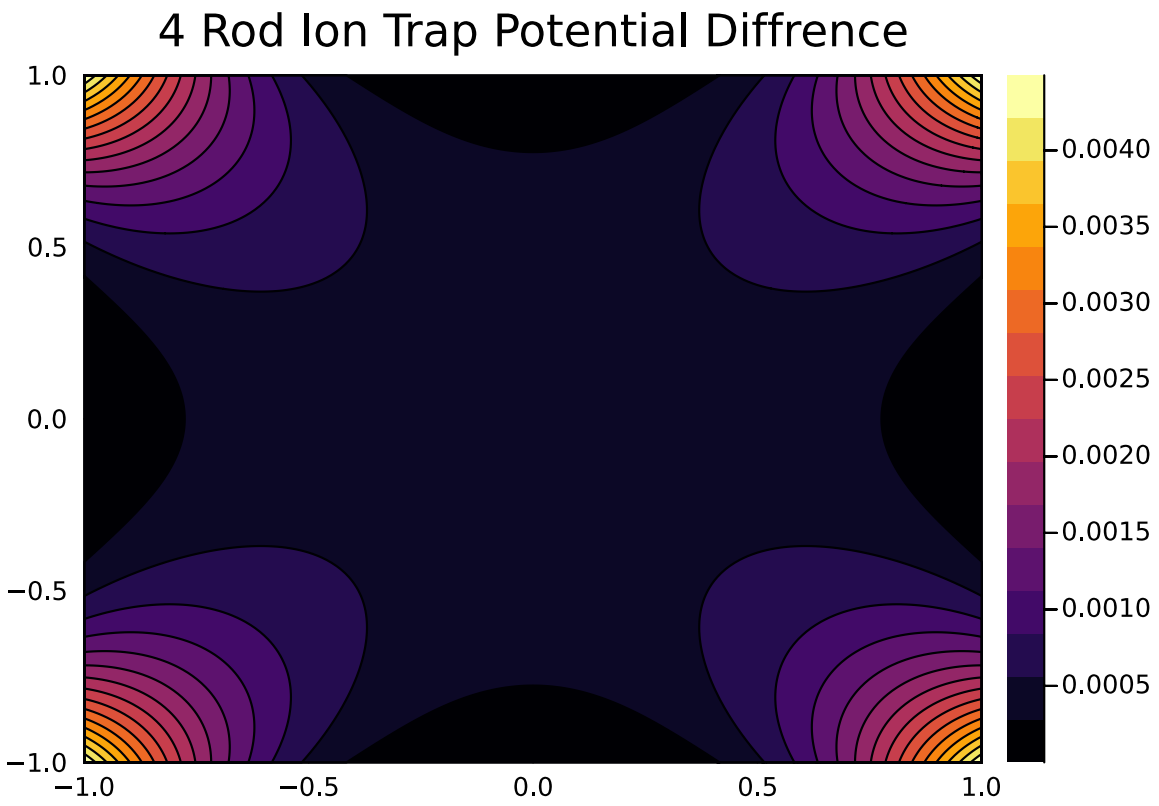

Figure 4.4: Difference between the four rod trap with symmetrically applied RF voltages of +V on the horizontal electrodes and -V on the vertical electrodes, and a trap that have +2V applied to the horizontal

as the segments get smaller they will will cluster towards the corners. A plot of the configuration for boundary points and charge points for a single square is shown in Figure 4.5, additionally the plot for a five wire trap is shown in Figure 4.6, where a circle bounding the domain of radius 40 is not shown, but is included in the simulation.

Now for a surface trap it is normal for the electrodes left and right of the middle electrode to be set to the same voltage, in this case they are set to +1V. Assigning these voltages and looking at the potential right above the trap, is shown in Figure 4.7. The absolute error for this simulation is 0.0001. The main region of interest to look at here is around (0,3), as shown in Figure 4.8 where one can see a highly distorted quadrupole, the left and right are positive and the up and down would be negative. From this we can see that surface traps do not have nearly as clean a potential as 3d ion traps do.

Luckily in the case of this trap there is an analytic solution if the gaps between electrodes are

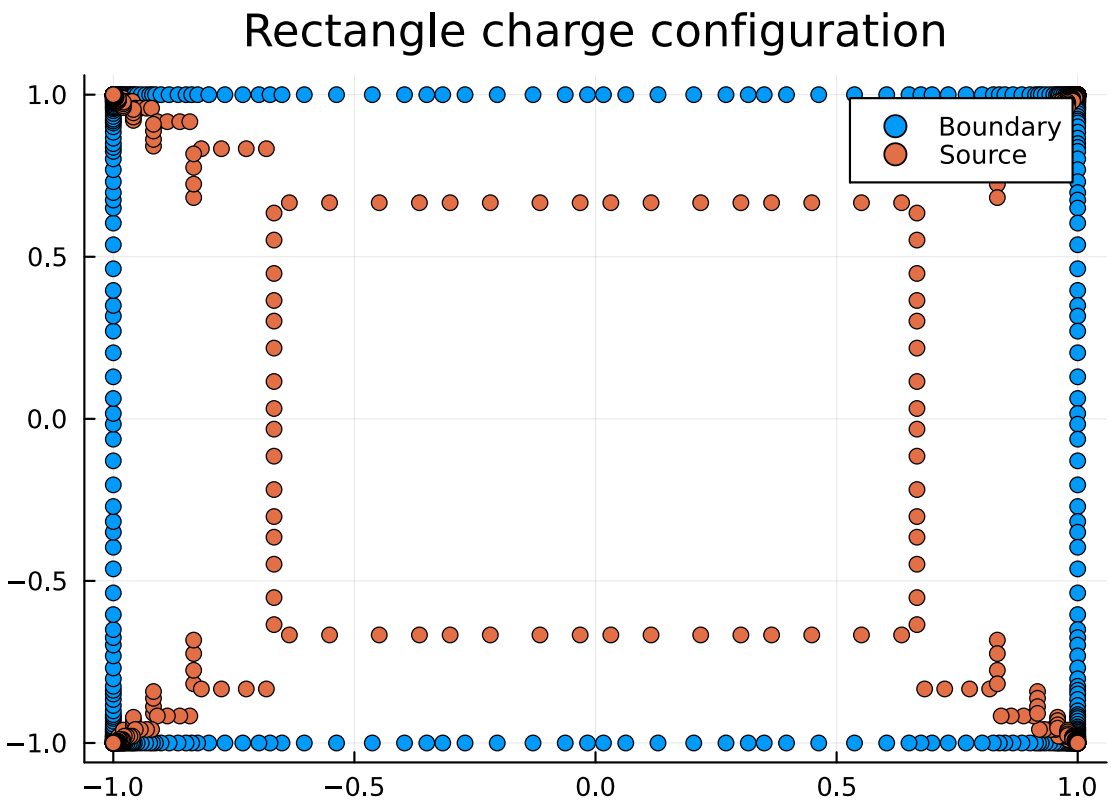

Figure 4.5: Clustering of charge points for a rectangle with sharp corners

assumed to go to 0, and if the ground plane of the trap extends to infinity, this reduces the problem to be two dimensional. The solution for a potential which is 1 over some region of a horizontal line and is 0 over the rest, all the way to infinity is given by,

$$\Psi_0(x_1, x_2) = \frac{1}{\pi}(\arctan\frac{a - x_1}{A - x_2} - \arctan\frac{b - x_1}{A - x_2}) \tag{4.2}$$

where x_1 and x_2 are the x and y coordinates, a and b are the positions of the edges of where the potential is 1, and A is the y coordinate of the line. This is the form as written in mathematical fields such as the Boundary Element Method. We can cast it into a more normal ion trap notation by setting the length of the middle electrode to be a, the length of the two outside electrodes to be b. Then we can write the analytic expression for the 5 wire trap as

$$\Psi(x, y) = \frac{V}{\pi}(\arctan\frac{a/2 + b - x}{y} - \arctan\frac{a/2 - x}{y} - \arctan\frac{a/2 + x}{y} + \arctan\frac{a/2 + c + x}{y}) \tag{4.3}$$

which is the expression appearing in [21] just shifted over so it is symmetric about the y=0 axis.

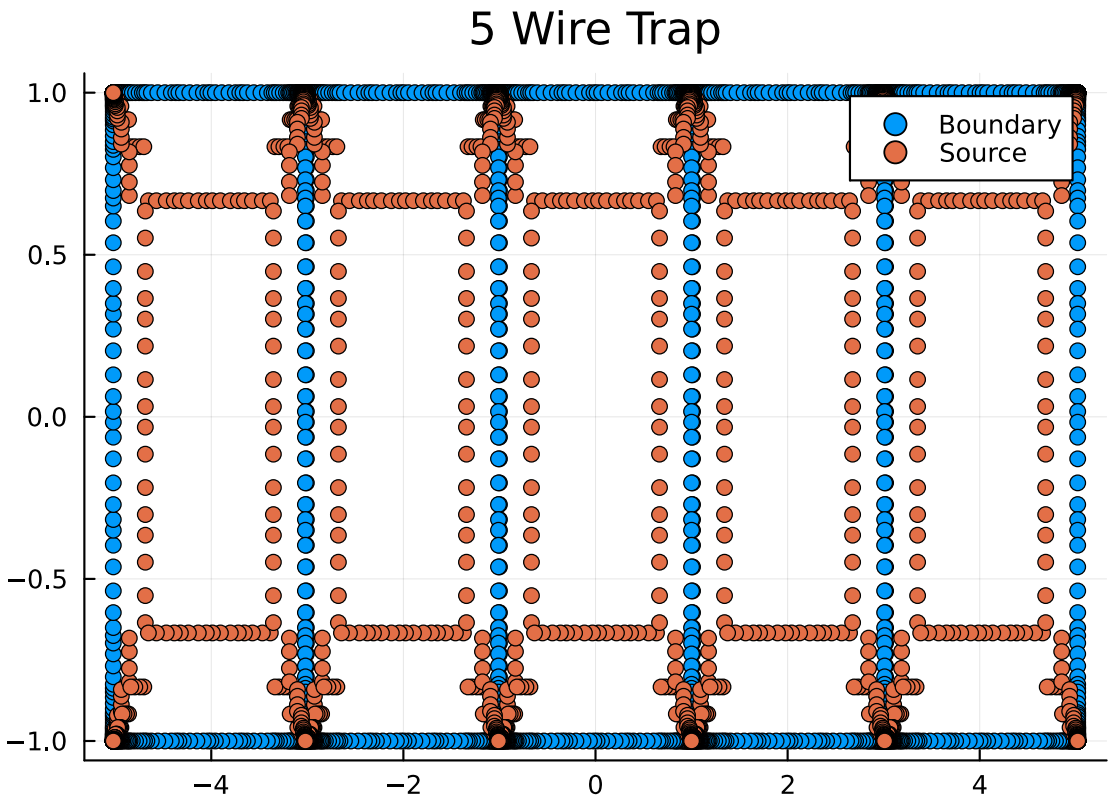

Figure 4.6: Configuration of points for a 5 wire surface trap, with a gap between each electrode of 0.01

Now using this analytic expression we can plot the potential as shown in Figure 4.9.

We can see the difference between the simulated and analytic potential in Figure 4.10. We see nearly no difference on most of the surface, except for a small peak around the location of the gaps. This will obviously not be correct as the analytic assumes there are no gaps but our simulation includes gaps of size 0.01. We see that these gaps only slightly effect the potential. The other difference we can see is that the difference between the two almost looks like the same shape but shifted upwards. This is due to our approximation that the ground plane was not infinite. Overall we can see a difference around .5 % around the trapping region.

5 wire conformal surface ion trap

Clustering points to the corners ends up requiring many more points than for simple shapes that do not have corners, in the previous case around 1000 points were needed for 1e-3 error. To get around this we can find an approximation to a square, however just rounding the corners does not

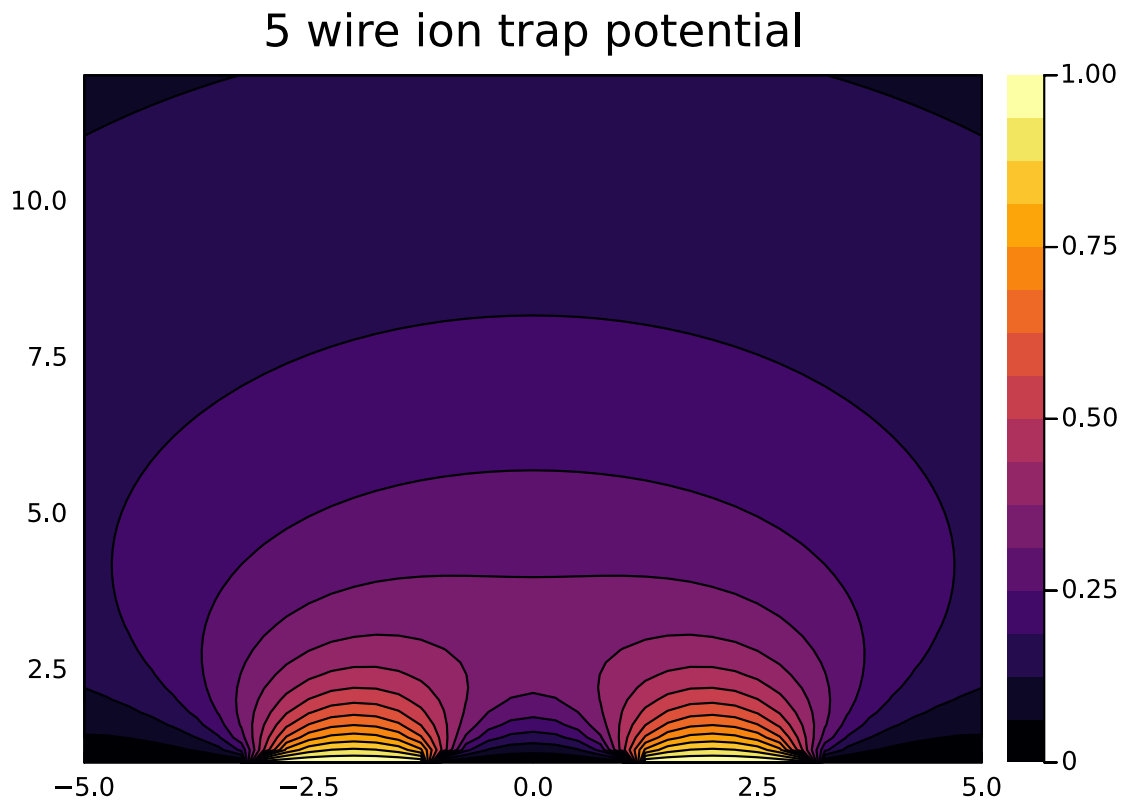

Figure 4.7: Potential of a 5 wire ion trap

provide good results. This is due to the fact that rounding the corners might change the fictitious boundary in a nontrivial way. One solution to this is that we can find a transformation that takes a shape like a circle, where we know the fictitious boundary, to another shape. The solution we can employ is a conformal transformation which takes the exterior of a circle to the exterior of a rounded cube [24] as shown in Eq 4.4.

$$F(w) = a(\frac{1125}{1024}w - \frac{203}{2048}w^{-3} + \frac{1}{2048}w^{-7}) \tag{4.4}$$

The result of this transformation applied to a circle of radius $a = 1$, and a fictitious boundary of a circle of radius .75 is shown in Fig 4.11. We can see that the fictitious boundary is nontrivially changed and near the rounded corners as there is a clustering of charges around the corners.

This gives results as good as a circle, and with only tens of points we can get errors around 1e-10. While the rounding of corners does deviate significantly from the sharp corners, we expect our ion to be far enough away from the corners, that the rounding of the corners does not dramatically change the results. This approximation is not necessary in the 2d case as shown with clustering,

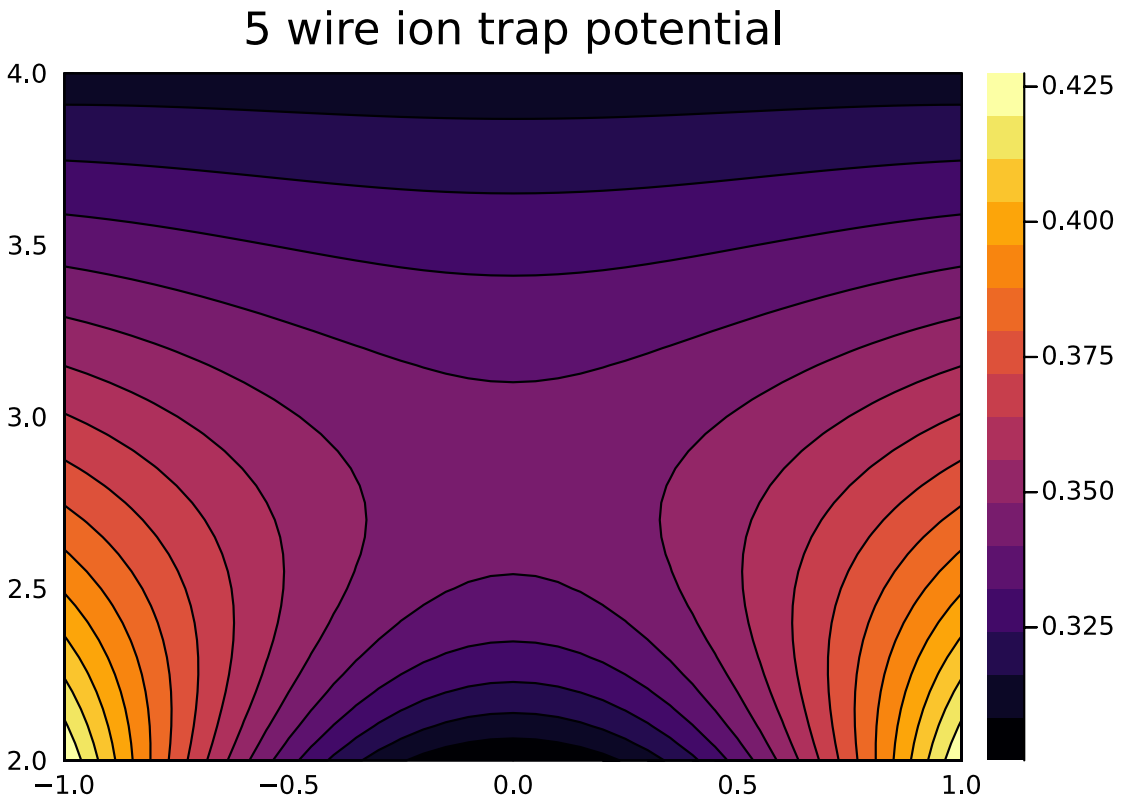

Figure 4.8: Zoomed in potential of a 5 wire ion trap

but in the 3d case it is extremely valuable as will be shown later. We can then plot the difference between this potential and the simulated potential with sharp corners in Figure 4.12

From this we can see that the effects of rounding the corners are only meaningful around the corners. Near the region where the ion will be the difference is around 1e-6 and thus we can say that the effects of rounding the corners is small.

4.1.3 Conclusion to 2D Traps

For these potentials which have a translational symmetry along the z axis, making most of them mass spectrometers instead of traps, we can simulate most geometries. Multiply connected domains, and domains with corners can be simulated quite well in a short amount of time. In particular, these techniques are very easy to program, and by having the maximum principle the error on the boundary can be checked easily as well. This allows one to be fully sure of results, such as the case in Fig 4.4, which showed the difference between the vertical electrodes being held at +1V and horizontal being held at -1V compared to the vertical being held at +2V and the horizontal being

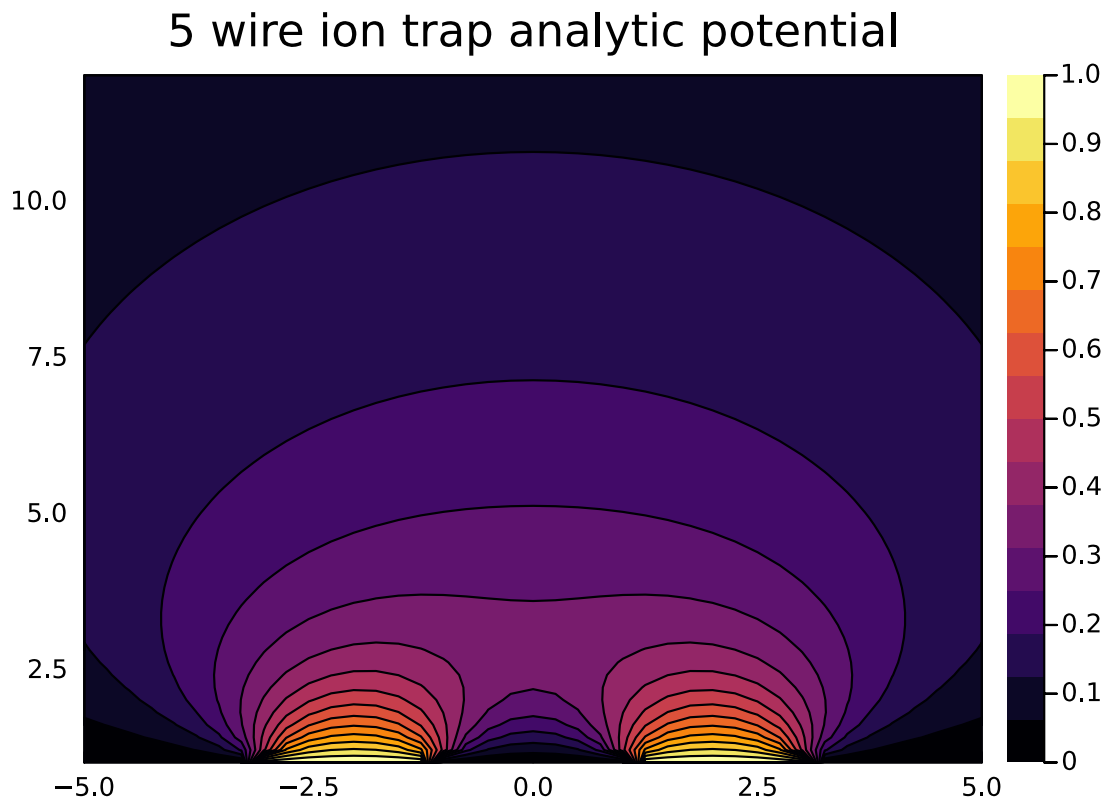

Figure 4.9: Analytic Potential of a 5 wire ion trap

held at 0V. Because we have the precision to measure such a difference, and because we are able to check every fact of the simulation due to its short size, we can be sure of our answers.

4.2 3D Traps

We can now turn our focus onto traps which trap ions in three dimensions. For shapes that do not have any symmetries we can use a point charge $1/r$ and for shapes which have symmetry about a axis of revolution we can use the fundamental solution of a ring of charge. Unlike the fundamental solution in two dimensions, both of these fundamental solutions decay to 0 at infinity, and thus do not need an outer cover to truncate the domain.

4.2.1 3D Toroidal Hyperbolic Trap

This trap is a revolved version of the hyperbolic ion trap. Meaning that we revolve our hyperbolic geometry a distance, D, about the axis of revolution. The result of this rotation is that our trapping

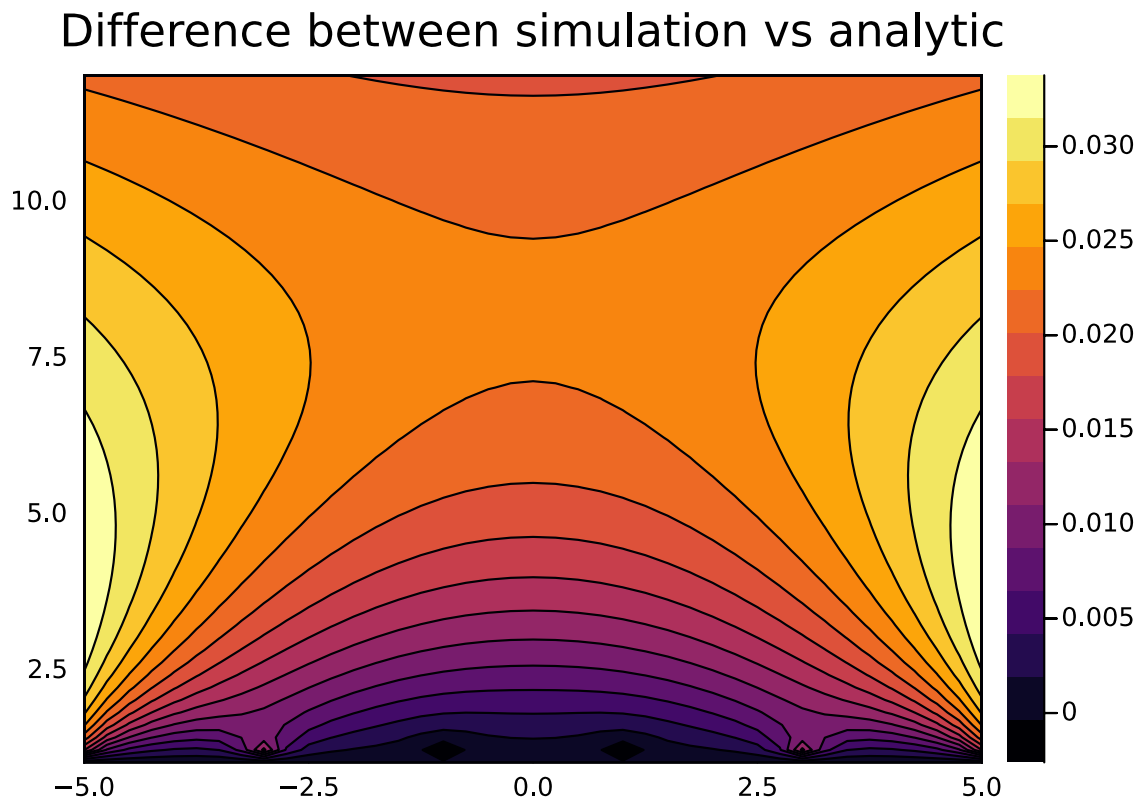

Figure 4.10: Difference between analytic and simulated potentials

region is not a single point in 3d but forms a ring in 3d. If we revolve our shape a distance of 5 from the central axis, we can see the potential in Figure 4.13.

We do see a significant problem from this trap configuration, which is that the potential does not look like a perfect quarupole anymore. To start, the center of the trap does not coincide with the geometric center of the trap, and appears to be shifted about .1 to .2 away. We can also notice that the potential is not symmetric about this new center. These effects can be explained by looking at the fundamental solution of a geometry with axial symmetry, a ring charge as previously shown in Figure 3.5. We noticed previously that the potential was not symmetric on the left and right of the ring, and now if we create a potential using many of these asymmetric potentials, in a symmetric fashion we would expect to have an asymmetric potential overall. In this way the curvature of the trap plays a big part in what the potential looks like.

Some of the earliest traps which featured a similar toroidal geometry were RF storage rings [40, 9], however, they focused on making the curvature of the trap big enough that there would be no effects of the curvature. Recently, mass spectrometers [26] have started focusing on this trap

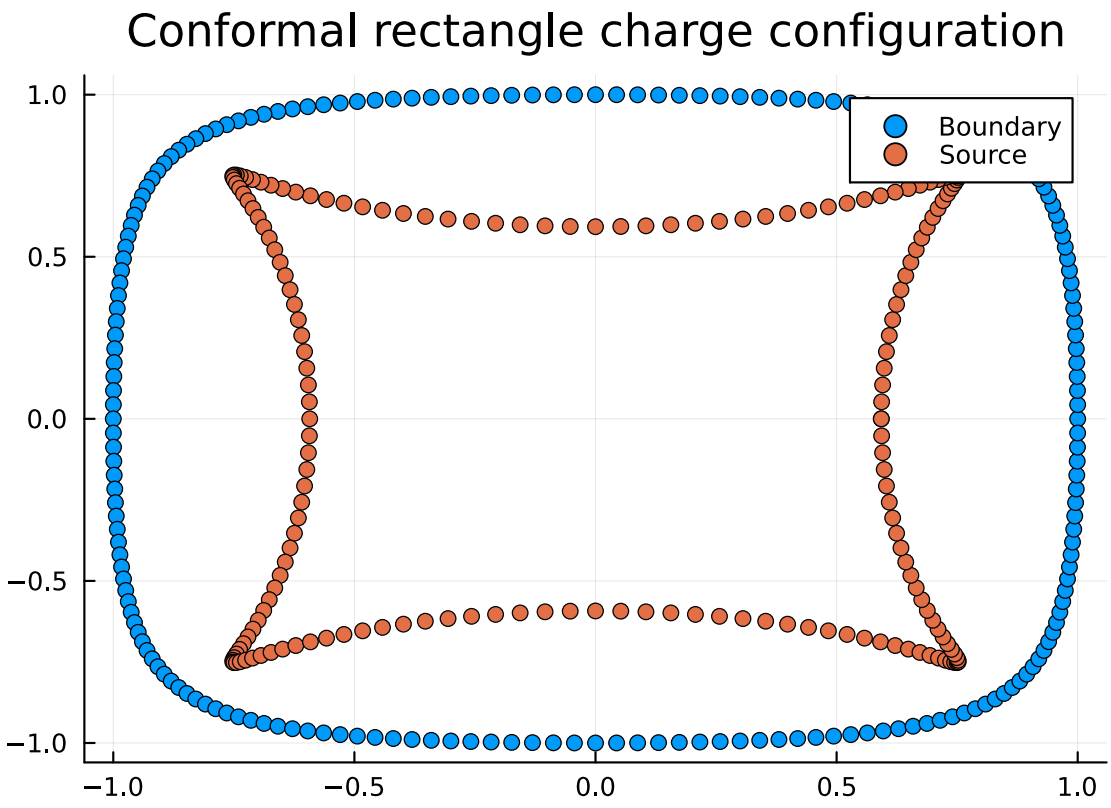

Figure 4.11: Distribution of points after the conformal transformation

geometry, and have found that these distortions due to curvature led to bad mass spectrometry performance. The exact form of these distortions is still being focused on in terms of a perturbation [41], or in terms of a different basis set of the toroidal harmonics [18].

4.2.2 Four Rod Toroidal Trap

As seen in the last section toroidal traps do not behave exactly like their linear counterparts. This section will focus on the more practical to machine version of a hyperbolic trap, the four rod toroidal ion trap. This is like the hyperbolic trap where we will take the linear version of the trap and turn it into a ring. A CAD rendering can been seen in Figure 4.14.

Since trap has axial symmetry, we can now use a fundamental solution that has the same axial symmetry as our trap, the ring charge, once again. Figure 4.15 shows a configuration of source points and boundary points, with the distance from an electrode to the center being, r, and the distance from the geometric center of the trap to the rotation axis being D.

For a normal linear ion trap if we rotate this trap around it geometric center such that it forms

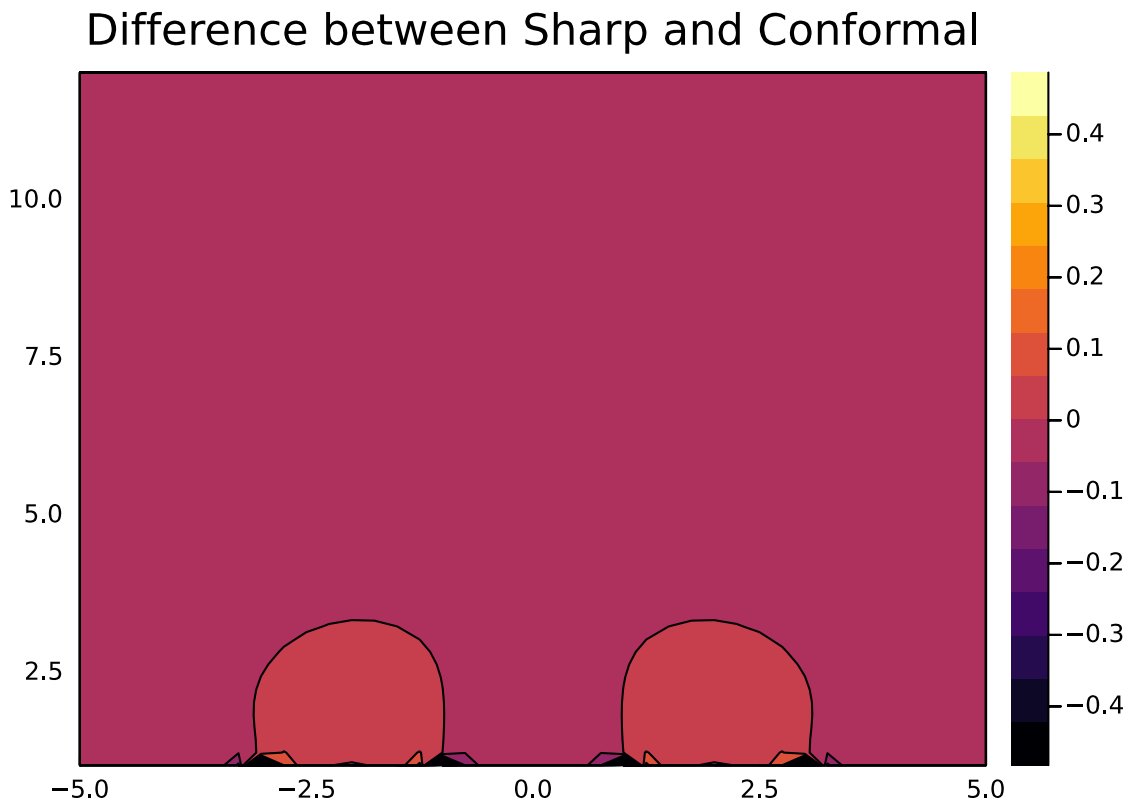

Figure 4.12: Difference between rounded rectangle and sharp rectangle five wire ion trap

an “x” shape, there is no physical difference in the field because of this. However, for this trap if we were to rotate it to be an “x” but keep the rotation axis the same, it will no longer be the same trap, due to the angle of the trap with the rotation axis being changed. Two configurations will be studied here, the “+” configuration, as shown in Figure 4.15 and the “x” configuration as shown in Figure 4.16.

For these traps we will investigate a few voltage configurations. One being a Symmetric RF voltage, where the top and bottom electrodes are applied a voltage of +1V and the left and right have -1V applied in the “+” configuration, and is rotated by 45 degrees counterclockwise in the “x” configuration. This potential is common to apply the RF pseudo potential of our trap. Another voltage configuration is a Asymmetric RF Voltage, where the electrodes previously at +1V are now at +2V and the -1V electrodes are held at ground.

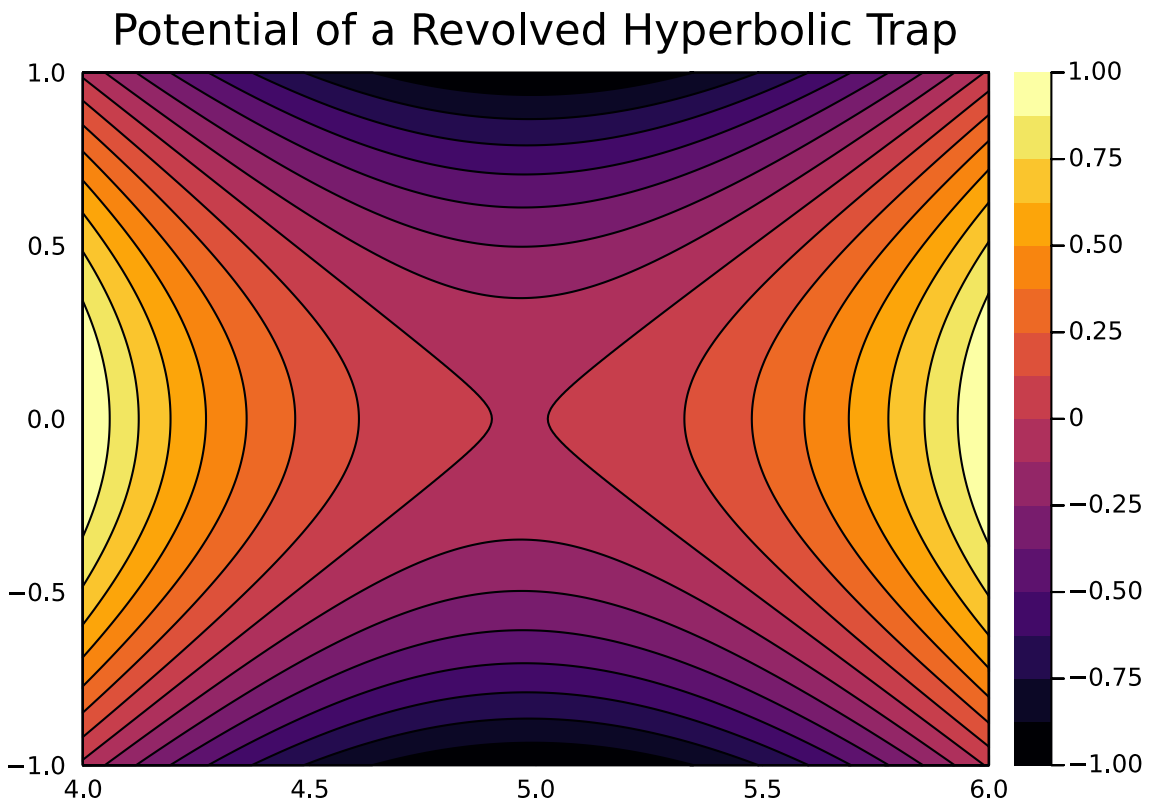

Figure 4.13: Potential of a hyperbolic trap revolved a distance of 5 from the central axis.

+ configuration

If we set up our ion trap in a "+" configuration, as in Figure 4.15, in the Symmetric RF Voltage configuration, with the vertical electrodes having positive RF voltage and the horizontal electrodes having a negative RF voltage, we can see the resulting potential in Figure 4.17. We see that the geometric center of the trap and the center of the potential do not align as seen in [25]. The geometric center of the trap is located at (5,0) but the potential's saddle point is located at (4.97,0) thus there is a leftward shift. A reason for this can be seen by looking at the potential caused by a ring of charge, in Figure 3.5. The potential on the inside of the ring is greater than the potential on the outside of the ring. At the geometric center, since this is inside of the outer ring, it will feel a greater force compared to the inner ring, in which the geometric center is outside. Thus, the point where these two potentials are equal is shifted towards the inner ring.

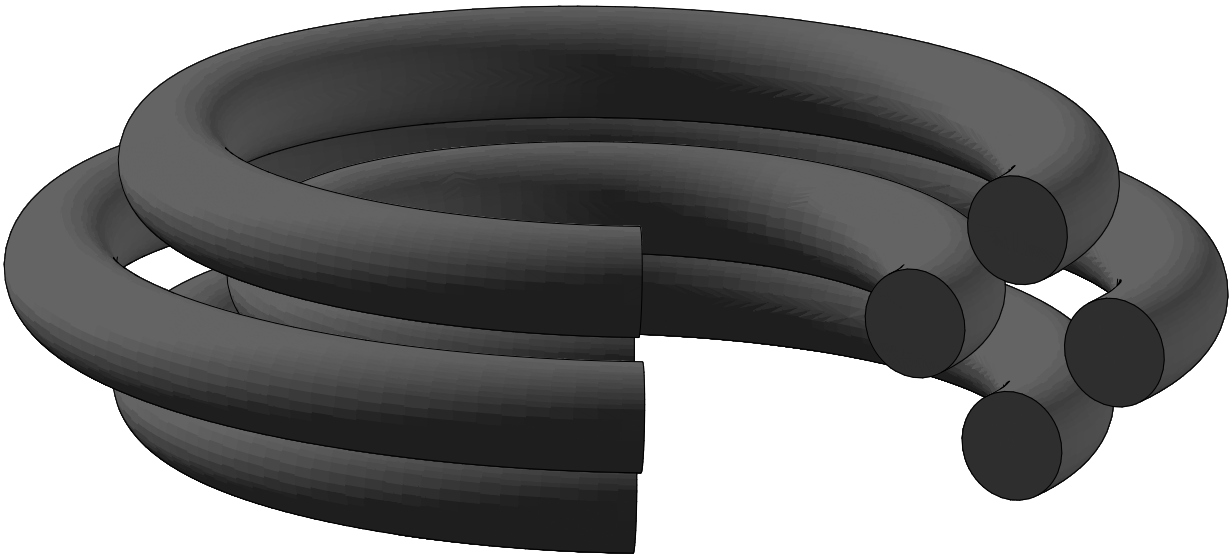

Figure 4.14: CAD rendering of a toroidal four rod ion trap in a plus configuration. Note a slice has been cut out such that the internal structure can be seen, however, the actual trap will form a complete circle.

x configuration

Now we can look at the "x" configuration as well, as shown in 4.16. We can first look at the Symmetric RF Configuration, with the electrodes on the negative diagonal being set to +1V and the electrodes on the positive diagonal being set to -1V.

From Figure 4.18, we can see that there is also an axis shift of the same magnitude as the "+" case. This is expected since we still have inner and outer electrodes which have different charateristics.

An even more interesting results occurs if we apply an rf to only two of the electrodes, instead of applying them to all of the electrodes, previously called the Asymmetric RF configuration. Looking at the Figure 4.19 we can see that there is a very small shift not only horizontally but also vertically. The horizontal position is 4.97 which is consistent with the previous simulations, however the vertical position of the minimum is at -.0044.

In the previous case we had symmetry due to our electrode placement such that any difference in the y direction would cancel out. However in this configuration there is no symmetry along the y axis, and thus the potential does not have to lie along the y axis. An important note is that this vertical shift causes a problem for trap designs which separate the DC and RF components to separate electrodes. In this case the RF and DC centers will not be at the same place due

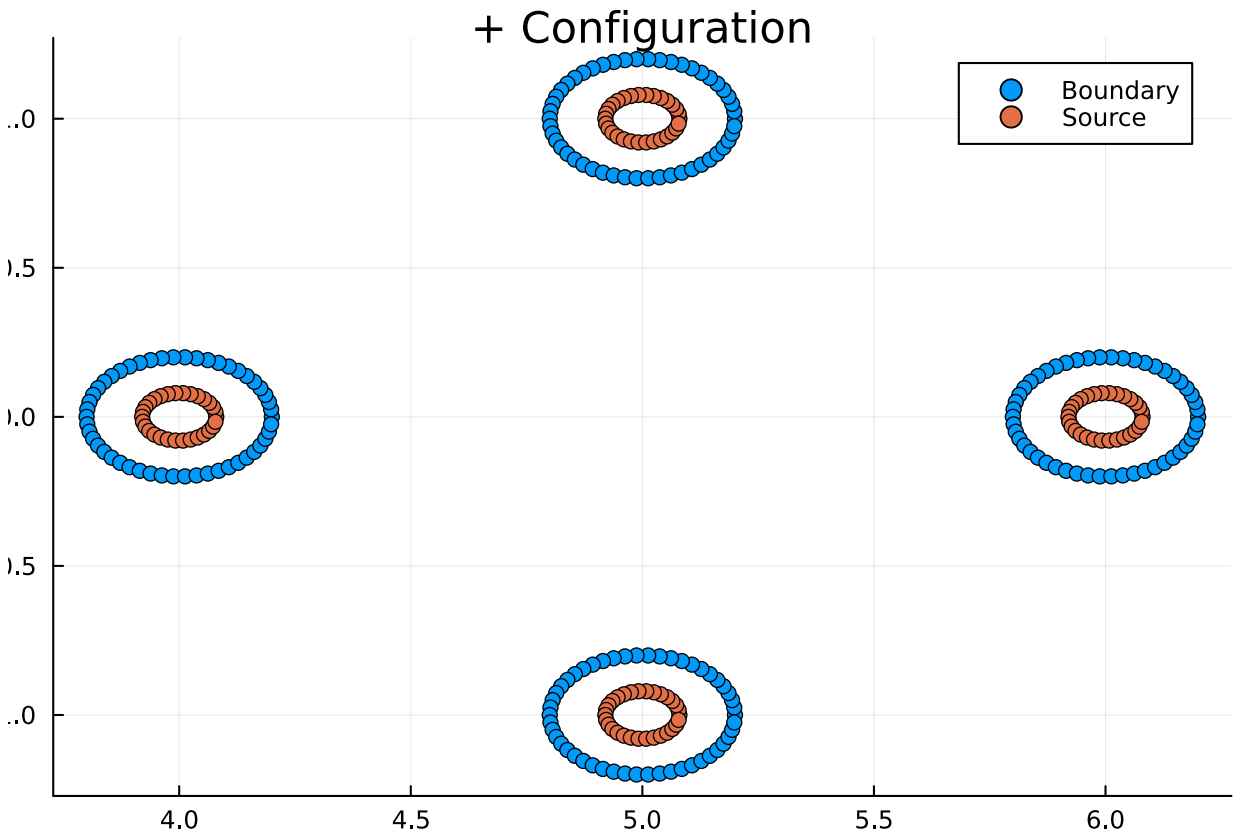

Figure 4.15: Example of a four rod toroidal trap in the "+" configuration with r=1, D=5

to the vertical shift. This causes the DC potential to push the ion off the RF pseudopotential minimum, which will result in excessive micromotion [5]. Note that this is also a problem for the "+" configuration as well, since the horizontal electrodes create a field not at the geometric center while the vertical electrodes will.

4.2.3 Toroidal Surface Trap

We can also perform this same toroidal analysis for a five wire ion trap. For this we can perform the same trick and take the 5 wire ion trap's parameters and use the fundamental solution of a ring of charge to take the linear version of the trap and turn it into a version with toroidal symmetry. Let us choose a trap which features five conformal rectangles with each having a diameter of 2 and the spacing of the centers being 2.3. We can also let the radius of the rotation axis, R, be 40. These dimensions should have similar ratios to those planned in [42]. The position of source points and boundary points are shown in Figure 4.20. Now for a five wire trap it is common to apply the same voltage to the first electrodes to the left and right of the middle. We can see the results of doing

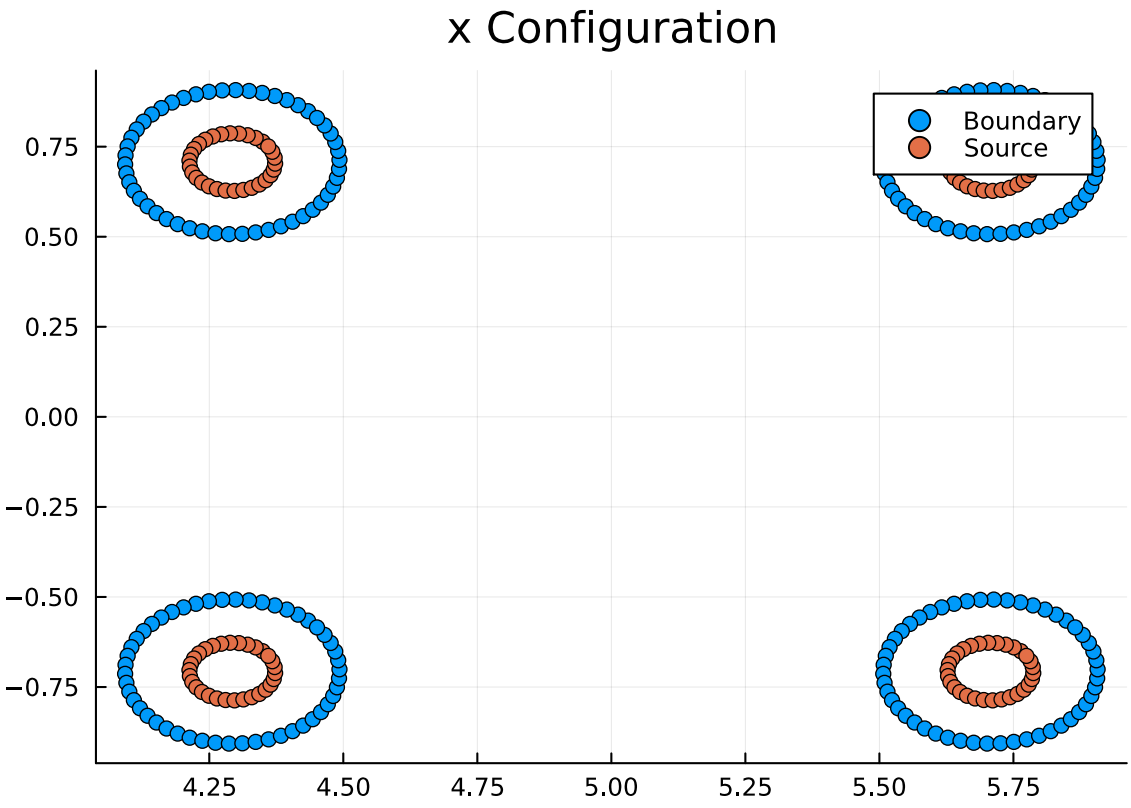

Figure 4.16: Example of a four rod toroidal trap in the "x" configuration with r=1, D=5

so in Figure 4.21.

Similar to the four rod toroidal traps, we see that the potential is asymmetric. However, this is actually a good thing in this case, as if the potential was symmetric then one of the trap's principal axes would be aligned perpendicular to the surface. This presents a problem for laser cooling, since the laser will have to travel parallel to the surface to prevent hitting the surface of the trap, and thus if a trap axis is perpendicular to the beam it will not be cooled [1]. However, an angle of 15% off the vertical was found to be the best [6], and the angle here is not that big, so methods to shift the potential's principal axis such as asymmetrically applying voltages, or adjusting the size of electrodes could be necessary [20].

Another thing to note, is that the potential is shifted to the right instead of to the left in this case. This can be explained by the grounded electrode in the middle, it should reduce the potential on the left more than on the right causing the potential to move to the right.

In addition, in [42], a mixture of an RF and DC potential was applied to the outer ring electrode to create a centripetal force inwards to counteract an outwards centrifugal force caused by rotating

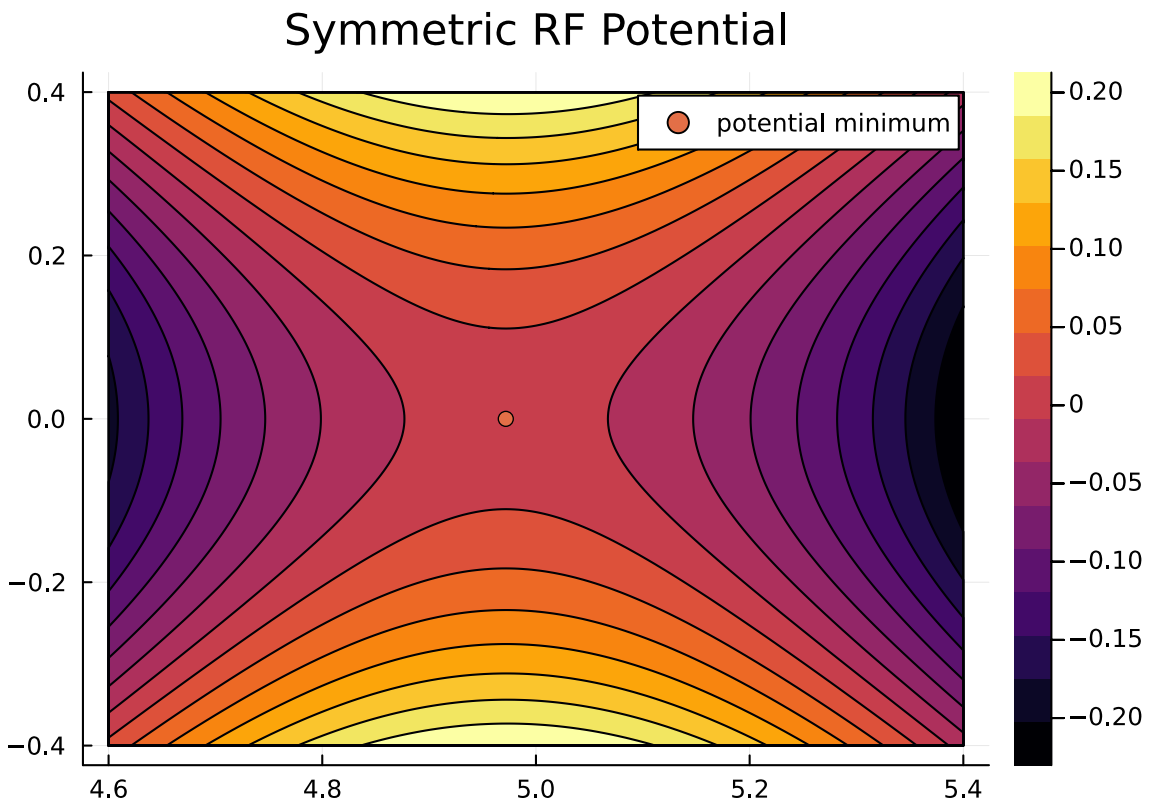

Figure 4.17: Example of the potential of a four rod toroidal trap in the "+" configuration with r=1, D=5

an ion around the ring. This has been simulated in Figure 4.22. If we want this potential to cancel out a centrifugal force, then we would want its E field component to be pointing perfectly to the left (inwards), as the centrifugal force would point to the right (outwards). Looking at the current plot we see that the E field produced by this potential points upwards and to the left. While the leftwards component of the field can be canceled by the centrifugal force, the upwards will drive the ion off of the potential minimum and causes excessive micromotion. Therefore, this quality is undesired and presents a problem.

The current simulations have not included the effects of the segemented electrodes, which break the axial symmetry. However, if we break axial symmetry then using a ring charge as the fundamental solution is incorrect. Thus instead of using ring charges we have to use point charges instead. However, to get a high enough density of points to get around a 1% error, in the case of having around 100 control electrodes, is likely to be in the range of 30,000 to 40,000 points. Since we are solving a linear least squares system and cannot use iterative methods due to the ill

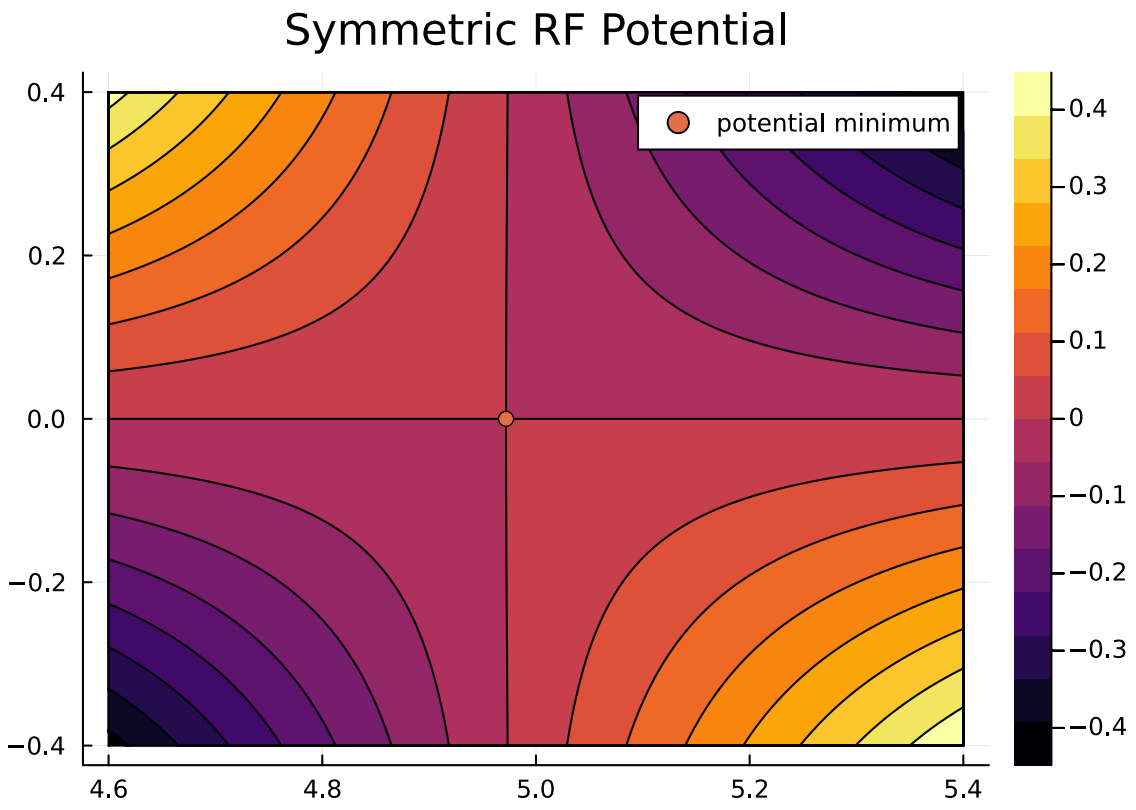

Figure 4.18: Example of the Symmetric RF potential of a four rod toroidal trap in the "x" configuration with r=1, D=5

conditioning, this is unfeasible. However, this trap is made to have many trap sites which are all identical to each other, and thus we have a periodic radial symmetry.

As mentioned in chapter 2, we can now create a green's function that captures this radial periodic symmetry, and thus we only have to simulate one trap site instead of all of them. This means that the trap can now simulate even a potentially infinite number of trap sites due to this symmetry. We can define that our trap has symmetry every eight electrodes and that there are 96 electtodes in total. Yet, the segemented electrodes still present a problem due to their sharp corners, which are not easy for the MFS to simualte. At this point we will simplify the electrodes dramatically and approximate them as spheres. This approximation will not produce the correct field but it will show us the general characteristic of the field. The boundary points and source points are shown in Figure 4.23, and the Potential is shown in 4.24, and checking the error on a grid about twice as fine gives a 4 percent error. Comparing this potential to Figure 4.21 we see that this approximation does have a decently big effect on the potential. The center has been shifted, which

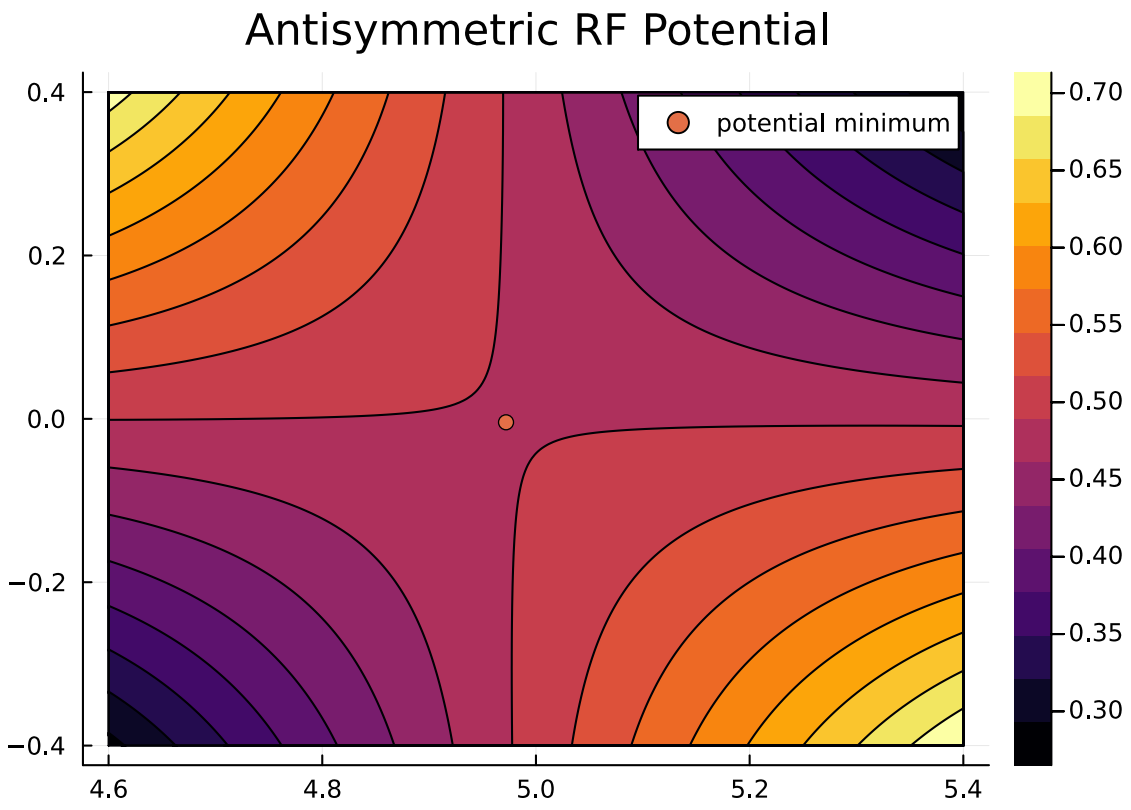

Figure 4.19: Example of the Asymmetric RF potential of a four rod toroidal trap in the "x" configuration with r=1, D=5

is quite a big effect. While approximating the outer electrodes as sphere results in a significant difference as compared to the previous simulation, we can still gain some insights from it, but for computing a high accuracy potential, this approximation is not valid.

Now we can simulate the potentials applied in [42] which are that the potentials on the control electrodes goes 0V, +V, 0V, -V, 0V. The potential created by the control electrodes is shown in Figure 4.25, along the same plane as the RF potential was previously shown. We can note that this potential is anconfining as expected however, its saddle point is not at the same position as the RF's saddle point. We can see that since there is no vertical symmetry to our trap that the minimum created by the control electrodes does not have to be at the same position as potential created by the ring electrodes. This shift is not good as the DC potential will shift the ion off of the RF minimum and cause excessive micromotion. Another problem is that the principal axes of the DC and RF components are not aligned, which is an assumption in the Matthieu equations. The effects of this were explored in [32], and they found that this is generally safe, and the only

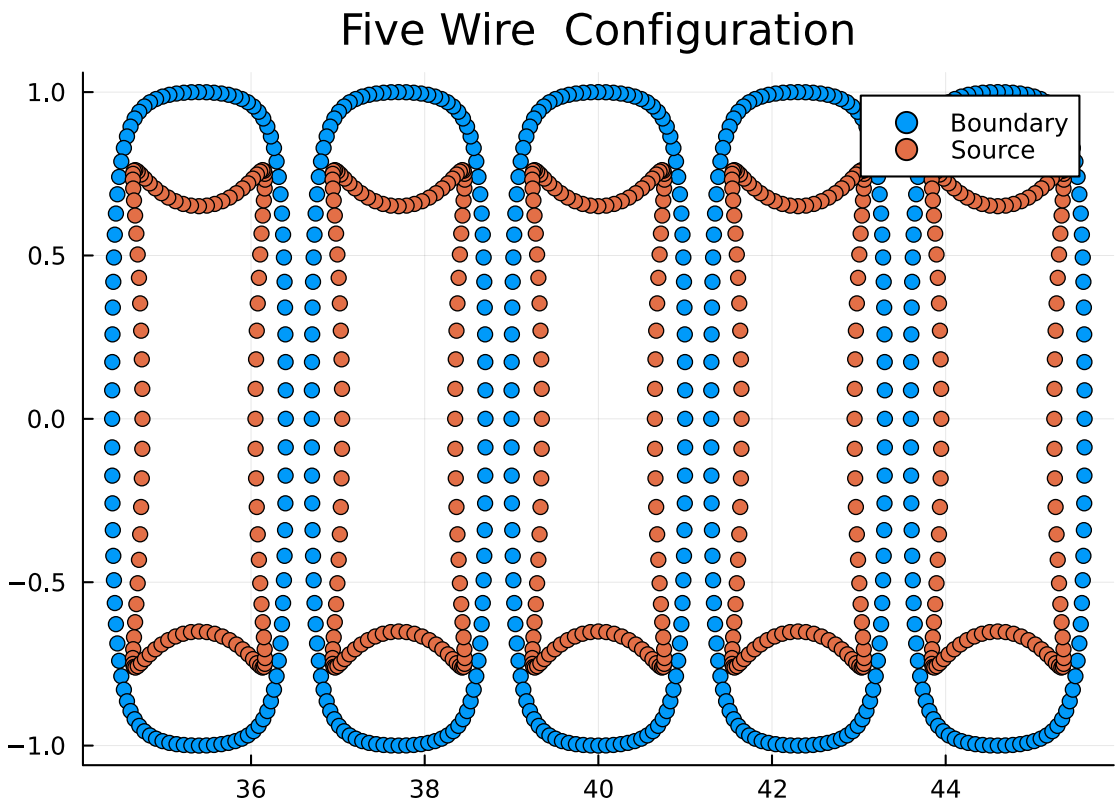

Figure 4.20: Distribution of points for the MFS solution to a five wire toroidal ring trap

effects are that the stability region's size is underestimated.

4.3 Conclusion

Overall, we can see that the Method of Fundamental Solutions does well to simulate many trap designs. In addition, because the physical intuition for the method is strongly rooting in the traditional teaching of Electricity and Magnetism courses, we can easily answer confusing questions such as why the potential saddle point does not coincide with the geometric center of an ion trap, though viewing it as a summation of ring charges. In this way the intuitive explanation is echoed by the numeric method.

In our simulations, we have noticed a few concerning facts arising from the toroidal geometry. One being that the trap center and geometric center do not align. This poses a problem for traps with split AC and DC components since, the DC field will push our ion off the minimum potential. This also presents itself as problem for the surface toroidal trap as well. In addition, it is clear

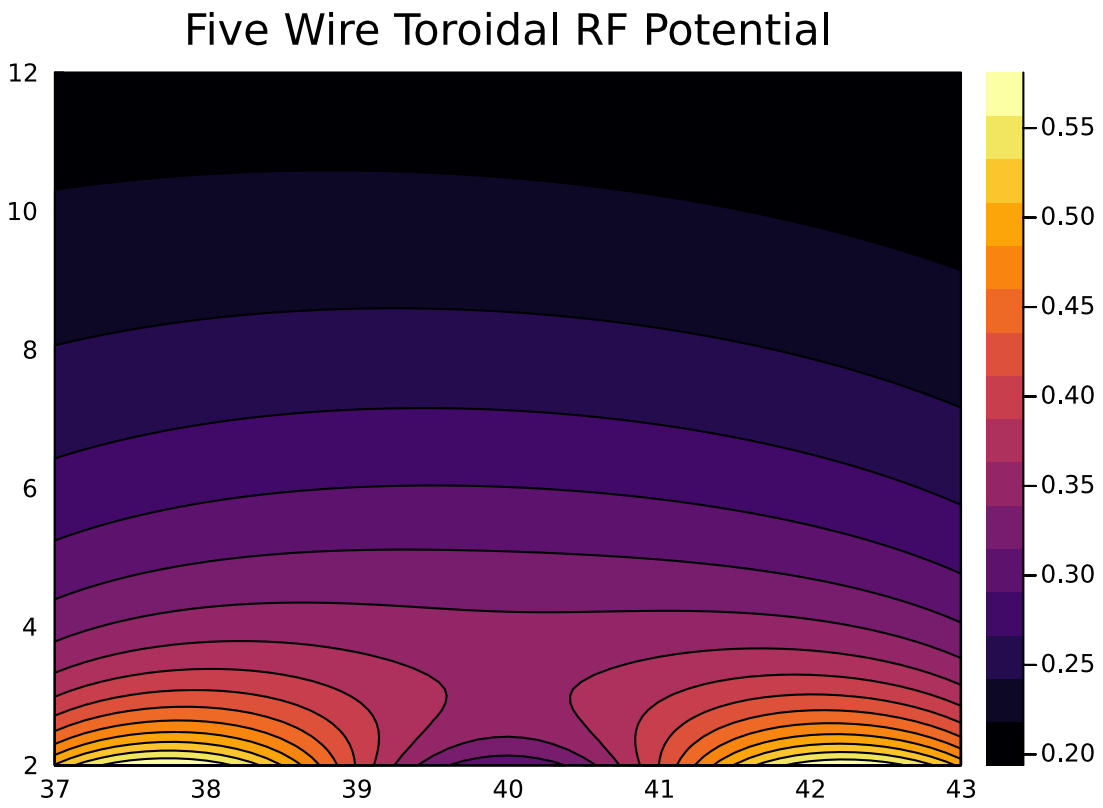

Figure 4.21: Potential due to a five wire toroidal ring trap with a voltage on the two electrodes next to the center electrode turned on

that there is some perturbation to our potentials due to the curvature of the traps. While the previously listed problems are more pressing, it would be interesting to find out what the nature of this perturbation is.

Since the MFS converges with a little amount of points, and also since modifying the geometry of our simulation only involves changing how our points are arranged, due to the meshless nature of the MFS, we can explore if we can minimize these undesired quantities with ease. This will be the focus of the next chapter.

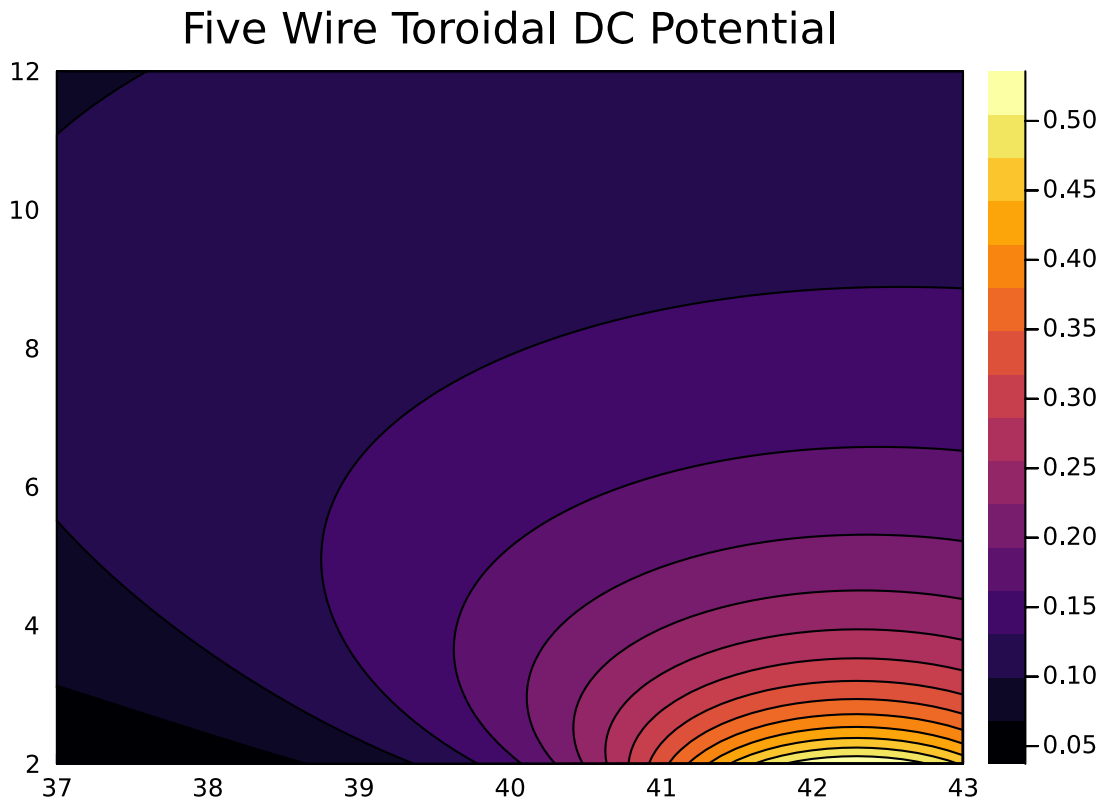

Figure 4.22: Potential due to only the right center wire

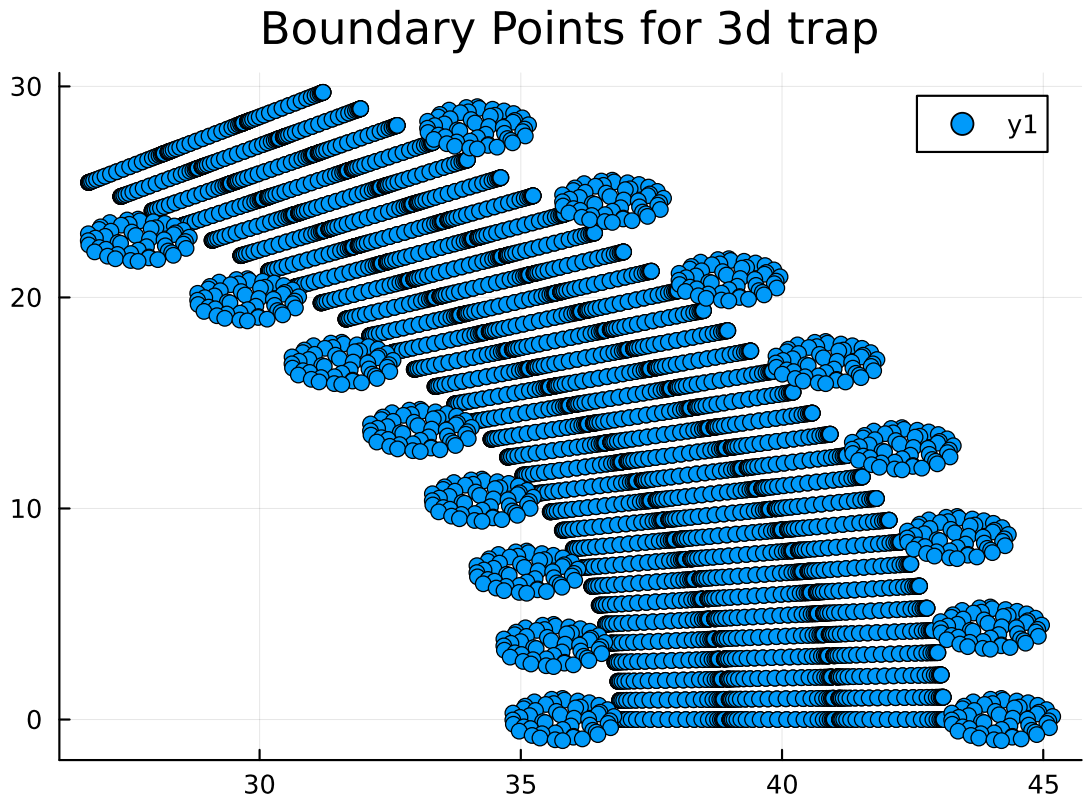

Figure 4.23: Overhead view of distribution of boundary points for a ring trap with segemented electrodes. Note that only 1/8 of the total trap needs to be simulated due to symmetry

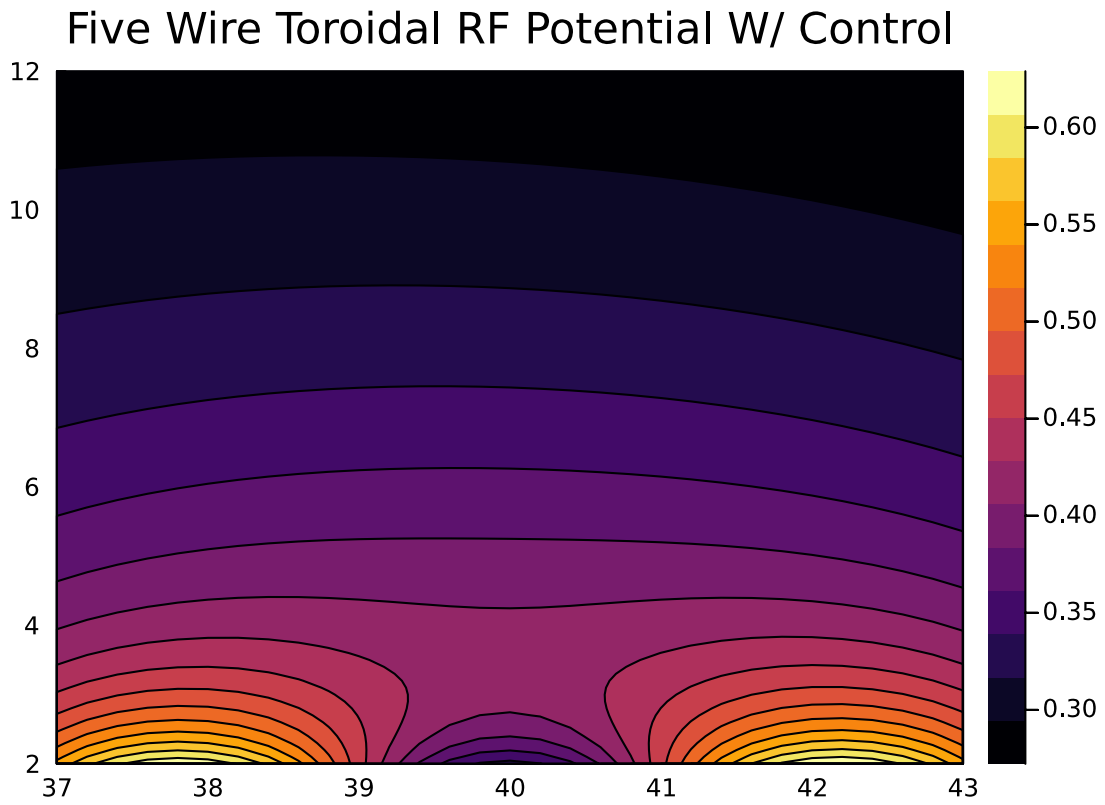

Figure 4.24: RF Potential of a surface toroidal trap with control electrodes

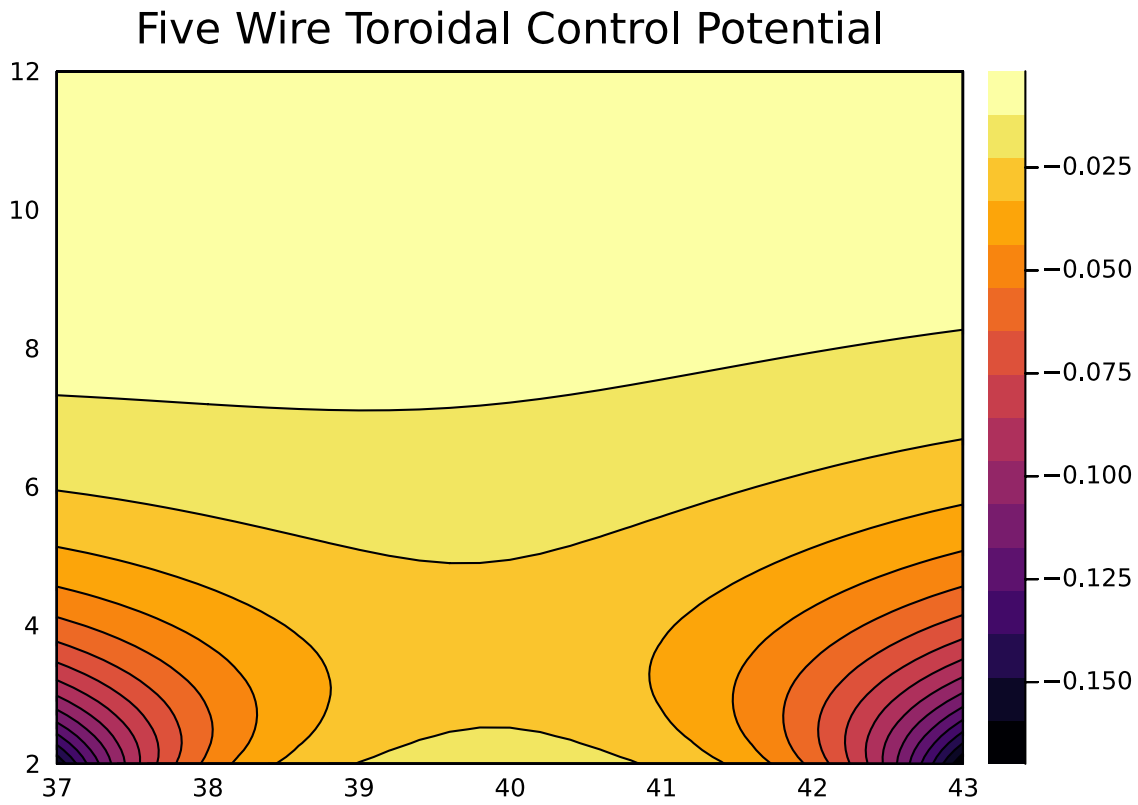

Figure 4.25: DC Potential of a surface toroidal trap with control electrodes

Chapter 5

Optimizing Ion Trap Potentials

As shown in the previous section, the typical intuition of ion traps falls apart when dealing with toroidal ion traps. Features such as the mismatch of the geometric center and the potential minimum's location, the mismatch of the DC potential's center to the RF potential's center, seem to be unique to toroidal ion traps. This chapter will focus on seeing if we are able to fix these kinds of issues. In addition to these 0th order qualities of the fields, we can also look at higher order effects on our fields. In doing so we will find that the standard Multipole Expansion of our trap's potential does not accurately capture our trap, and a possible trap design will be proposed which potentially can fix this issue.

5.1 Matching Centers

As seen in the previous chapter, there are cases where the DC center and RF center do not match in four rod toroidal traps with split DC and RF electrodes, and also in surface toroidal traps. If the centers do not match then DC potential will push the ion off of the RF null causing excessive micromotion. In addition, if the ion is pushed off the center, then nonlinear effects of the field will be amplified. For ion traps, these nonlinear effects, are usually assumed to be nearly zero because of the ion being on the RF null. So the problem of mismatched centers is bad in many ways, and needs to be corrected.

5.1.1 Four Rod Toroidal Trap

+ configuration

We will first look again at our four rod toroidal in the "+" configuration. For this trap we would expect that if we increase the voltage on the innermost electrode relative to the outermost electrode, that our saddle point would move to the right. We then want to find a way to find the saddle point and perform numeric minimization until the saddle point is at the location we want. In this way we can set up an optimization problem that finds the ratio of these two such that the saddle point is in the location we want.

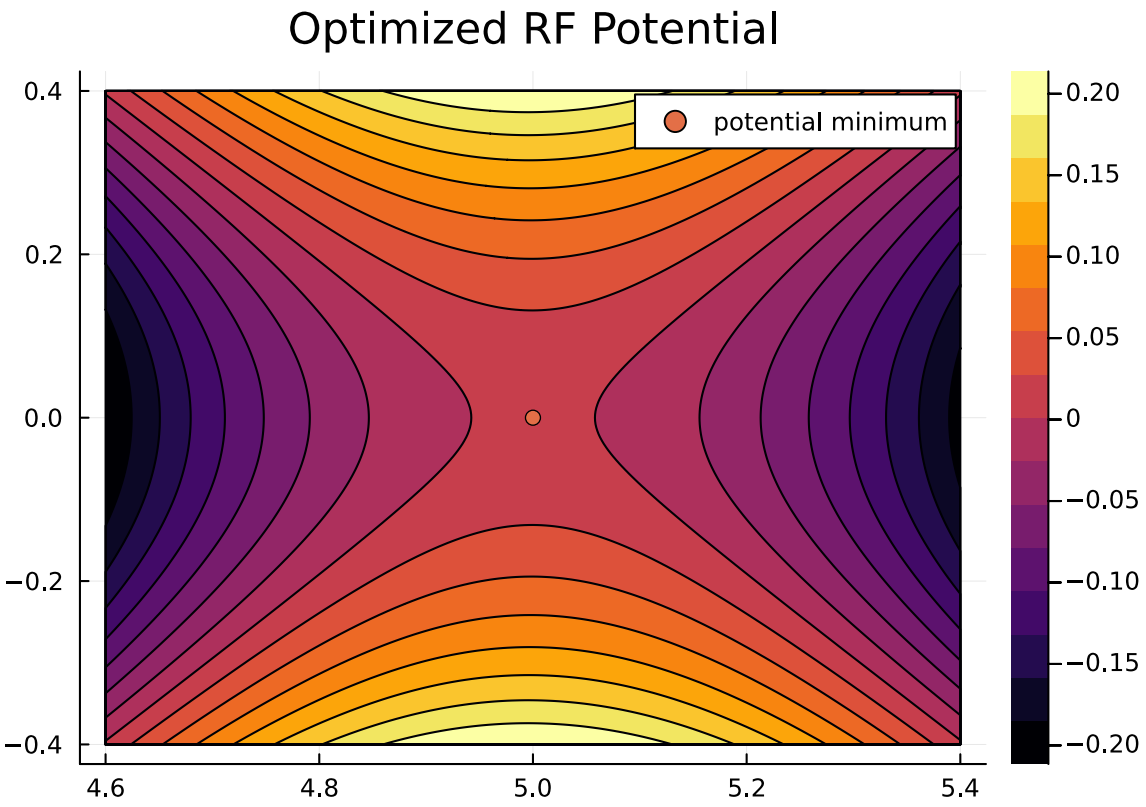

Figure 5.1: Optimized RF Potential of a 4 rod toridal trap in the "+" configuration

We can start our analysis with the RF potentials. Starting with the vertical electrodes voltage of +1V and the horizontal electrodes voltage of -1V, we obtain, a saddle point to the minimum of our potential by changing the voltages to .915V for the top and bottom electrodes a voltage of -.54V for the outer ring electrode, and a voltage of -1.31V for the inner ring electrode. The potential can

be seen in Figure 5.1 This follows what we expect, in that the the top and bottom electrodes are the same because when they are the same their contribution to the potential is along the y=0 line, and they cannot provide any shift along the horizontal direction, and the inner electrode now has a higher voltage to force the saddle point to the right.

x configuration

We can also perform the same analyses for the "x" configuration. We can look for the voltages that make the RF potential minimum at the geometric center, these are a voltage of 4.12 V on the inner rings and a voltage of 2.59 V on the outer rings. We can see the potential in Figure 5.2. In this case we see that there is no longer the shift which moves the potential leftwards, because we have increased the potential on the inner ring which will move the potential to the right.

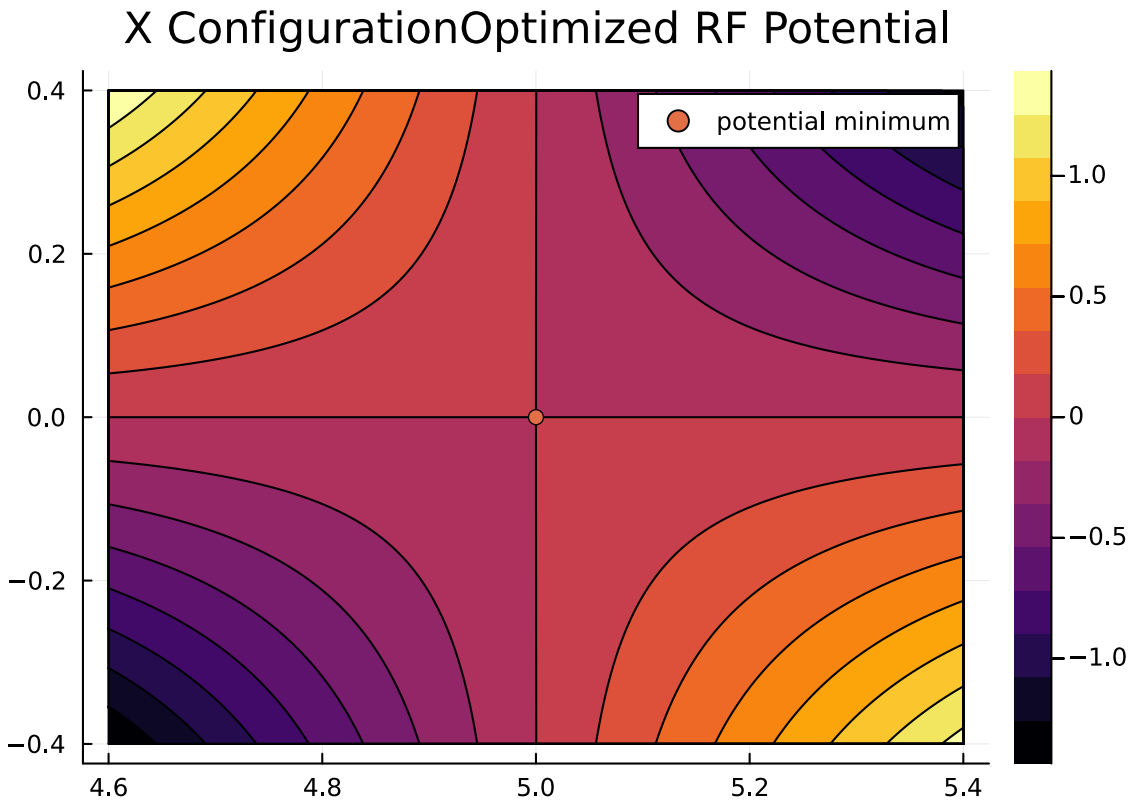

Figure 5.2: Optimized RF Potential of a 4 rod toridal trap in the "x" configuration

One last configuration we can consider is the split RF and DC case where we only applied a voltage to two of the electrodes. Previously we saw that the potential for this was shifted both

vertically and horizontally. Unfortunately, when doing the optimization for this setup, the potential minimum was not able to be located at the geometric center. This is understandable since, we only have one degree of freedom in this case, the ratio of our two electrodes. Since we have no symmetry there is no guarantee that we can find a potential at an arbitrary spot. However if we loosen our search that we need a potential that lies on xy plane then we find that a voltage of 1.12V on the inner electrode and 1.09V on the outer electrode, creates a saddle point at (4.96,0). Using this point we can realize a split DC and RF electrode configuration, since the vertical shift is eliminated.

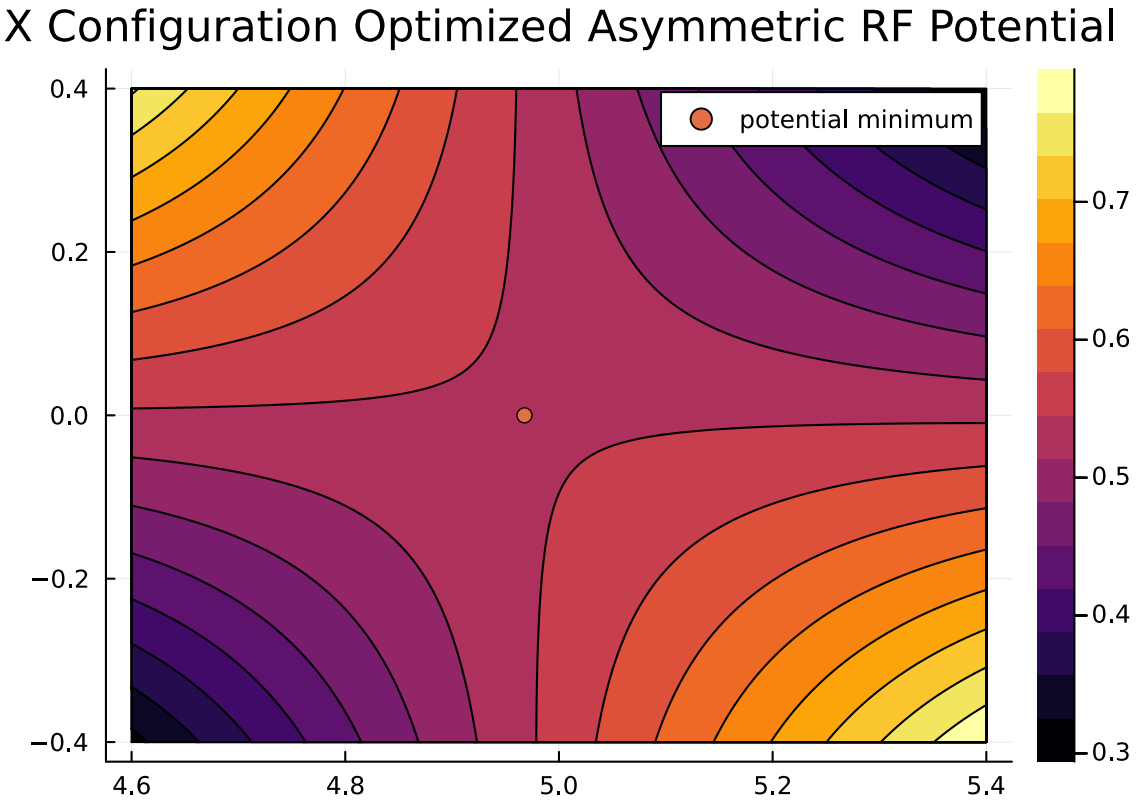

Figure 5.3: Optimized RF Potential of a 4 rod toridal trap in the "x" configuration, with voltages only applied to the top left and bottom right electrodes

Overall, the toroidal geometry introduces many interesting challenges due to the asymmetry of the ring charge fundamental solution, luckily a majority of these can be solved by setting the voltages on each electrode to specific ratios. Currently I have looked at the "x" and "+" configurations, however, these problems will present themselves for ion traps at any arbitrary angle. Overall, one must design a toroidal trap such that the RF and DC centers align, either through exploiting

symmetry, or by making sure that the potential created by the electrodes has no vertical shift.

5.1.2 Toroidal Surface Trap Control Electrodes

As seen before if we take a voltage sequence used to shuttle an ion for a linear trap and apply it to a surface trap, we run into problem because the DC potential's minimum in general, will not be in the same position as the RF potential minimum. This is the case because we have lost vertical symmetry through the trapping point, due to the surface trap nature. This means that we need to find a way to get the voltages to form a potential at the correct position, but also we want to specify the curvature of the potential used to trap the ion along a certain position of the ring. One way to perform this optimization based on [21], is to note that at the center of the trap we want the gradient of the potential in all three spatial directions to be 0, and for the confinement dimension it we can specify its 2nd derivative to be a specific value. We get the constraints

$$\sum_i V_i \nabla \phi_i = \vec{0} \tag{5.1}$$

$$\sum_i V_i \partial_z^2 \phi_i = A_{zz} \tag{5.2}$$

where ϕ_i are the green's functions of the electrodes we want to use to control the field, and V_i are the voltages we apply to each. Then by performing a least squares fit we will get an answer which minimizes the sum of the squares of the applied voltages $\sum_i V_i^2$ by the definition of least squares. For this method additional constraints can be applied, such as specifying the curvature in the x and y directions as well, or specifying a tilt to the potential.

Another method to find the potential is presented in [35] and phrases the problem as trying to perform an ill-conditioned fit to a specific potential. They define a function that describes the potential shape they want Φ and then pick the points $x_1, x_2, ..., x_m$ along the trap axis, and then aim to find the values of V_i that best fit this potential. Which can be written

$$\Phi_i = \sum_i A_{ij} V_j \tag{5.3}$$

However, since there are only 8 independent control electrodes, and the potential might need to be specified in hundreds of places, then this is quite likely to be ill-conditioned. As a result the norm of the vector of V_i is likely to be large, and thus the voltages needed to create the desired potential would be experimentally unfeasible. They are able to reduce the ill-conditioning, and thus the required voltage by performing a Singular Value Decomposition of the matrix A,

$$\vec{v} = USV^T\vec{\Phi} \tag{5.4}$$

with $\vec{v}$ being the vector of V_i, $\vec{\Phi}$ being the potential Φ evaluated at the desired points along the trap axis, S being the diagonal matrix which has the singular values and, U and V being unitary matrices. The singular values act as a generalization of an eigenvalue decomposition, and thus the bigger a singular value is the more important it is. In fact if we only consider the first r singular values of the matrix, and set the rest to 0, this matrix is the best r rank approximation to our original matrix [13].

Then what they did was modify the singular values following

$$s_i'^{-1} = \frac{s_i}{s_i^2 + \alpha^2} \tag{5.5}$$

with α being the Thikonov regularization parameter, and as it is decreased, more of the smaller singular values will be reduced. This results in a more well conditioned matrix at the expense of accuracy.

This then gives the solution to our problem as

$$\vec{v} = VS'^{-1}U^T\vec{\Phi} \tag{5.6}$$

with S' being a matrix with the regularized singular values.

However, this method does not specify anything about the shape of the potential in the xz plane, and in my testing this resulted in the minimum being very far from the ideal location. While we could incorporate more points to specify the potential in the xz plane, this would dramatically increase the ill-conditioning due to the difference in discretizing a single dimension vs three, and adding a term like in the first to make the gradient 0 at the center, would only make a small difference, if all points are equally weighted.

Due to this the method used to find the minimum was a mixture of the two methods mention previously, the matrix was constructed in a similar manner to the first method [21], but using SVD and Thikonov regularization to regularize the matrix as in [35]. Additionally, a term to constrain the value of the potential minimum to -0.75 was added. Using this method we can obtain the required voltage on an electrode to move it through a full zone, with a full zone being 1/8 of the full ring due to symmetry. The results of no regularization are shown in Figure 5.4, and with a regularization parameter of $\alpha = .005$ in Figure 5.5.

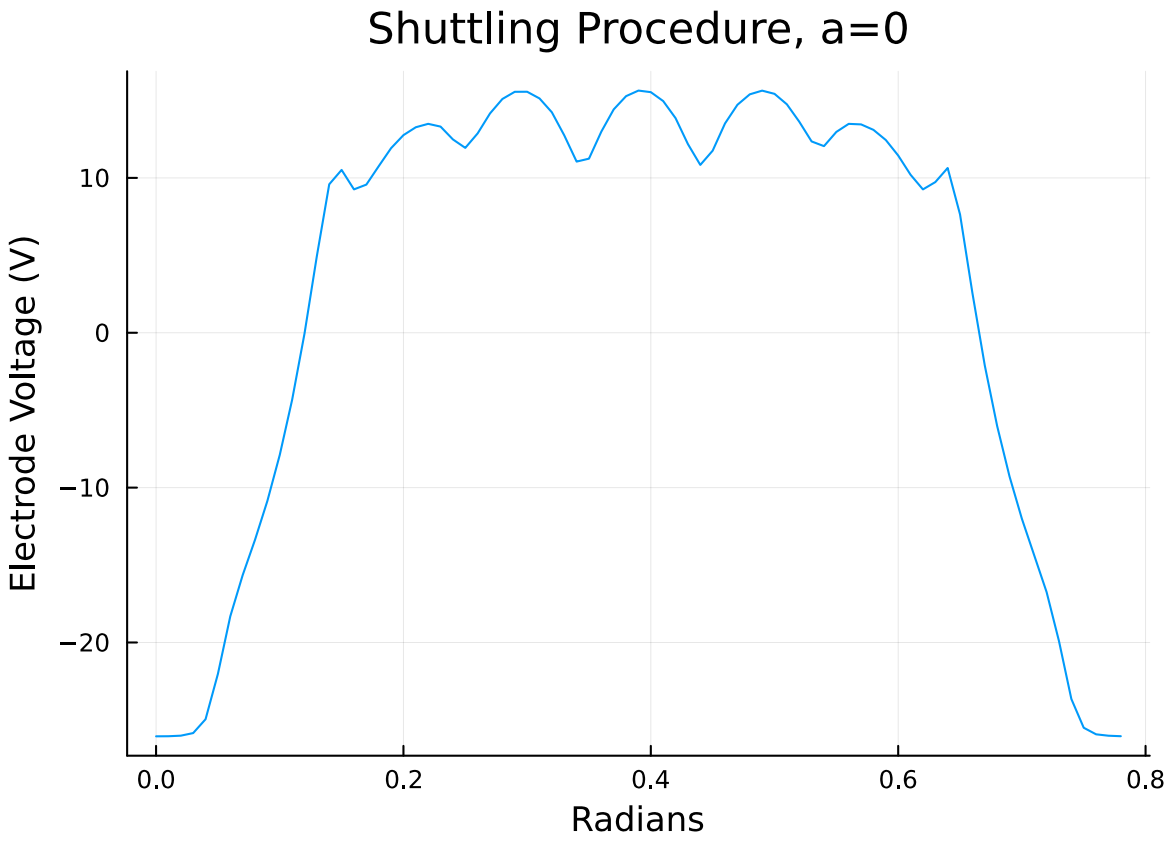

Figure 5.4: Voltage applied to control electrodes to shuttle ions, with no regularization

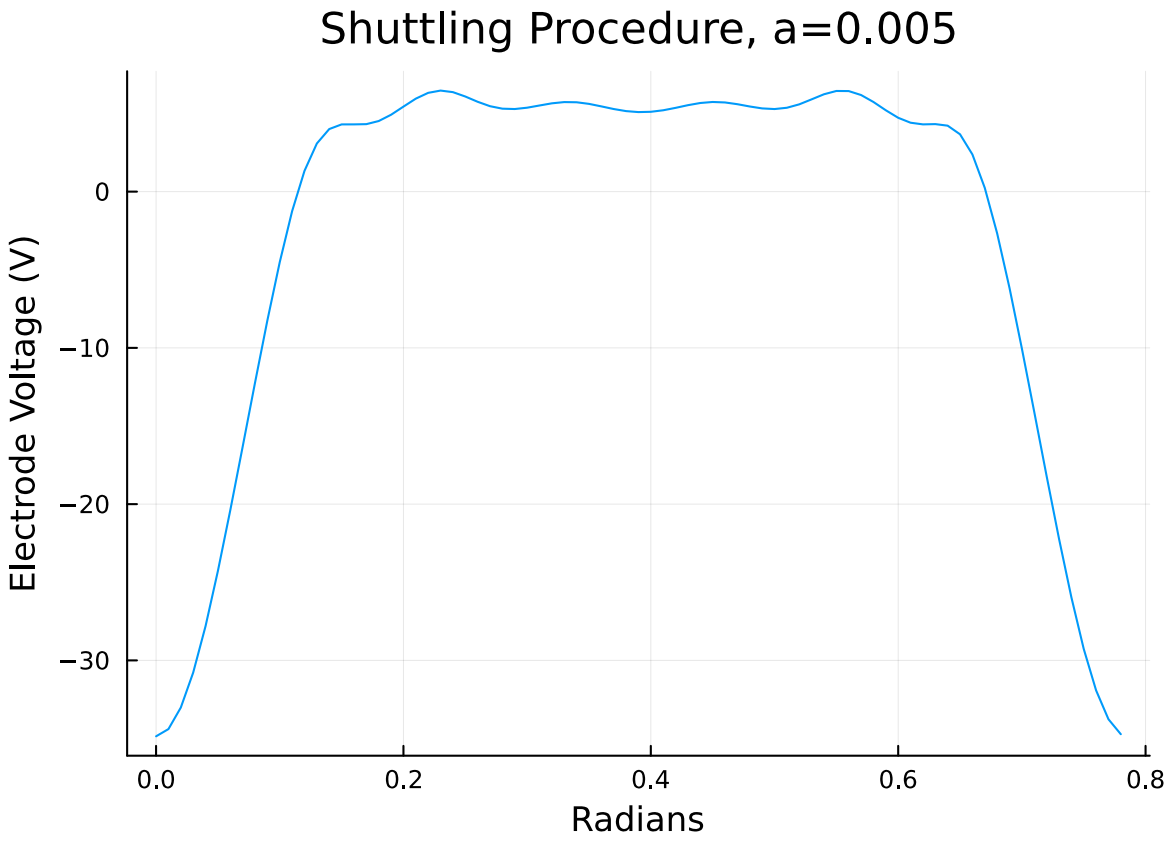

Figure 5.5: Voltage applied to control electrodes to shuttle ions, with $\alpha = .005$

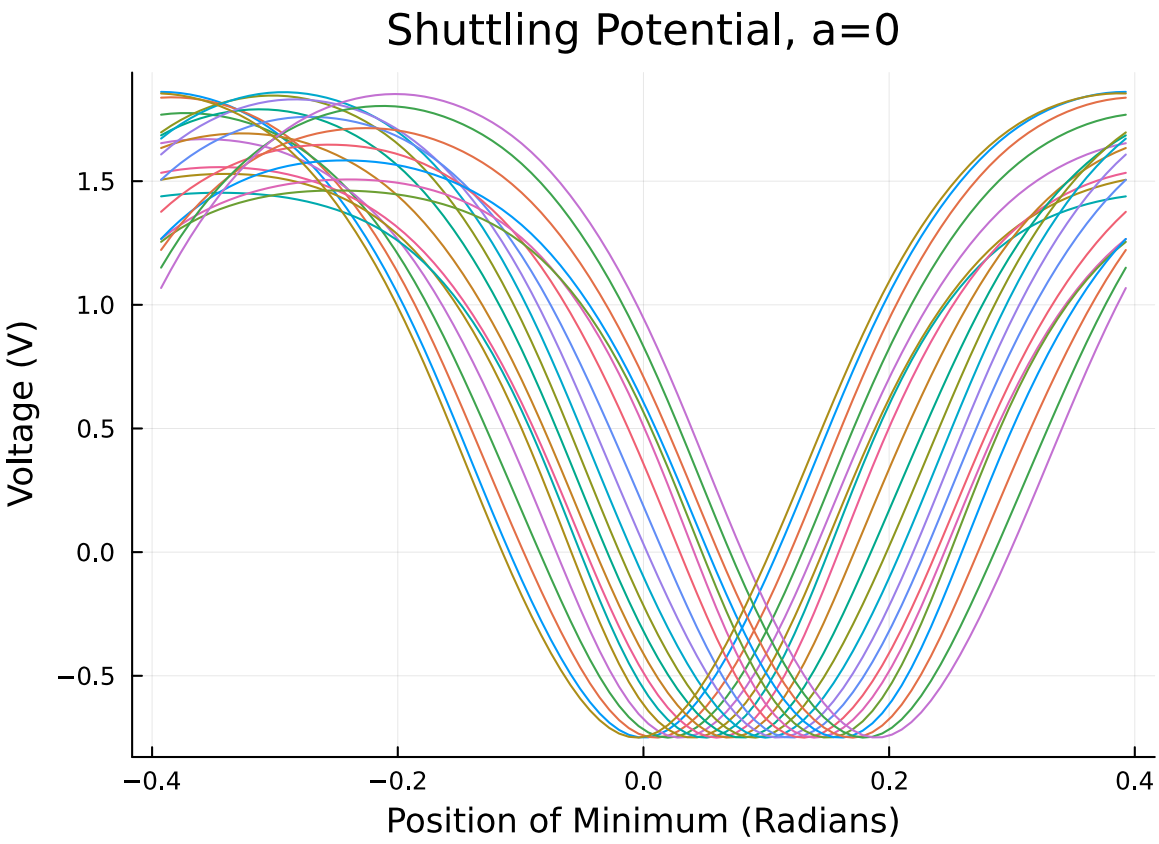

Figure 5.6: Potential created along trapping circle, without regularization

While this is for a single electrode, due to the symmetry of the trap, the other electrodes have the same voltage profile with just a phase shift. We can see that the applied voltage has been smoothed out when we include a regularization term. Also note that the voltages have been scaled so the regularization term and non regularized terms are nearly the same. We can see the effect on the potential produced by each in Figure 5.6 for no regularization and for Figure 5.7 with regularization.

In the case without regularization we see that the potential looks quite good as it is translated along, and it also looks good with regularization. The main difference we see is farther away from the minimum, the potentials deviate more for the unregularized case. We do see that the regularized case is not able to keep the potential smoothly at a single value, and it nearly completely ignores the requirement that the potential minimum is at -0.75V. Lastly we can look at the potential created radially without regularization in Figure 5.8 and with regularization in Figure 5.9.

However, we do find some problems with regularization as indicated by the previous plots. As we increase our regularization we increase how off the potential minimum is from the expected

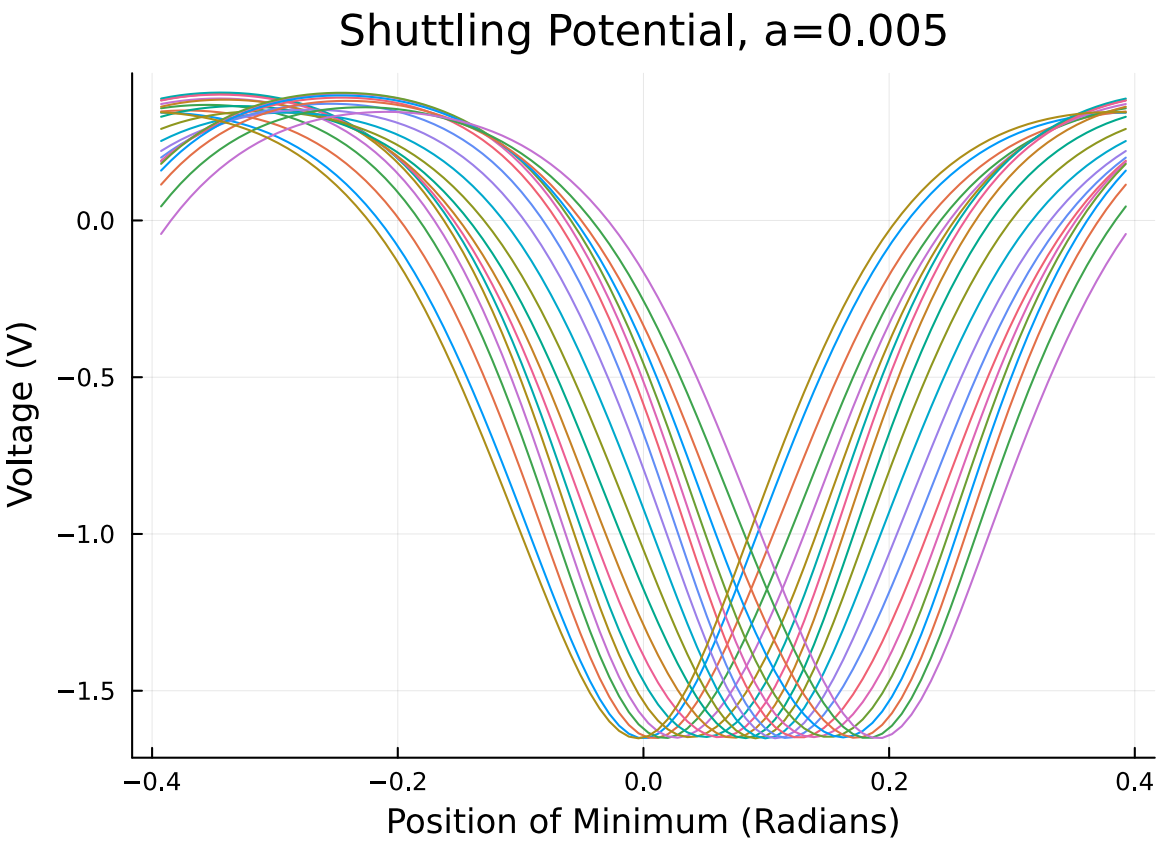

Figure 5.7: Potential created along trapping circle, with $\alpha = .005$

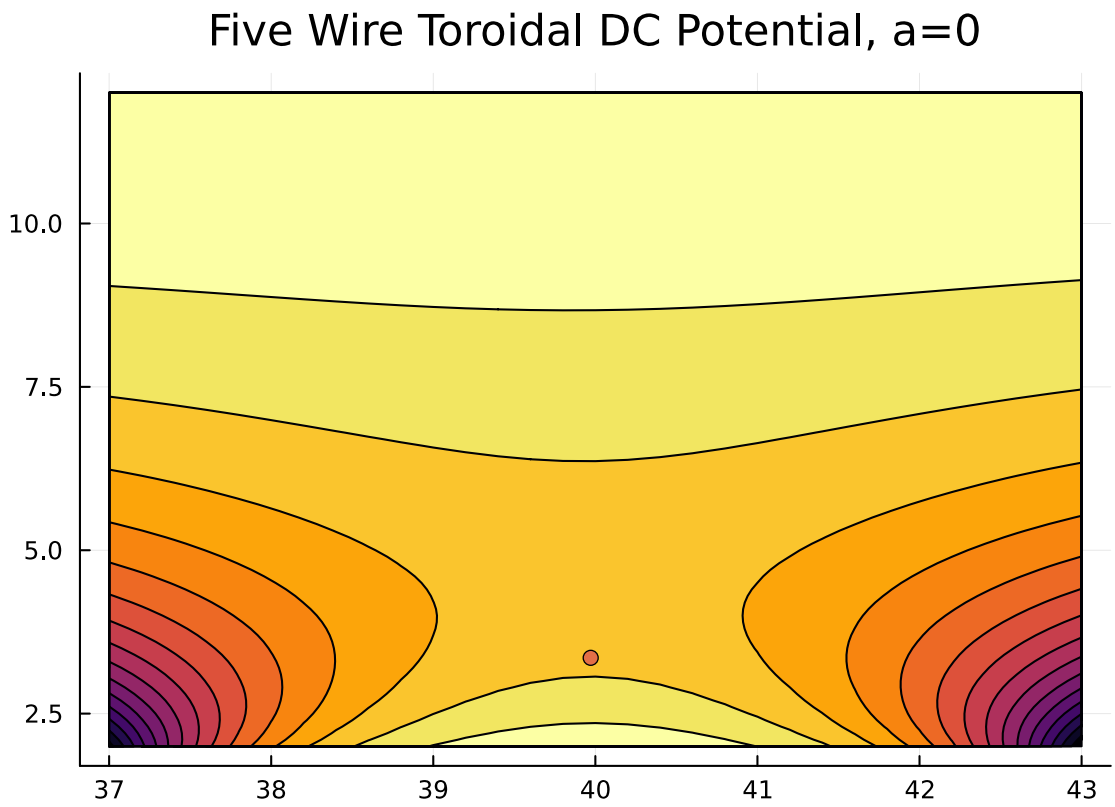

Figure 5.8: Radial Potential, without regularization

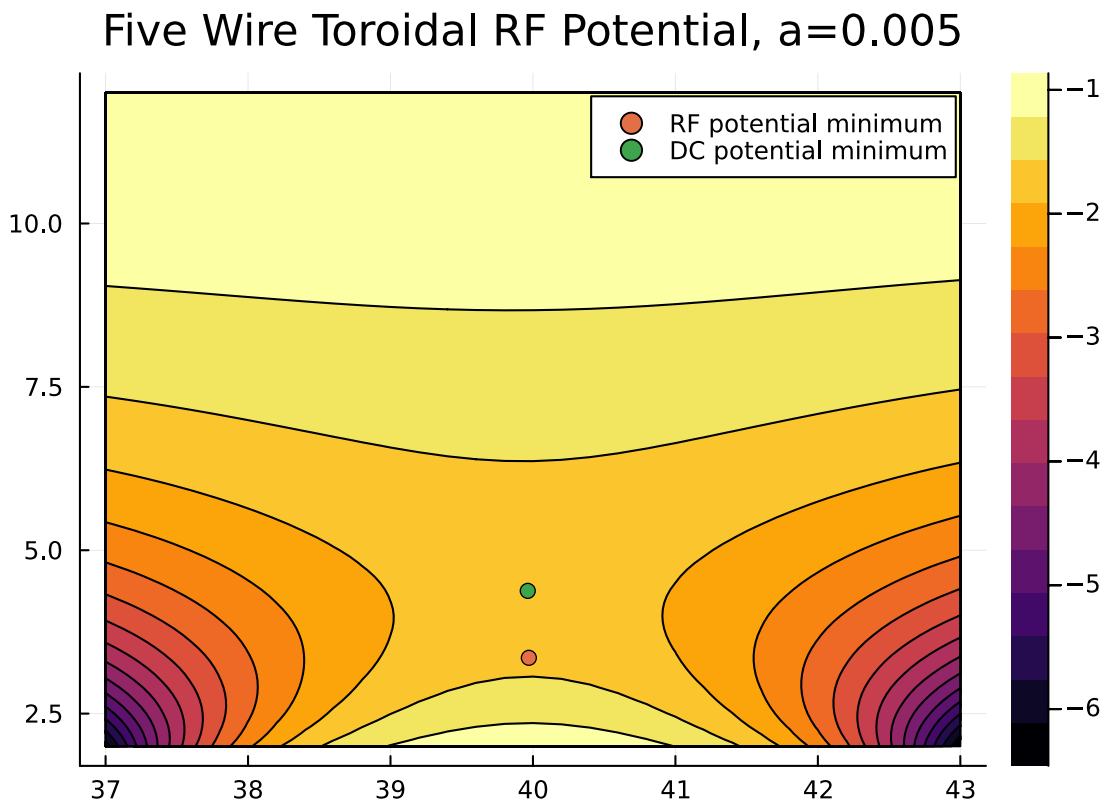

Figure 5.9: Radial Potential, with $\alpha = .005$

value. For a value of $\alpha = .005$ the difference between RF and DC centers is off by nearly 1.5, while it is 1e-6 for the unregularized case. Also we can note many other behaviors such as the potential's minimum changing as it moves along the circle, what it's higher order components are, and even specifying the shape of the potential in the radial direction. All of these can be added to our optimization problem as well, but they come at the cost of increasing the ill conditioning. The use of SVD and Thrikonov Regularization provides a method to choose a compromise between experimentally obtainable voltages and creating the ideal potential.

Overall, we can make the center of the potential created by the control electrodes to be at the same position as the center of the RF minimum, if we do not use regularization. Regularization does smooth out our potentials and should make it more experimentally realizable but there seems to be quite adverse effects on the location of the potential. This is quite bad and shows that regularization might have to be applied with a careful hand. We have currently only optimized a few parameter, just the E field to be 0, the curvature tangentially, and what the value of the potential at the minimum is. If we wanted to align the principal axes of the control and RF potentials then we would need to specify all nine values of the Hessian matrix. In this case regularization along with weighting the most important parameters, could be highly necessary.

5.2 Multipole Expansion of Four Rod Toroidal Trap

We have currently shown that many of the undesirable properties of toroidal ion traps can be minimzed or eliminated. However, we have only considered the impacts near the trapping center, and thus have not really considered how the field itself is changed. We have seen that by introducing a toroidal structure that the potential changes quite dramatically and thus we should try to characterize this change. We can begin by considering a harmonic expansion of our potential.

Let us start our simulation by considering a standard four rod toroidal trap with parameters, r=1, R=1, D=5. The plot of the potential is shown in figure 5.10, and we can see the asymmetry in the x direction as seen before. Let us now expand this potential in terms of the first 20 harmonic polynomials, and then look at how well the harmonic polynomials are able to reproduce this potential. The difference between the two is shown in Figure 5.11, and we see quite bad results, with the error being .012, in a box of size 1 around the geometric center. We would expect that the harmonic polynomials would produce much better results, and be able to converge to our potential easily, since they should be able to reproduce solution to Laplace's equation in this domain. The only difference here is the toroidal geometry, which appears to have a dramatic effect on our

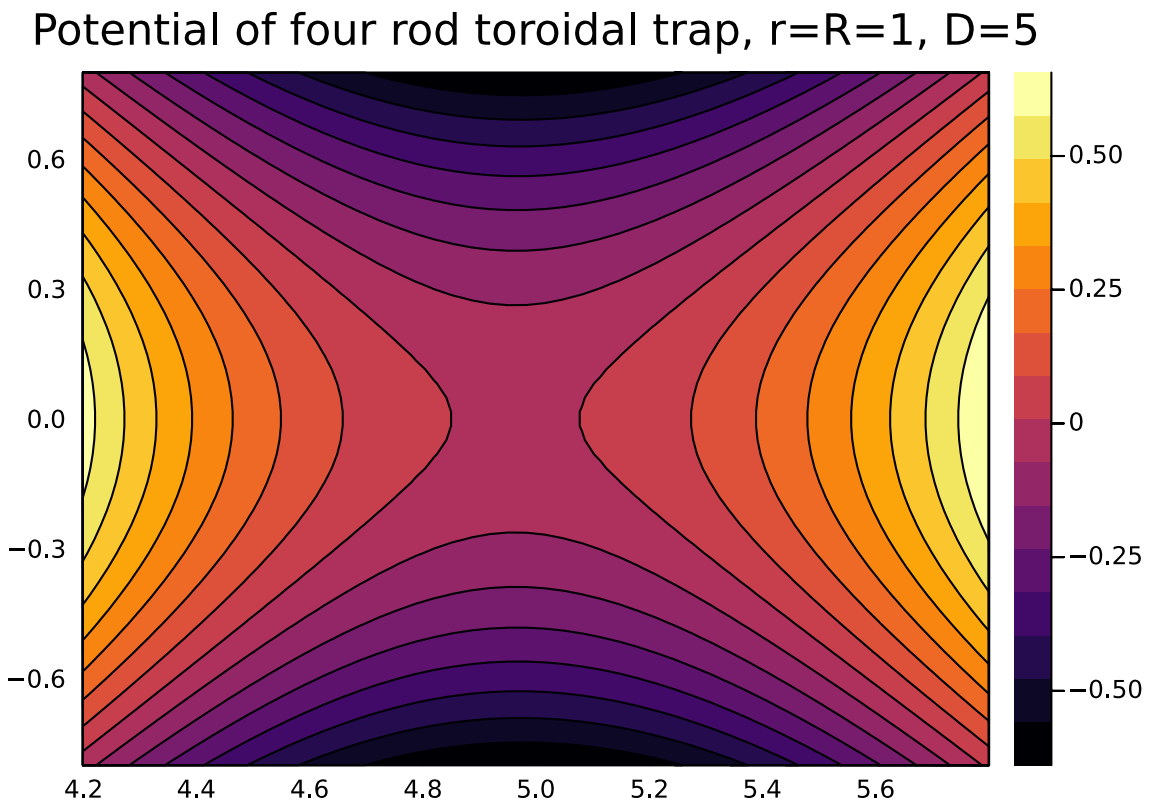

Figure 5.10: Potential due to a four rod toroidal trap with r=R=1, D=5

potential.

The paper [41], offers a solution to this problem. They perform a perturbative analysis on the trap and find that **only** along the radial axis, x, is there an effect to the potential due to the curvature of the trap, but not in the y axis. They find corrections to the x axis of

$$u = A * (\frac{x^2}{r_0^2} - \frac{r_0}{3D}\frac{x^3}{r_0^3})\frac{r_0^2}{4D^2}\frac{x^2}{r_0^2} + \frac{r_0}{3D}\frac{x}{r_0} \tag{5.7}$$

with A being an arbitrary potential. Since these correction terms only effect the x axis and not the y, then they lie outside of the space that the harmonic polynomials can reproduce. To check that our results agree we can perform a fit of our potential only along the x axis by a polynomial of 10th order, the coefficients are shown in Table 5.1, from this we can see quite a good agreement with their perturbative analysis. However, we can also note that these pertubative terms do not lie in the space of harmonic polynomials as evidenced by the error on our fit. This causes a problem that there appears to be parts of our field which do not obey a multipole expansion.

As a last attempt to try to cancel out these perturbative terms, we can try the "x" configuration

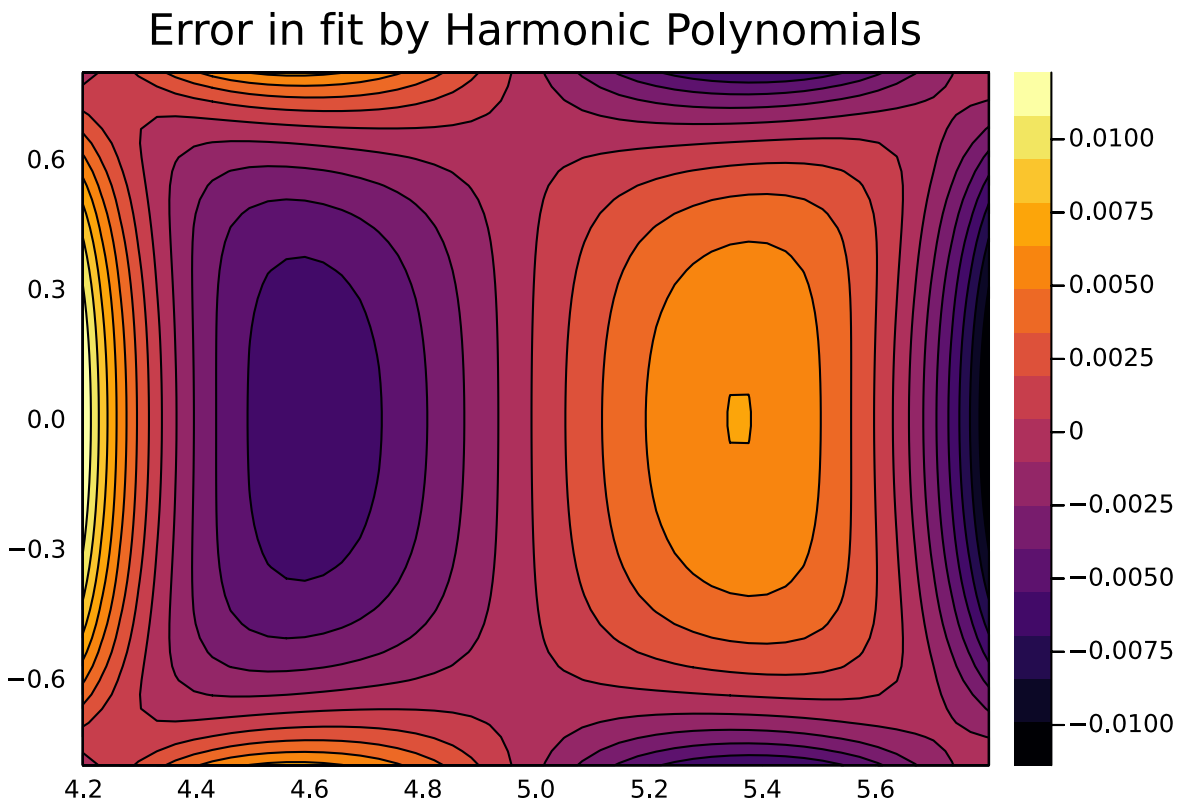

Figure 5.11: Error in Harmonic Fitting

of the four rod toroidal trap, and make our harmonic polynomials aligned with the axes of the trap. In this way if harmonic polynomials are tilted by 45 degrees that is the maximum amount they can deviate from the previous case. We can see the results in Figure 5.12. We see that this potential is shows all the same characteristics as the "+" configuration and thus we see that this perturbation is indeed a fact of the space and independent of how our quadrupole is aligned. Thus this error represents a field that is not representable by the harmonic polynomials.

This poses a problem, since most of the analysis on the anharmonic terms of an ion trap are in terms of a multipole expansion. Having a component of our field which is not able to be expressed by a multipole expansion means that additional theory would have to be done to characterize this field and to see how the dynamics are altered as a result. One alternative solution is to have a high aspect ratio trap, as these preturbations appear to scale in terms of r/D, so increasing the aspect ratio would decrease their effects.

Table 5.1: Coefficients of a linear fit along the x axis of a toroidal four rod ion trap

Coefficient	Numeric	Theory
A1	.072268	.066666
A2	.982997	1
A3	-.061429	.066666
A4	.010496	.01

5.3 Toroidal Harmonics

Since a multipole expansion of our potential appears to not be able to properly reproduce our field, we might consider a basis set which includes the toroidal nature of our space. These are the toroidal harmonics and their expressions can be found in [18].

To roughly see the nature of them a plot of the 2nd toroidal harmonic is shown in Figure 5.13. We can already see that these show some of the same behaviors as seen by the toroidal four rod ion trap, and thus we might think that we fully reproduce its potential using these.

If we now use these to expand our potential and plot the error in Figure 5.14, we see that they behave in a more regular pattern, and we are able to reproduce our potential in this basis, with the maximum error being 1e-9 with only the first 11 toroidal harmonics.

One of the reasons that the harmonic polynomials fail is due to the axis of symmetry. If we naively guess that a basis of our potential is a revolved quadrupole around the axisymmetric axis, then when its potential reaches the axisymmetric axis, it would suffer a discontinuity in its derivative. The toroidal harmonics are continuous on the axisymmetric axis, and thus we see why they are the correct ones to expand toroidal potentials with.

However, a consequence of this is that the toroidal harmonics do not offer a very intuitive picture to our problem. The paper [19] finds that toroidal quadrupole's stability diagram exhibits resonance lines in many parts, and proposes some values of the toroidal hexapole which minimize certain values of these resonance lines. So while we can expand our field in terms of toroidal harmonics, they do not offer an intuitive answer to many questions.

An alternative approach would then be to ask if there is a combination of toroidal harmonics which approximates a perfect quadrupole field, and how this could be used to create an ion trap. My proposal is that such a field would need many controllable knobs, and thus we can create a toroidal surface trap which has more than three inner rings, but perhaps has nine or more rings. Then we can look for the voltages needed to be applied on each of our electrodes such that a perfect

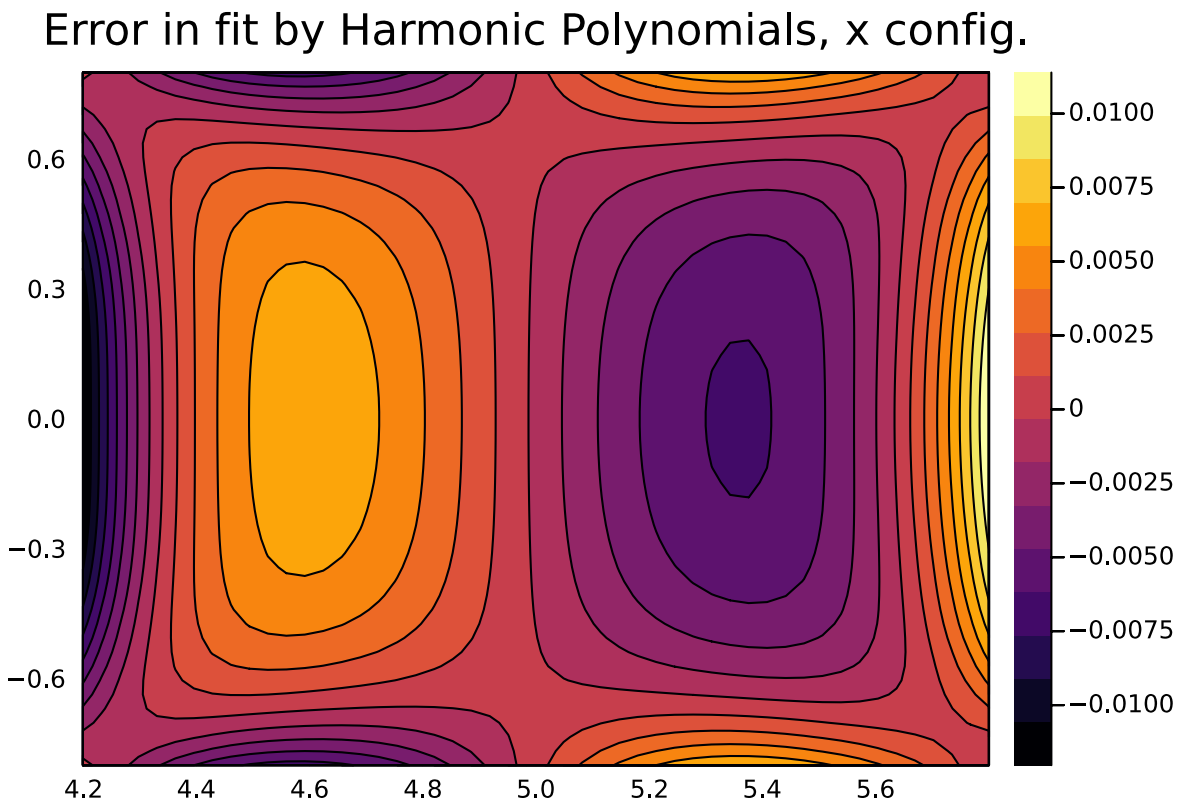

Figure 5.12: Error in Harmonic Polynomial fit of x configuration

quadrupole is created in the region we are interested in. This would be an ultimate test if there are parts of the field which are uncapturable using harmonic polynomials.

5.3.1 2N+1 Wire Trap

Overall we can see that for a 3d trap it appears to be impossible to really eliminate many of these higher order terms, since the curvature adds terms as low as a hexapole which would normally be forbidden by symmetry. If we cannot design a potential through the optimization of geometry then perhaps we can design the potential that we want through brute force. For an ion trap like a surface trap adding more ring electrodes is trivial to do, and each of these ring electrodes acts as a new function to which we can use to approximate any other function. In this way adding more ring electrodes adds more terms to use to tune our potential to be what we want. In another view this allows us more tunable parameters to tune out the undesired components of our field. This approach was taken in [4], to minimize the field at the center of a toroidal surface trap composed of an upper and lower plate. The current proposal is to perform the same analysis but with the

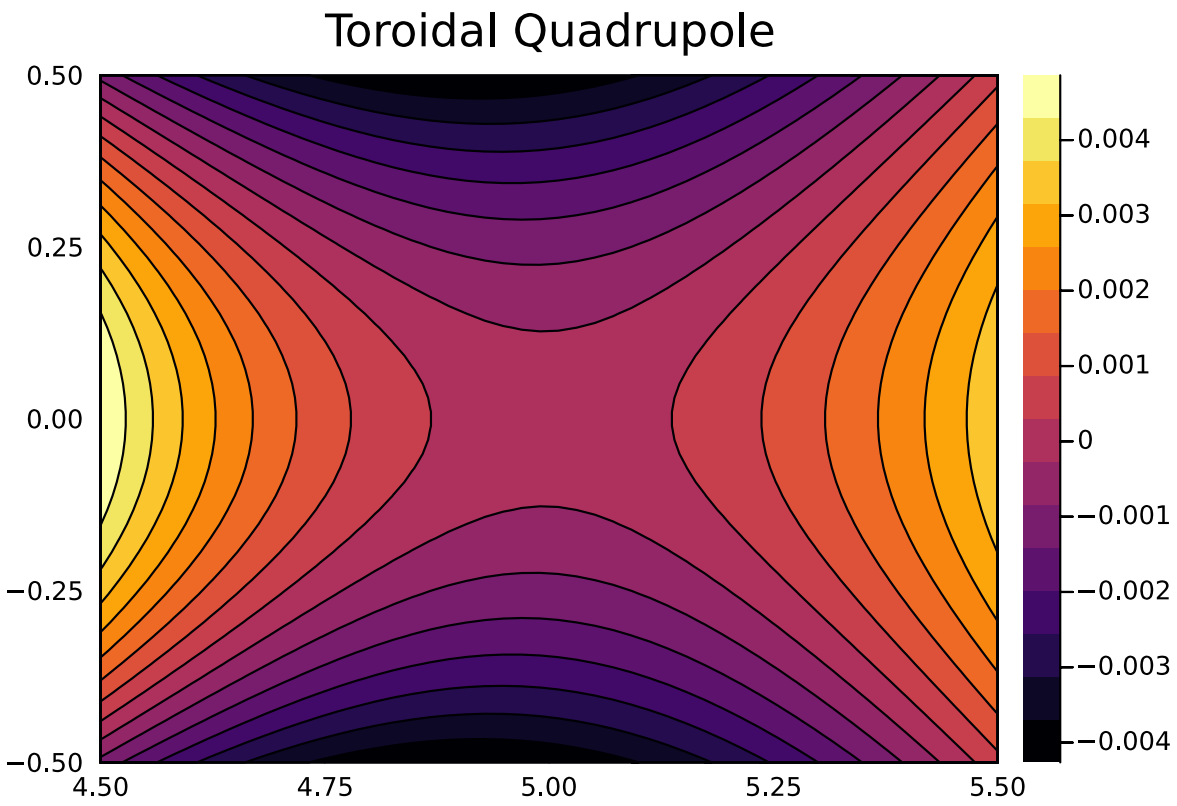

Figure 5.13: The Toroidal Quadrupole for a toroidal coordinate system which has a torus of radius 5

the trapping potential not at the center and with only a single plate.

We can set up a simulation to perform this. We can set up 2n+1 conformal rectangles separated from each other by a distance d, and we know where to place our charges for a conformal rectangle. This trap design will give us two more electrodes as compared to the five wire design. Now for each of these electrodes, m electrodes, we can construct a Green's function G_j by solving for the charges that make the nth electrode equal to 1 while the other boundary points of each electrode are 0.

Now with these green's functions if we want to find a specific potential then we only need to sample that potential as a set of data sites, and then perform a least squares regression to find the correct combination of parameters that gives the best reproduction of that answer. However, it is more informative if we take each of our Green's functions and expand them in terms of harmonic polynomials, since we are working in 2d. In chapter 2 only the real parts were considered, and now the imaginary parts are included as well. The imaginary parts only represent a rotation of the real part by 90 degrees, and will need to be included to represent an arbitrary potential.

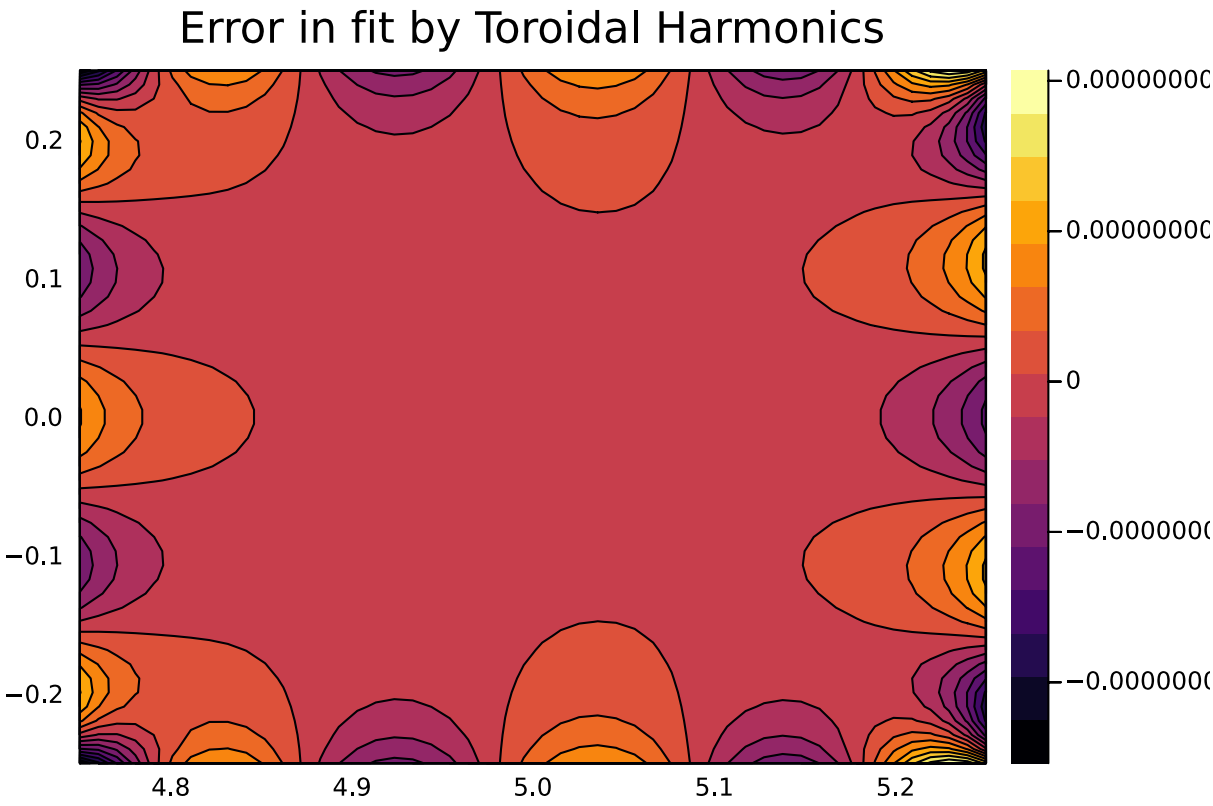

Figure 5.14: Error in Toroidal Harmonic Fitting

$$\phi_{n,1} = Re((x+iy)^n) \tag{5.8}$$

$$\phi_{n,2} = Im((x+iy)^n) \tag{5.9}$$

From potential theory we know that for a well behaved domain that is simply connected that these should be able to reproduce any function. Thus if we take points near the trapping region both of these criteria should be satisfied, as that part of our domain is well behaved. But these polynomials will fail to characterize the domain in all of space (note that they go off to infinity and don't obey our boundary conditions). We can then write each of the Green's functions for our electrodes as a linear expansion of harmonic polynomials.

$$G_j = \sum_{i=0}^{n} A_{j,i}\phi_{i,1} + \sum_{i=1}^{n} A_{j,i+n}\phi_{i,2} \tag{5.10}$$

And we can now say that our total potential is then a sum of these green's functions

$$\Phi(x,y) = \sum_{j=1}^{m} V_j G_j \tag{5.11}$$

Where V_j is the potential applied to each electrode. Now that we have expressed our Green's functions in terms of Harmonic Polynomials we can then look to solve for a potential in terms of harmonic polynomials, which in this case we want to maximize the quadrupole term.

$$\begin{bmatrix} A_{0,1} & A_{1,1} & A_{2,1} & \dots & A_{m,1} \\ A_{0,2} & A_{1,2} & A_{2,2} & \dots & A_{m,2} \\ \vdots & & & \ddots & \\ A_{0,2n} & A_{1,2n} & A_{2,2n} & \dots & A_{m,2n} \end{bmatrix} \begin{bmatrix} \mathrm{V}_1 \\ V_2 \\ \vdots \\ V_n \end{bmatrix} = \begin{bmatrix} \mathrm{A}_0 \\ A_1 \\ \vdots \\ A_n \end{bmatrix} \tag{5.12}$$

This matrix is underdetermined if we want to determine n of the coefficients for harmonic polynomials A_n with only m electrodes, when $2n > m$, meaning it would have to be solved using least squares. Thus as we use more ring electrodes we should be better able to make more of the terms what we want. In addition, as more rings are added, we have more rings of different sizes, and thus they should have more and more different harmonic terms.

To optimize our trap we will choose to center our harmonic polynomials at (40,3) which is close to the trap center of a standard 5 wire trap and keep this height for all simulations. This gives us a ratio of the trap radius to the radius of rotation of around 1/13, if we assign r to be the height from the surface. While for a surface trap this ratio can be pushed even further down and thus have less of a curvature, the current ratio seems to be reasonable for even 3d traps, and should represent a reasonable ratio.

We will optimize our potential such that the quadrupole term is set to 1 and all other terms are set to 0, and these are sampled in a square region of side length 1 centered around the determined center. The results are shown in Table 5.2, showing the first few coefficients of the harmonic polynomials, with the fit including the first 10 real and imaginary harmonic polynomials, as well as the trap center location, how good the fit using harmonic polynomials is compared to the numeric solution, and the maximum voltage difference applied.

From this we see that we have nearly no control with the 5 wire trap, and even the minimum is not in the correct place. As we increase the number of electrodes we see that all of the harmonics except for the quadrupole $\phi_{2,2}$ start to go to 0 and $\phi_{2,2}$ beings to approach the set value for it of 1, we also see the trap center being at the correct position. However, we do not see the harmonic polynomials being able to reproduce the field any better as we increase the number of electrodes.

Table 5.2: Fit by N electrodes

Coefficient	5 electrodes	7 electrodes	9 electrodes	11 electrodes
ϕ_0	-.041495	-.004366	-.000101	8.09e-7
$\phi_{1,2}$	.006387	-.002110	.004100	2.56e-5
$\phi_{2,2}$	-.207465	-.690754	-.979462	-.999623
$\phi_{3,2}$	.000272	.003610	-.001139	-4.75e-5
$\phi_{4,2}$	-.024436	.162623	-.104157	-.009997
$\phi_{1,1}$	-.394819	-.068692	-.002510	-2.89e-5
$\phi_{2,1}$	-.000261	.004032	.000769	3.767e-5
$\phi_{3,1}$	.078325	.424112	.079129	.0025764
$\phi_{4,1}$	-.000244	-.001959	.001277	9.97e-5
center	(40.54,8.092)	(39.99,4.05)	(39.99,4.001)	(39.99,4.00001)
error	.000710	.00269	.00289	.0028
ΔV (V)	17.15	115.7	674.6	2872

This can indicate that we are increasing the value of higher order harmonic polynomials which were not included in the fit.

Perhaps the most concerning fact is the required voltage to produce the desired field. From nine electrodes to eleven electrodes, we don't see a change in the quadrupole coefficient, meaning the potential should be nearly the same strength between the two, but we see the maximum potential difference between the electrodes being around four times bigger. We can look at the voltages applied in the eleven electrode case to see what is going on. From left to right the voltages are,

$$1246V, -1280V, 258V, -21V, 18V, -22V, 274V, -1420V, 1451V$$

which shows a trend that the farther away electrodes need to have a very high voltage to contribute to the field at the center of the trap, and also that while one electrode contributes a curvature, the next electrode partially cancels out that curvature. This causes the alternating signs between each electrode.

Overall, the issue of the maximum voltage required poses quite an issue to the actual creation of the trap. In addition, while we can minimize certain harmonic polynomials, we did not reproduce the actual potential, meaning that our combination of toroidal harmonics could not make a quadrupole looking potential. Perhaps the best explanation for why this is the case is by showing the difference between the potentials in Figure 5.15

We see that the difference between our numerically calculated potential and the fit has all of the same characteristics of revolving a four rod ion trap into a toroidal four rod ion trap. Because of this, we can conclude that there is no way for the harmonic polynomials to exactly reproduce a

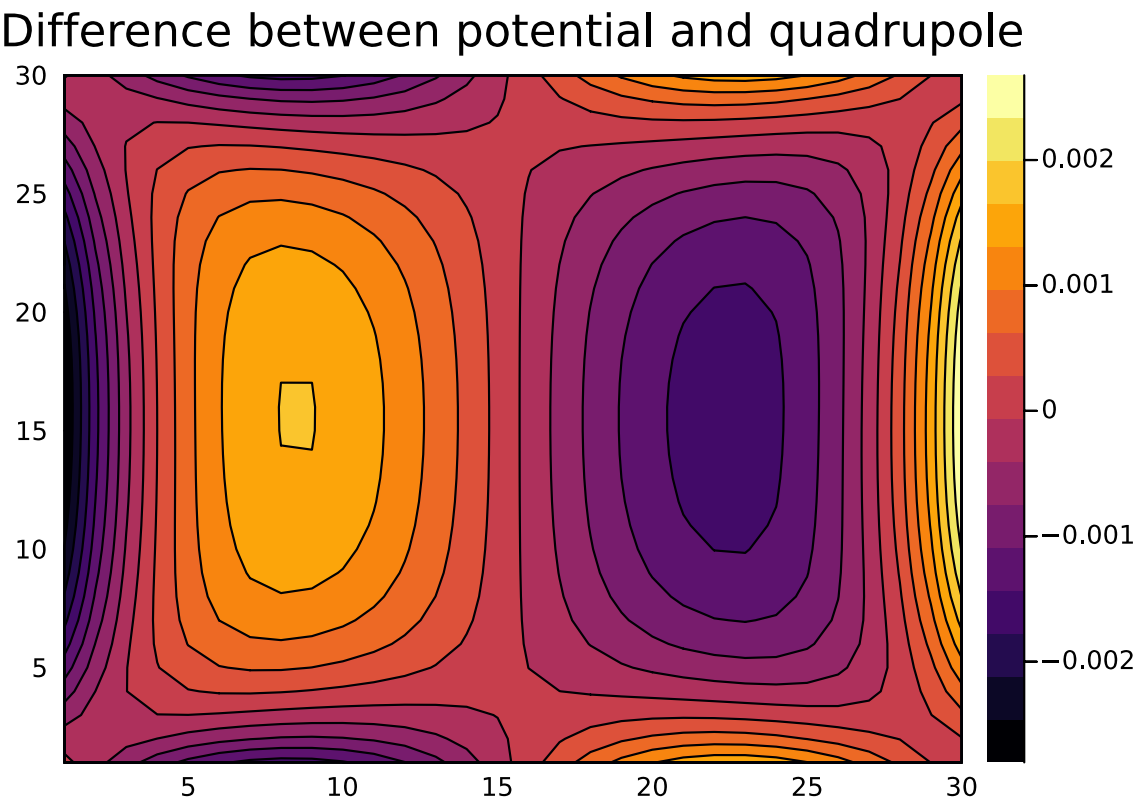

Figure 5.15: Difference between the optimized potential of an 11 electrode ring trap and an ideal quadrupole

field that obeys a toroidal geometry. In addition, the exact nature of these fields seems to be more complicated for ion trap designs that have more anharmoncity, as shown by the surface ion trap having an opposite shift to the perturbative analysis.

This means that the only thing to change is the aspect ratio of the trap, but even for an aspect ratio of 30 there would still be a 1 percent contribution to the x^3 perturbation term, which is likely too large to only be considered a small perturbation. The dynamics simulations performed by other members in the group have gone off the assumption that a revolved quadrupole is possible and thus finding out which terms to include to fully reproduce the potential are needed.

Overall, the issue of toroidal geometries will always be present and cannot be optimized out. Because of this if the aspect ratio is not large enough, then the potential cannot be explained using a standard multipole analysis. To get around this, working in terms of toroidal harmonics, will be able to reproduce the potential, but then Mathieu's equations are not written in terms of these potentials.

5.3.2 Adding a DC Potential

While the previous section showed that there unavoidable harmonics associated with the toroidal geometry, their effects might be minimized if the ion is able to be kept near the RF minimum. We have already seen a procedure to transport the ion around the ring using a DC potential, which is able to have the potential centered at the RF minimum, to prevent the DC potential shifting the ion off the RF minimum, but we have not considered the effects of the centrifugal force on the ion as it rotates around the ring. There is a high chance that this field will move our ion off the RF minimum, which makes the effects of the toroidal geometry much bigger. As proposed in [42] a DC centripetal force is planned to be supplied to counteract this force. When first simulating the fields in Chapter 3, we say that only applying a DC potential to the outer electrode would not create a field pointing exactly inwards, but inwards and upwards. To get around this we can use the same method as in the previous section and use more electrodes to create a better approximation to a constant E field inwards. Since a constant E field is provided by a dipole potential, a hope is that the difference between the toroidal dipole and normal dipole is less than the difference of the toroidal quadrupole and the normal quadrupole.

We can fist look at the potential of a surface trap with 3 rings, which is shown in Figure 5.16. For this potential to be created voltages of -5.7V, .003V, 5.9V needed to be applied to the three electrodes. We can see that the potential is not exactly in the x direction but it is much better than applying a voltage on a single electrode. We can also investigate the case of having 5 ring electrodes to apply voltages to. The result can be seen in Figure 5.17, and we can see that this potential better approximates an E field in the x direction over a larger range. The voltages from left to right are -15.1V, -1.1V, 0.6V, .79V, 17.4V. These voltages are around 3 times larger, but the potential is obviously much better. Overall there is once again a trade off to getting a good potential, but different to the quadrupole case, these potentials seem to be much more experimentally realizable. Adding more electrodes does not dramatically change the resulting potential, so it might seriously be worth considering a 7 wire toroidal trap to improve the inwards pointing E field.

5.4 Conclusion To Chapter

Overall, we have demonstrated that many qualities of our trap can be adjusted, including where the center of the RF and DC potentials are, the curvature of the DC potential along the ring of the trap, and the harmonics of the trap. For all of these parameters, it was shown that using a method

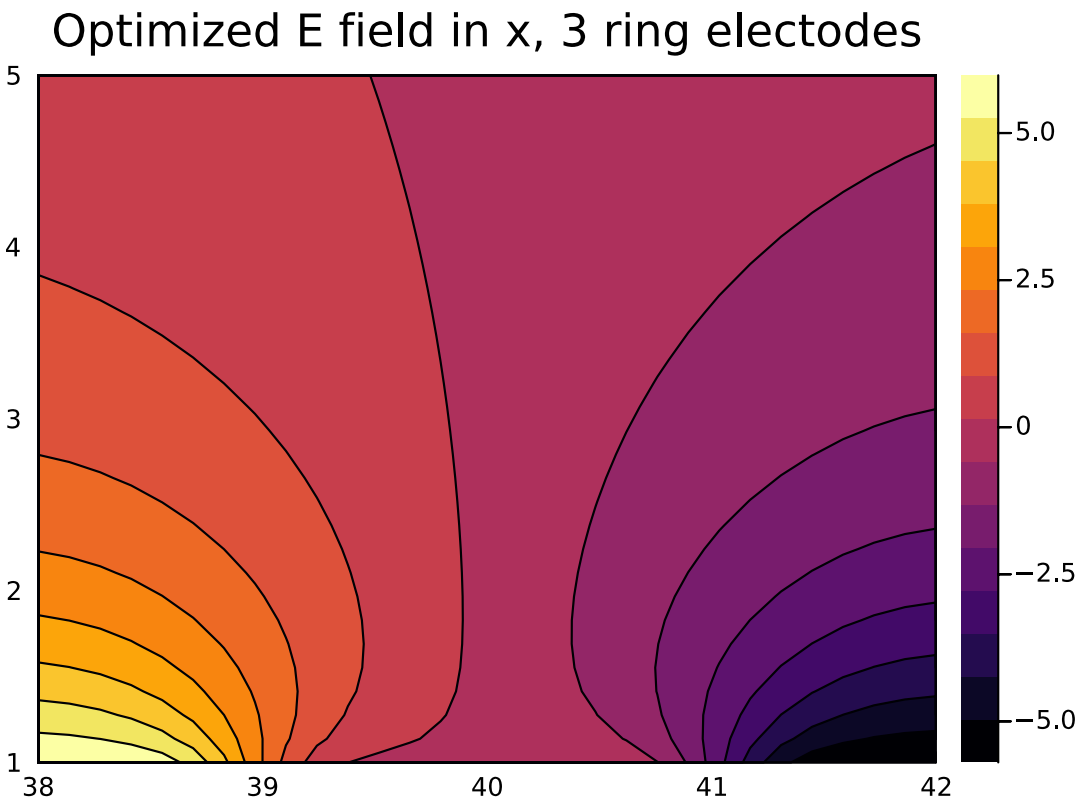

Figure 5.16: E field in the X direction created with only 3 ring electrodes.

such as SVD and Thrikonov regularization can reduce the required voltages on the electrodes to an experimentally viable level. With these techniques the initial simulation of a ring trap can be carried out, and this can aid in the initial design of such a trap. For fully 3d geometries, too many approximations to the shapes of the electrodes we applied to fully trust the resulting field. Numeric methods that can deal with corners better, such as the Boundary Element Method or Finite Element Method, could be used to finalize the field. The simplicity of the MFS and its speed for approximating many simple shapes allows it to still have a great deal of value in rapid prototyping and design.

However, we have seen that no matter how many degrees of freedom are given, a set of rings cannot fully approximate the potential caused by a revolved quadrupole. This means that considering the potential in terms of toroidal harmonics or dealing with the exact potential of a simulation will need to be considered. On a good note, if a certain ratio of toroidal harmonics is need then the 2N+1 wire trap should be able to provide that potential, so the method can work for future simulations with the only change being to specify the toroidal harmonic ratio instead of the harmonic

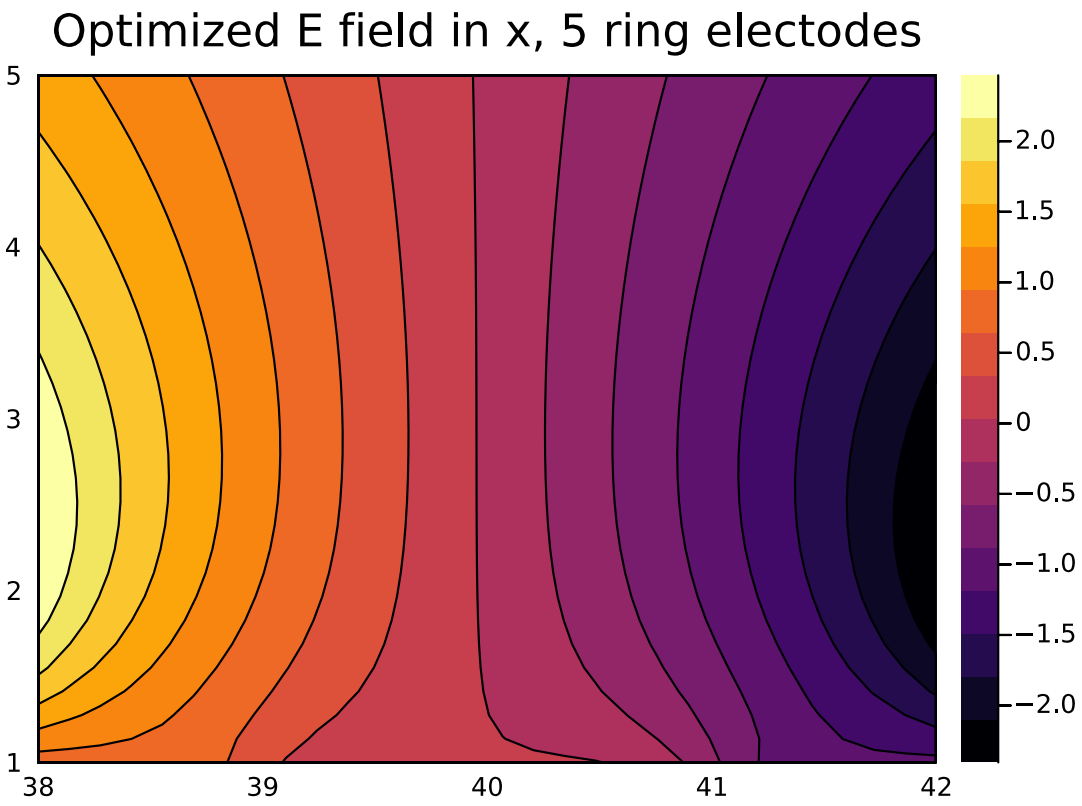

Figure 5.17: E field in the X direction created with only 5 ring electrodes.

polynomial ratio.

Currently there appear to be many possible problems but also many possible solutions. Some of the problems being the minimization of anharmonic terms of a surface trap, the anharmonicity due to low aspect ratios, and the voltage required to create the ideal potential. A surface trap allows for the a high aspect ratio, but the potential is not clean, and applying an E field in the x direction requires many electrodes at fixed ratios. In addition, there are often stray fields present due to patch charges, which have to be compensated for. The NIST ring trap [37] originally used its control electrodes just to compensate for stray fields. Even with 80 electrodes they still were not able create a ring potential as good as they desired. This could pose a big problem in the future as it increases the number of parameters needed to be controlled considerably. Another alternative approach would be to create a toroidal 4 rod trap, which would have a cleaner potential. However, since we require tangential control of the ion, a single ring would need to be broken up into 80 pieces, which would be difficult to make reliably, and would only get harder as the aspect ratio increased. A last alternative would be to have two copies of the surface trap arranged such that

they share an axis of symmetry but are displaced vertically. In this way the potential would be much better, and less control would be needed due to the additional axis of symmetry. However, the characteristic length, r, of the trap will be much larger than a surface trap, and thus the aspect ratio will be lower. Another issue is misalignment which will become more of an issue as the aspect ratio is increased.

Chapter 6

Conclusion

It has been shown in this work that the Method of Fundamental Solutions has been able to be used to simulate the potential of many ion traps. The simplicity of the method, as well as the maximum principle giving an absolute error bound, presents itself as a method which is easy to learn, code, and analyze. This technique has been demonstrated to work well for many ion trap configurations, and can work for many problems besides Laplace's equation.

Using this method many unintuitive facts about toroidal ion traps were considered such as the difference between the geometric center and trapping center, the vertical axis shift in the "x" configuration with split RF and DC electrodes, and the distortion to the potential due to the toroidal geometry. Not only were these effects simulated, but many of them were able to be compensated for, by changing the voltages applied to the electrodes or by changing the trap's geometry. The main effect that was not able to be compensated for was the inability to create a revolved quadrupole potential. This was ultimately determined to be an unavoidable consequence of the toroidal geometry.

Currently, there seems to be no ideal trap which has a high aspect ratio so the Mathieu equations are valid, no experimental difficulties such as patch charges or stray fields, and which doesn't required an extreme amount of control to perform correctly. However, the consequences of the toroidal geometry on the experiment have not been fully considered. There is a chance that low aspect ratio traps could be fine for the experiment. Thus, theoretical and experimental work on shuttling of an ion in a low aspect ratio toroidal trap could give insights on the impact of these effects.

Bibliography

[1] D. Allcock, J. Sherman, D. Stacey, A. Burrell, M. Curtis, G. Imreh, N. Linke, D. Szwer, S. Webster, A. Steane, et al. Implementation of a symmetric surface-electrode ion trap with field compensation using a modulated raman effect. *New Journal of Physics*, 12(5):053026, 2010.

[2] C. J. Alves. On the choice of source points in the method of fundamental solutions. *Engineering analysis with boundary elements*, 33(12):1348–1361, 2009.

[3] C. J. Alves and S. S. Valtchev. On the application of the method of fundamental solutions to boundary value problems with jump discontinuities. *Applied Mathematics and Computation*, 320:61–74, 2018.

[4] D. E. Austin, B. J. Hansen, Y. Peng, and Z. Zhang. Multipole expansion in quadrupolar devices comprised of planar electrode arrays. *International Journal of Mass Spectrometry*, 295(3):153–158, 2010.

[5] D. Berkeland, J. Miller, J. C. Bergquist, W. M. Itano, and D. J. Wineland. Minimization of ion micromotion in a paul trap. *Journal of applied physics*, 83(10):5025–5033, 1998.

[6] R. B. Blakestad. *Transport of trapped-ion qubits within a scalable quantum processor*. University of Colorado at Boulder, 2010.

[7] C. Chen, A. Karageorghis, and Y. Li. On choosing the location of the sources in the mfs. *Numerical Algorithms*, 72:107–130, 2016.

[8] W. Chen and M. Tanaka. A meshless, integration-free, and boundary-only rbf technique. *Computers & Mathematics with applications*, 43(3-5):379–391, 2002.

[9] D. Church. Storage-ring ion trap derived from the linear quadrupole radio-frequency mass filter. *Journal of Applied Physics*, 40(8):3127–3134, 1969.

[10] T. W. Drombosky, A. L. Meyer, and L. Ling. Applicability of the method of fundamental solutions. *Engineering Analysis with Boundary Elements*, 33(5):637–643, 2009.

[11] J. Durandau, J. Wagner, F. Mailhot, C.-A. Brunet, F. Schmidt-Kaler, U. Poschinger, and Y. Bérubé-Lauzière. Automated generation of shuttling sequences for a linear segmented ion trap quantum computer. *Quantum*, 7:1175, 2023.

[12] D. M. Eades, R. A. Yost, and R. Cooks. Black canyons for ions stored in an ion-trap mass spectrometer. *Rapid communications in mass spectrometry*, 6(9):573–578, 1992.

[13] C. Eckart and G. Young. The approximation of one matrix by another of lower rank. *Psychometrika*, 1(3):211–218, 1936.

[14] J. Franzen. The non-linear ion trap. part 4. mass selective instability scan with multipole superposition. *International journal of mass spectrometry and ion processes*, 125(2-3):165–170, 1993.

[15] Z. Fu, Q. Xi, Y. Gu, J. Li, W. Qu, L. Sun, X. Wei, F. Wang, J. Lin, W. Li, et al. Singular boundary method: A review and computer implementation aspects. *Engineering Analysis with Boundary Elements*, 147:231–266, 2023.

[16] P. K. Ghosh. *Ion traps*. Oxford university press, 1995.

[17] T. Hasegawa and J. J. Bollinger. Rotating-radio-frequency ion traps. *Physical Review A*, 72(4):043403, 2005.

[18] J. M. Higgs, B. V. Petersen, S. A. Lammert, K. F. Warnick, and D. E. Austin. Radiofrequency trapping of ions in a pure toroidal potential distribution. *International Journal of Mass Spectrometry*, 395:20–26, 2016.

[19] J. M. Higgs, K. F. Warnick, and D. E. Austin. Field optimization of toroidal ion trap mass analyzers using toroidal multipoles. *International Journal of Mass Spectrometry*, 425:10–15, 2018.

[20] S. Hong, M. Lee, H. Cheon, T. Kim, and D.-i. ho. Guidelines for designing surface ion traps using the boundary element method. *Sensors*, 16(5):616, 2016.

[21] M. House. Analytic model for electrostatic fields in surface-electrode ion traps. *Physical Review A*, 78(3):033402, 2008.

[22] C.-O. Hwang and M. Mascagni. Electrical capacitance of the unit cube. *Journal of applied physics*, 95(7):3798–3802, 2004.

[23] J. D. Jackson. *Classical electrodynamics*. John Wiley & Sons, 2021.

[24] A. Komiyama. Arrangement of sources in the charge simulation method–the case of e-wave scattering by one perfectly conducting cylinder of convex cross section shape. *Electronics and Communications in Japan (Part I: Communications)*, 68(5):106–113, 1985.

[25] A. N. Kotana and A. K. Mohanty. Determination of multipole coefficients in toroidal ion trap mass analysers. *International Journal of Mass Spectrometry*, 408:62–76, 2016.

[26] S. A. Lammert, W. R. Plass, C. V. Thompson, and M. B. Wise. Design, optimization and initial performance of a toroidal rf ion trap mass spectrometer. *International Journal of Mass Spectrometry*, 212(1-3):25–40, 2001.

[27] H.-K. Li, E. Urban, C. Noel, A. Chuang, Y. Xia, A. Ransford, B. Hemmerling, Y. Wang, T. Li, H. Häffner, et al. Realization of translational symmetry in trapped cold ion rings. *Physical review letters*, 118(5):053001, 2017.

[28] Z.-C. Li. Combinations of method of fundamental solutions for laplace's equation with singularities. *Engineering Analysis with Boundary Elements*, 32(10):856–869, 2008.

[29] Y. Liu. *The numerical solution of frequency-domain acoustic and electromagnetic periodic scattering problems*. Dartmouth College, 2016.

[30] H. Loh, K. C. Cossel, M. Grau, K.-K. Ni, E. R. Meyer, J. L. Bohn, J. Ye, and E. A. Cornell. Precision spectroscopy of polarized molecules in an ion trap. *Science*, 342(6163):1220–1222, 2013.

[31] A. D. Ludlow, M. M. Boyd, J. Ye, E. Peik, and P. O. Schmidt. Optical atomic clocks. *Reviews of Modern Physics*, 87(2):637, 2015.

[32] A. Ozakin and F. Shaikh. Stability analysis of surface ion traps. *arXiv preprint arXiv:1109.2160*, 2011.

[33] R. Schaback. Adaptive numerical solution of mfs systems. *The Method of Fundamental Solutions-A Meshless Method*, pages 1–27, 2008.

[34] T. Shigeta and D. Young. Mathematical and numerical studies on meshless methods for exterior unbounded domain problems. *Journal of Computational Physics*, 230(17):6900–6915, 2011.

[35] K. Singer, U. Poschinger, M. Murphy, P. Ivanov, F. Ziesel, T. Calarco, and F. Schmidt-Kaler. Colloquium: Trapped ions as quantum bits: Essential numerical tools. *Reviews of Modern Physics*, 82(3):2609, 2010.

[36] J. Stark, C. Warnecke, S. Bogen, S. Chen, E. Dijck, S. Kühn, M. Rosner, A. Graf, J. Nauta, J.-H. Oelmann, et al. An ultralow-noise superconducting radio-frequency ion trap for frequency metrology with highly charged ions. *Review of Scientific Instruments*, 92(8), 2021.

[37] B. Tabakov, F. Benito, M. Blain, C. R. Clark, S. Clark, R. A. Haltli, P. Maunz, J. D. Sterk, C. Tigges, and D. Stick. Assembling a ring-shaped crystal in a microfabricated surface ion trap. *Physical Review Applied*, 4(3):031001, 2015.

[38] L. N. Trefethen. *Spectral methods in MATLAB*. SIAM, 2000.

[39] E. Urban, N. Glikin, S. Mouradian, K. Krimmel, B. Hemmerling, and H. Haeffner. Coherent control of the rotational degree of freedom of a two-ion coulomb crystal. *Physical Review Letters*, 123(13):133202, 2019.

[40] I. Waki, S. Kassner, G. Birkl, and H. Walther. Observation of ordered structures of laser-cooled ions in a quadrupole storage ring. *Physical review letters*, 68(13):2007, 1992.

[41] X. Zhou, C. Xiong, G. Xu, H. Liu, Y. Tang, Z. Zhu, R. Chen, H. Qiao, Y.-H. Tseng, W.-P. Peng, et al. Potential distribution and transmission characteristics in a curved quadrupole ion guide. *Journal of the American Society for Mass Spectrometry*, 22:386–398, 2011.

[42] Y. Zhou, J. O. Island, and M. Grau. Quantum logic control and precision measurements of molecular ions in a ring trap: An approach for testing fundamental symmetries. *Physical Review A*, 109(3):033107, 2024.

Curriculum Vitae

Trevor Taylor

TrevorTaylor1280@gmail.com

Education

University of Nevada, Las Vegas *2021 - current*

Masters in Physics

Department of Physics and Astronomy

University of Nevada, Las Vegas *2016 - 2021*

Bachelors in Physics

Department of Physics and Astronomy

Papers and Presentations

Trevor Taylor, Exploring new physics with Molecular Ions, Poster ACS WRM meeting 2022

Academic Achievements

Russell L. Brenda Frank Scholarship *Fall 2021 - present*

Kenneth R. Sites Physics Scholarship *August 2020 - Summer 2021*

Nevada Millennium Scholarship *May 2018 - present*

Explore Knowledge Academy Valedictorian *May 2018*